TECHNISCHE UNIVERSITÄT MÜNCHEN

Fakultät für Chemie

Professur für Molekulare Katalyse

Time and Temperature dependent Reactivity Studies of a Dipyridine Ethinyl Ligand with Zinc(II)

and

Synthesis and Characterization of new Precursors for the Deposition of Refractory Metals from Ionic Liquids

Christiane Michaela Egger

Vollständiger Abdruck der von der Fakultät für Chemie der Technischen Universität München zur Erlangung des akademischen Grades eines

Doktors der Naturwissenschaften (Dr. rer. nat.)

genehmigten Dissertation.

Vorsitzender:	Prof. Dr. Tom Nilges
Prüfer der Dissertation:	1. Prof. Dr. Fritz E. Kühn
	2. Prof. Dr. Klaus Köhler

Die Dissertation wurde am 16.07.2020 bei der Technischen Universität München eingereicht und durch die Fakultät für Chemie am 01.09.2020 angenommen.

Die vorliegende Arbeit wurde im Zeitraum von Juli 2016 bis Februar 2020 an der Professur für Molekulare Katalyse der Technischen Universität München angefertigt.

Mein besonderer Dank gilt meinem Doktorvater

Herrn Prof. Dr. Fritz E. Kühn

für die Aufnahme in seinen Arbeitskreis, das entgegengebrachte Vertrauen und die damit verbundene finanzielle und wissenschaftliche Freiheit, Forschungsthemen frei zu gestalten und uneingeschränkt verfolgen zu können. Vielen Dank für Ihre Unterstützung sowie die spannende und lehrreiche Zeit.

DANKSAGUNG

Ganz besonderer Dank gilt **Dr. Oliver Schneider**. Danke Oliver für viele hilfreiche Anregungen, für die Unterstützung bei organisatorischen Belangen des Projekts und die Organisation sämtlicher Projektmeetings. Vielen Dank auch an **Ludwig Asen**, **Dr. Lukas Seidl**, **Göktug Yesilbas** und **Esther Eke** für die gute Zusammenarbeit. An dieser Stelle möchte ich mich auch bei den übrigen Projektpartnern des GALACTIF-Projektes bedanken, für die gute Zusammenarbeit, die Ausrichtung der Projektmeetings und die schönen Abende mit interessanten Gesprächen.

Ein großer Dank geht an Frau **Ulla Hifinger**. Vielen Dank, dass Sie mich immer mit so viel Geduld und Freundlichkeit in allen bürokratischen Belangen unterstützt haben.

Ich danke auch Herrn **Dr. Robert Reich**, für hilfreiche Anregungen und sämtliche Unterstützung in letzten Jahren, seien es fachliche oder organisatorische Dinge gewesen.

Vielen Dank an **Jens Oberkofler** für das Messen der Kristalle und an **Ulrike Ammari**, dafür, dass du dir immer so viel Zeit für das Messen meiner Elementaranalysen genommen hast.

Ich danke meinen Laborkollegen **Lorenz**, **Sebastian**, **Alex** und **Dani** für die angenehme Arbeitsatmosphäre und die ausgezeichnete musikalische Unterhaltung. **Marco**, deine „Musik“ werde ich wohl nie vergessen. **Nadine**, du warst eine wunderbare Laborpartnerin und es war mir eine Freude dir den Siegestanz beizubringen.

Vielen Dank an **Dr. Tommy Hofmann**, **Dr. Florian Groche** und den gesamten **AK Kühn**, für die unkomplizierte Aufnahme in den Arbeitskreis, die angenehme Arbeitsatmosphäre, die Seminar-Room-Raves, die vielen Mittags- und Kaffeepausen und das ein oder andere Feierabendbier.

Caro, vielen Dank für Alles! Mit dir habe ich in den letzten Jahren sämtliche Höhen und Tiefen (nicht nur) des Studiums gemeistert. Du bist mir immer bedingungslos zur Seite gestanden. Ohne dich hätte ich es wohl nicht geschafft und dafür bin ich dir unendlich dankbar.

Vielen Dank an meine **Freunde**, die immer ein offenes Ohr haben, mich unterstützen und für den nötigen Ausgleich abseits der Uni sorgen.

Ich danke meiner Familie und insbesondere meinen **Eltern** für den Rückhalt und das große Vertrauen, das ich genießen darf. Ihr habt mir immer viele Freiheiten gegeben und ohne eure bedingungslose Unterstützung würde ich heute bestimmt nicht die Danksagung meiner Doktorarbeit schreiben.

In diesem Leben ist jeder mutig, der nicht aufgibt.

Sir James Paul McCartney

TABLE OF CONTENTS

ABSTRACT

In the first part of this work fundamental studies towards the reaction behavior between a zinc compound and several dipyridine ethinyl ligands were conducted. These ligands, bearing a variety of functional groups (OMe, COOH, NH_2, NHBoc, $NBoc_2$), were synthesized and converted with $Zn(OTf)_2$ in acetonitrile. The results reveal that isolable defined products can be obtained by applying ligands with an amine group and its Boc protected derivatives ($NBoc_2$ and NHBoc). The product which is derived from the amine ligand (**2**^{Zn}) exhibits a polymeric sandwich structure corresponding to SC-XRD analysis, suggesting that the NH_2 moiety is of vital importance for product formation. In dependence of the reaction temperature, two novel coordination polymers (**5**^{Zn} and **6**^{Zn}) are received upon conversion of the Boc protected amine ligands with $Zn(OTf)_2$ in CH_3CN. Single crystal XRD measurements of **6**^{Zn} with the NHBoc ligand shows a one-dimensional coordination polymer with a layer structure, while **5**^{Zn} reveals a two-dimensional layer structure, in which the $NBoc_2$ moiety acts as a chelator for zinc(II) within the coordination polymer.

In the second part of this thesis the synthesis of new precursors for the electrochemical deposition of refractory metals from ionic liquids was conducted. Refractory metals exhibit many beneficial properties, which is the reason why many components are functionalized by coatings with these metals to improve their properties like their corrosion resistance. Currently metallic coatings are realized by electrodeposition from aqueous solutions, but due to the narrow potential window of water this method cannot be used for refractory metals. Hence, the medium had to be changed to ionic liquids (ILs) because of their wide electrochemical window amongst others. But the electrodeposition of some refractory metals only led to metal layers of poor quality because of the formation of subhalides and other side products which disturb the layers by applying halides as source of refractory metals. Therefore, the precursors, which were used for the deposition, had to be changed as well. The approach in this work was the application of nitrile stabilized metalorganic complexes with weakly coordinating anions with the idea of generating a ‘naked’ cation to circumvent the mentioned detriments. Nitrile stabilized metalorganic complexes with Ti, V, Nb, W and especially Cr and Mo were synthesized bearing different weakly coordinating anions such as BF_4^-, $CF_3SO_3^-$ or TFSI. Furthermore, their solubility in ionic liquids and their electrochemical behavior were investigated. The results reveal that all tested complexes are soluble in all different ionic liquids and that they exhibit a high stability in the ILs, but unfortunately only low concentrations of 0.07 M were obtained. It was recognized that a better solubility can be received if the complex and the IL contain the same anion which is why Cr and Mo complexes with the TFSI anion were generated. For both metals, complexes were obtained which still contained acetate ligands of the starting material. However, in the case of Mo, this compound revealed a superior solubility in the ILs. In addition, higher solubilities in the ILs were obtained in more polar ILs such as ACh TFSI or MEMP TFSI and also by applying complexes with additional NO ligands as in the case for W. Basic electrochemical studies of some selected Cr and Mo complexes only showed low currents in different EQCM measurements and for $[Cr(NCC(CH_3)_3)_4][BF_4]_2$ (**10**) as well as for $[Mo_2(NCCH_3)_7][CF_3SO_3]_4$ (**22**) deposits could be obtained, however further investigations are necessary.

ZUSAMMENFASSUNG

Mehrere dipyridin-ethinyl-Liganden mit verschiedenen funktionellen Gruppen (OMe, COOH, NH_2, NHBoc und $NBoc_2$), wurden synthetisiert und mit $Zn(OTf)_2$ in Acetonitril umgesetzt. Grundlegende Studien bezüglich des Reaktionsverhaltens zwischen Zink und dieser Liganden wurden durchgeführt, welche zeigten, dass mit den Liganden, die eine Aminogruppe oder deren Boc-geschützte Derivate ($NBoc_2$ and NHBoc) aufweisen, definierte isolierbare Produkte erhalten werden können. SC-XRD des Produktes aus der Umsetzung mit dem Amin-Liganden weist eine polymere Sandwichstruktur auf, welche zeigt, dass die NH_2-Gruppe von entscheidender Wichtigkeit für die Produktbildung ist. Die temperaturabhängige Reaktion des Boc-geschützten Amin-Liganden mit $Zn(OTf)_2$ in Acetonitril führt zu zwei neuen Koordinationspolymeren. Die Röntgenstrukturanalyse der Einkristalle zeigt, dass für den NHBoc-Liganden ein eindimensionales Koordinationspolymer mit einer Schichtstruktur vorliegt, wohingegen für den $NBoc_2$-Liganden ein Koordinationspolymer mit einer zweidimensionalen Schichtstruktur vorliegt, bei dem die $NBoc_2$-Gruppe als Chelator für Zink(II) innerhalb des Koordinationspolymers agiert.

Im zweiten Teil dieser Arbeit wurde die Synthese neuer Präkursoren für die elektrochemische Abscheidung von Refraktärmetallen aus ionischen Flüssigkeiten (IL) untersucht. Refraktärmetalle verfügen über einige nützliche Eigenschaften, weshalb viele Bauteile mit Beschichtungen dieser Metalle funktionalisiert werden, um so die Eigenschaften zu verbessern. Derzeit werden metallische Beschichtungen durch elektrolytische Abscheidung aus wässriger Lösung hergestellt. Aber aufgrund des engen Potentialfensters von Wasser kann diese Methode nicht für die Refraktärmetalle angewendet werden. Wegen ihres breiteren elektrochemischen Fensters wurden ILs dafür eingesetzt. Aber die Abscheidung dieser Metalle aus ILs führte nur zu Metallschichten von schlechter Qualität mit Einlagerungen von Subhalogeniden. Deshalb mussten auch die Präkursoren ausgetauscht werden, aus denen die Abscheidung erfolgt. Der Lösungsansatz dieser Arbeit waren nitrilstabilisierte Komplexe mit schwachkoordinieren Anionen zu verwenden mit dem Hintergrund ein ‚nacktes' Kation in Lösung zu generieren. Derartige Komplexe wurden mit Ti, V, Nb, W und vor allem Cr und Mo hergestellt mit BF_4^-, $CF_3SO_3^-$ oder TFSI als Anion. Deren Löslichkeit in ILs und elektrochemisches Verhalten wurde untersucht, mit dem Ergebnis, dass zwar alle Komplexe in allen ILs löslich sind und eine hohe Stabilität aufweisen, aber meistens nur mit geringer Konzentration von 0.07 M. Eine bessere Löslichkeit kann erreicht werden, indem der Komplex und die IL das gleiche Anion enthalten. Deshalb wurden vor allem Cr und Mo Komplexe mit dem TFSI Anion hergestellt. Für beide Metalle wurden Produkte erhalten, die teilweise noch Acetatliganden aus dem Edukt enthielten. Für den entsprechenden Mo-Komplex wurde eine vergleichsweise hohe Konzentration erhalten in ILs wie Ach TFSI oder MEMP TFSI. Außerdem wurde für die W-Komplexe, die zusätzliche NO-Liganden enthalten ebenfalls eine hohe Löslichkeit erhalten. Grundlegende elektrochemische Untersuchungen wurden für einige Cr- und Mo-Komplexe durchgeführt, zeigten aber nur niedrige Ströme in verschiedenen EQCM-Messungen. Für $[Cr(NCC(CH_3)_3)_4][BF_4]_2$ (**10**) und $[Mo_2(NCCH_3)_7][CF_3SO_3]_4$ (**22**) wurden dünne Metallschichten erhalten, wozu aber weitere Untersuchungen notwendig sind.

List of Abbreviations

°C	Degree Celsius
Å	Ångström
ACh	acetylcholine
AN	acetonitrile
av.	average
BMIm	1-butyl-3-methylimidazolium
BMMIm	1-butyl-2,3-dimethylimidazolium
BMP	1-butyl-1-methylpyrrolidinium
BMPip	1-butyl-1-methylpiperidinium
Boc	*tert*-butyloxycarbonyl
BPh_4	tetraphenylborate
cf.	compare, abbreviation from Latin ‘conferatur’
cP	Centipoise
CP	Coordination polymer
Cp	Cyclopentadienyl $(C_5H_5)^-$
cryst.	crystallized
CV	Cyclic voltammetry
CVD	Chemical vapor deposition
δ	chemical shift
D	dimensional
d	doublet
DCM	dichloromethane
DMAP	4,-*N,N*-dimethylaminopyridine
DMF	Dimethyl formamide
DMSO	Dimethyl sulphoxide
DTMA	*N*-decyl-*N*,*N*,*N*-trimethylammonium
EA	Elemental analysis
e.g.	for example, abbreviation from Latin ‘exempli gratia’
EMIm	1-ethyl-3-methylimidazolium
EMMIm	1-ethyl-2,3-dimethylimidazolium
EMP	*N*-ethyl-*N*-methylpyrrolidinium
EPR	Enhanced permeability and retention
eq.	equivalent
EQCM	Electrochemical Quartz Crystal Microbalance
ESI-MS	Electrospray ionization mass spectrometry
et al.	and others, abbreviation from Latin ‘et alii / et aliae’

f	resonant frequency
FDA	Food and Drug Administration
FSI	Bis(fluorosulfonyl)amide
g	gram
h	hour
HTFSI	trifluoromethanesulfonimide
HTMA	*N*-hexyl-*N*,*N*,*N*-trimethylammonium
Hz	Hertz
IL	Ionic Liquid
j	current density
K	Kelvin
L	Ligand
LUMO	lowest unoccupied molecular orbital
m	multiplet
M	Metal
M	Molarity (mol/L)
Me	methyl
MeCN	acetonitrile
MEMP	1-(2-methoxyethyl)-1-methylpyrrolidinium
MEMPip	1-(2-methoxyethyl)-1-methylpiperidinium
MeOH	methanol
mg	milligram
MHz	Mega Hertz
min	Minute(s)
mL	milliliter
MOF	Metal organic framework
m. p.	melting point
m/z	mass to charge ratio
NHE	Normal hydrogen electrode
NMR	nuclear magnetic resonance
OAc	acetate
OMIm	1-octyl-3-methylimidazolium
OMMIm	1-octyl-2,3-dimethylimidazolium
ORTEP	Oak Ridge thermal ellipsoid plot
OTf	Trifluoromethane sulphonate / triflate
OTMIm	1-octyl-2,3,4,5-tetramethylimidazolium
$P_{6,6,6,14}$	Trihexyl(tetradecyl)phosphonium
PMIm	1-propyl-3-methylimidazolium

ppm	parts per million
PVD	Physical vapor deposition
q	quartet
r.t.	room temperature
RTIL	Room Temperature Ionic Liquid
TEBA	*N*,*N*,*N*-triethylbut-2-enammonium
TFSI	Bis((trifluoromethyl)sulfonyl)amide
s	singlet
SCC	supramolecular coordination cage
SC-XRD	Single crystal X-ray diffractometry
t	triplet
THF	tetrahydrofurane
V	Volt
vs.	versus
w	damping
WCA	weakly coordinating anion

I. Reactivity Studies of a Dipyridine Ethinyl Ligand with Zinc(II)

This chapter is published in C. M. Egger, C. H. G. Jakob, F. Kaiser, O. Rindle, P. J. Altmann, R. M. Reich and F. E. Kühn, *Eur. J. Inorg. Chem.* **2019**, 2019, 48, pp. 5059 – 5065.[1]

1. Introduction and Objective

Soon after the discovery of the cytotoxic effects of *cis*-diamminechloridoplatinum(II) (cisplatin) it was approved as an anticancer drug in the USA by the FDA and has been successfully applied since then. Despite its beneficial properties in therapy, cisplatin exhibits some severe detriments in the tumor treatment because cisplatin is not only active in tumor tissue, but also cytotoxic against several healthy cells. The consequence are some heavy side effects for the patients.[2] Thus, it is of great interest to reduce the secondary effects by improving the selectivity of cisplatin and its derivatives. One promising approach to minimize these drawbacks are supramolecular coordination cages (SCCs) as drug delivery systems. With this method, the active pharmaceutic is incorporated in a cage and the inclusion into cells can be alleviated. Further advantages of this method are, that the active ingredient can be enriched in the tumor tissue and selectively released. The principle to this procedure is the enhanced permeability and retention effect (EPR effect). The porous vascular structure and the poor lymphatic clearance of the tumor tissue form the basis of this principle. Thereby, macromolecules such as SCCs can easily diffuse into the malignant tissues where they are retained, because the lymphatic drainage is still functional in the normal tissue.[2a, 2b] McMorran and Steel referred to the first Pd_2L_4 cage (L coordinating *via* pyridyl-N) in 1998. This cage can encapsulate a hexafluorophosphate ion.[3] Since then, these compounds have become of increasing interest, as the cages can be ordinarily synthesized through self-assembly by mixing the metal precursors with the bidentate ligands.[4] Therrien *et al*. synthesized the first metallocage which can be used as a drug delivery system in 2008. It is about a metalorganic ruthenium-containing complex, which is able to encapsulate palladium or platinum acetylacetonato compounds and which possesses an extended cytotoxic activity against A2780 human ovarian cancer cells.[5] Most of the self-assembled M_2L_4 cages which are known so far, contain Pd(II) or Pt(II) as the metal but there are only few with other metals.[6] In order to follow the uptake, the distribution, and the localization of the active pharmaceutic in the body, fluorescent properties of these systems are very beneficial. But heavier metals such as palladium or platinum exhibit a strong influence on the fluorescent properties of a compound, which is why fluorescence quenching often occurs. There are only few examples with these metals which have a high fluorescence.[7] Thus, it is of significant interest to find compounds with which the fluorescence can be maintained by substituting palladium or platinum for lighter metals. But only few research groups such as Yoshizawa *et al*.[8] and Bu *et al*.[9] were able to successfully realize such compounds. At this point it has to be noticed, that the self-assembly of metal compounds with organic ligands can not only result in the formation of supramolecular cages, but also in coordination polymers (CP). This is influenced by various parameters such as external factors like temperature as well as internal factors like coordination geometry of the metal or the flexibility of the applied organic ligands.[10] In general, coordination polymers are polymeric structures with a broad spectrum of features. These can be attributed to the manifold combination possibilities of organic ligands with metal components. Therefore, their properties can be selectively adjusted by varying possible substituents of the organic ligands which makes them interesting for various applications.[11] The first CP was reported by Hofmann and Küspert, while Powell *et al.* revealed its structure.[12] Metalorganic frameworks (MOFs) form one subcategory of spatial CPs.[13] These are porous hybrid materials with a metal-coordination bond between the inorganic units and the organic ligands, which results in three-dimensional structures.[14] In

1995, O. M. Yaghi shaped the term MOF essentially.[15] A zinc based MOF (MOF-5) with Zn_4O units, which are connected by linear 1,4-benzenedicarboxylate linkers forming a cubic network was reported by O. M. Yaghi *et al*. The core of the cluster is composed of a single oxygen atom which is bound to four zinc atoms resulting in a Zn_4O tetrahedron. On each edge of the tetrahedron a carboxylate group is coordinated leading to a $Zn_4(O)(CO_2)_6$ cluster. This structure exhibits a high stability despite desolvation and temperatures of 3008 °C, which makes it an applicable material for gas storage.[16] Various coordination geometries such as tetrahedral, trigonal bipyramidal, square pyramidal and octahedral are possible geometries for the d^{10} metal zinc(II). Therefore, it can be applied for the synthesis of various CPs.

Some fluorescent supramolecular coordination compounds of palladium and platinum were previously examined using a dipyridine ethinyl ligand system and its derivatives holding a variety of functional groups such as NH_2 or COOH. The pyridine moieties always participated in the coordination, which enables the formation of metallocages.[4, 17] So the aim of this work was to investigate the suitability of this ligand system and some of its derivatives (NH_2, NHBoc, $NBoc_2$) for the potential generation of a fluorescence maintaining metallocage in combination with $Zn(OTf)_2$ as zinc(II) compound bearing in mind the feasible formation of a CP as a consequence of its several possible coordination modes compared to Pd(II) and Pt(II). The obtained products were characterized by single crystal X-ray diffraction and their stability was examined at various temperatures.

2. Results and Discussion

2.1 Reaction of the Ligands **1**-**4** with $Zn(OTf)_2$

The rigid bis-monodentate dipyridine ethinyl ligand **1** and its derivatives **2**-**4**, which were previously reported [4, 7c, 18] were reacted with $Zn(OTf)_2$ in acetonitrile. To begin with, ligand **1** was prepared without an *exo*-functionalization at the central aromatic system (see position X, Scheme 1) and was converted with $Zn(OTf)_2$ in CH_3CN. The aim was to get further insight into the reaction behavior of this unfunctionalized ligand with a zinc compound. Though, according to ^{1}H-NMR spectroscopy the conversion of ligand **1** with $Zn(OTf)_2$ did not lead to the formation of a defined product. In case of the formation of a complex or a cage, significant shifts of signals would have been possible to observe. As a consequence of this result several functional groups at the central aromatic system were introduced to this ligand system.

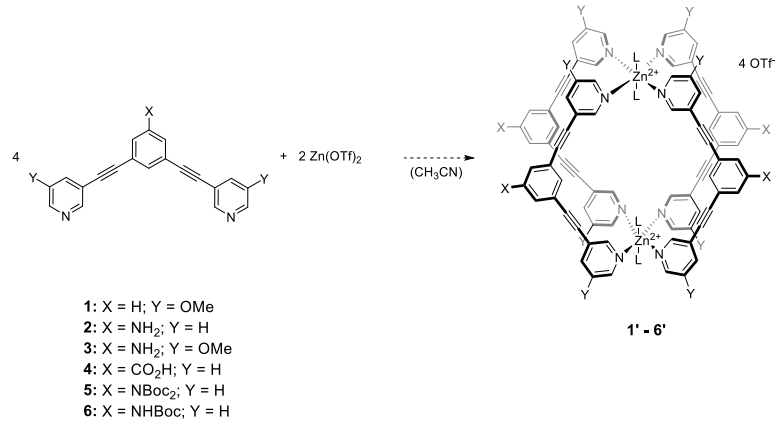

Scheme 1 Conversion of dipyridine ethinyl ligands **1**-**6** with zinc and the proposed structure of a supramolecular coordination cage (SCC). L corresponds to additional axial coordinated molecules such as solvents, water, counterions.[1]

In the next step, an amine group was incorporated at the central aromatic system resulting in ligand **2**. This ligand exhibits a good solubility in dipolar aprotic solvents. A Sonogashira cross-coupling reaction was used to synthesize the ligand after a literature procedure.[17b] After **2** was dissolved in acetonitrile, this solution was added to a solution of 0.5 equivalents of $Zn(OTf)_2$ in CH_3CN generating the precipitation of a light yellow solid within a few minutes. In Figure 1 the ^{1}H-NMR spectra of the time-dependent reaction development of **2** in CD_3CN during the reaction with $Zn(OTf)_2$ are depicted. Instantly after combining the solutions, a signal shift in the ^{1}H-NMR spectrum was observed. The first spectrum (red) is the spectrum of the pure ligand before the addition of the zinc salt. The second spectrum (green) was measured immediately after the addition of the zinc species and the third spectrum (blue) was detected after a reaction time of one hour at 25 °C. The fourth spectrum (purple) shows the signals of the isolated precipitate. After adding the zinc salt, the signal at 4.50 ppm of the free NH_2 group cannot be detected anymore in the ^{1}H-NMR spectrum. In comparison to the free ligand, the peaks of the protons, especially those adjacent to the coordination sites H_d and H_g, were significantly shifted to higher field. This is in contrast to the formation of a cage, in which these signals would have been shifted downfield as

previously reported for the Pd(II) and Pt(II) compounds.[7c-e] There were no additional signals observed during the further reaction. The formation of a defined species is indicated after these results, but not of a cage. Strikingly, the results of the elemental analysis of the obtained light yellow solid corresponded with a composition of $[Zn_2(\mathbf{2})_2(OTf)_2]_n$.

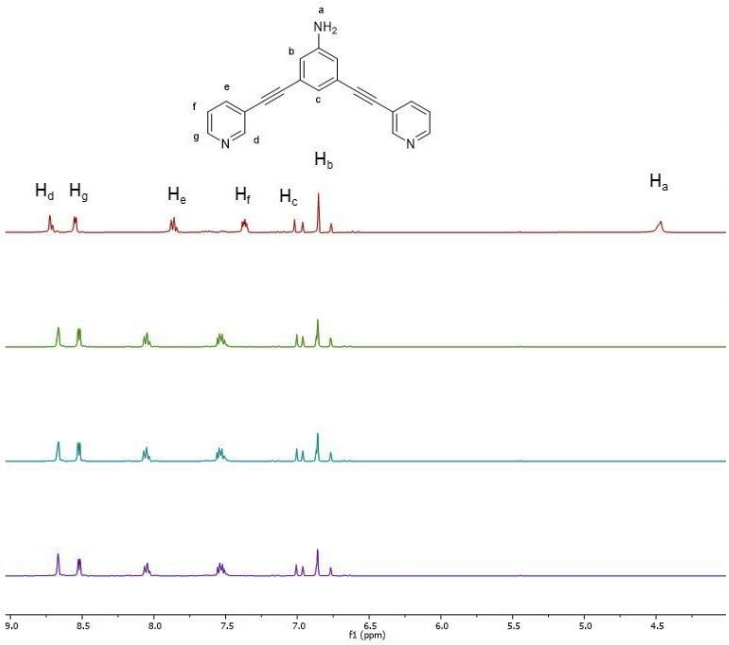

Figure 1 ^{1}H-NMR spectra during the reaction of ligand **2** with 0.5 eq. $Zn(OTf)_2$ in deuterated acetonitrile. Red: **2** before the addition of $Zn(OTf)_2$; green: immediately after combination of **2** and 0.5 eq. $Zn(OTf)_2$; blue: solution of **2** and 0.5 eq. of $Zn(OTf)_2$ in CD_3CN after a reaction time of 1 h at 25 °C; purple: isolated precipitate, see text for details.[1]

It was possible to obtain single crystals suitable for SC-XRD by layering a solution of **2** in acetonitrile with a solution of $Zn(OTf)_2$ in CH_3CN at 25 °C ($\mathbf{2^{Zn}}$). A non-solvable symmetry effect prevented a detailed discussion of the structure. However, the structure revealed the formation of a coordination polymer (CP) and the involvement of the NH_2 groups in the coordination additionally to the pyridine moieties appeared to be beyond doubt (see Figure 6, chapter I.5.1.2). A layer-type structure was observed which might be caused by π-π-interactions of the conjugated systems. By the introduction of additional functional groups with a +π-effect the donor strength of the pyridyl-nitrogen will be enhanced and therefore a coordination between the metal and the pyridyl groups will be favored over the coordination between the metal and a free NH_2 group. This could facilitate the formation of a metallocage. This assumption was examined by incorporating an electron donating methoxy group into the pyridyl moieties leading to ligand **3**. In a subsequent reaction, **3** was converted with $Zn(OTf)_2$ in CH_3CN at 25 °C. The reaction was also analyzed *via* ^{1}H-NMR spectroscopy and showed a similar behavior to the reaction with ligand **2** (cf. Figure 1). After the addition of the zinc salt, the proton signal of the NH_2 group was not observed anymore and the signals of the protons, which are adjacent to the pyridyl-N (H_d and H_g) were shifted to higher field. In consequence, modifying ligand **2** to ligand **3** presumably did again not result in the formation of a cage.

The coordination mode of the ligand system compared to a monodentate amine group was changed by introducing a carboxylic acid functionality at the central aromatic system of the general ligand system leading to ligand **4**. It could potentially also allow for a bidentate coordination mode and a different structure would be obtained. However, ligand **4** exhibited only a poor solubility in acetonitrile, which is why **4** was treated with $Zn(OTf)_2$ in DMF. Even at various temperatures, a precipitation of the product was not observed, which indicated, that an insoluble coordination polymer was not generated. Removing the solvent completely in order to isolate a soluble product might rather lead to a structural change, as it was published for several other coordination polymers.[19] Because there were no significant hints for the creation of a defined product without an amine as functional group, it was maintained in the ligand system for further investigations. Another method of resolution might be to vary the coordination mode of the ligand at the NH_2 position in that way, as the coordination *via* the N-atom will not be allowed anymore. Therefore, the NH_2 group was provided with the sterically demanding protective group *tert*-butylcarbonate (Boc) by reacting **2** with Boc_2O. The assumed π-π-interaction between the aromatic moieties of the ligands will be suppressed due to steric hindrance. This might inhibit the formation of a coordination polymer consisting of several two-dimensional layers as well. For this reason, the ligands **5** and **6** have been synthesized to take advantage of this effect and they were converted with $Zn(OTf)_2$ in acetonitrile. Another important point is, that the Boc groups may participate in coordination of zinc *via* O-atoms thus allowing access to a novel class of coordination polymers.

2.2 Synthesis and Characterization of the Ligands **5** and **6**

The reaction of **2** with di-*tert*-butyldicarbonate (Boc_2O) led to rigid, bis-monodentate pyridyl ligands **5** and **6** (Scheme 2). A subsequent DMAP mediated double amide coupling of **2** with Boc_2O resulted in a colorless solid after it was purified by column chromatography (DCM/MeOH = 99:1). The product revealed a good solubility in acetonitrile. The compounds **5** and **6** were characterized by ^{1}H- and ^{13}C-NMR spectroscopy (see Figures 10 and 11, chapter I.5.2). The di-substituted product **5** as well as the mono-*boc*-substituted product **6** were obtained as indicated by the ^{1}H-NMR spectrum (see Figure 10, chapter I.5.2). Despite the variation of some parameters such as the extension of the reaction time and an increase of Boc_2O, it was not possible to fully convert **6** into **5**. The extremely high chemical resemblance of **5** and **6** are the reason why the compounds are hardly separable by common purification methods. Even though it was unfeasible to separate **5** and **6** no residual free amine could be observed in the respective ^{1}H-NMR spectra. Due to the high steric demand both compounds suppress the coordination *via* the N-atom. For this reason, the inseparable mixture of **5** and **6** was used in further reactions with $Zn(OTf)_2$.

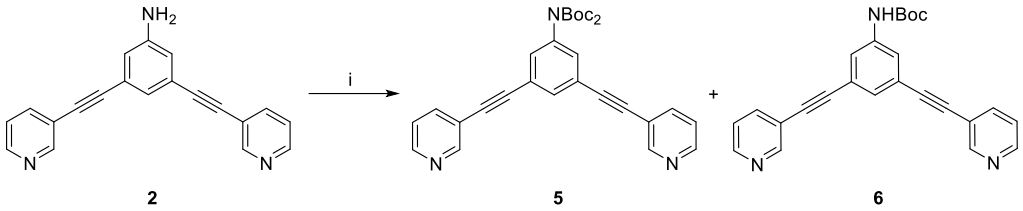

Scheme 2 Synthesis of the Boc protected dipridine ethinyl ligands **5** and **6**. Reagents and conditions: i) Boc_2O, [DMAP], (CH_3CN), room temperature, overnight. Boc_2O = di-tert-butyldicarbonate, DMAP = 4-N,N-dimethylaminopyridine.[1]

2.3 Treatment of the Ligands **5** and **6** with $Zn(OTf)_2$

The conversion of the ligand mixture **5** and **6** with $Zn(OTf)_2$ in acetonitrile resulted in different quantitative temperature dependent ligand transformations, as depicted in Scheme 3. Hence, beginning with a mixture of **5** and **6** three different coordination polymers $\mathbf{2}^{Zn}$, $\mathbf{5}^{Zn}$ and $\mathbf{6}^{Zn}$ were isolated and crystallized. The ligand transformation of **5** and **6** was conducted with 0.5 equivalents of $Zn(OTf)_2$ in CH_3CN at various temperatures. When the reaction was conducted at a temperature of 5 °C the colorless product $\mathbf{5}^{Zn}$ precipitated. At 25 °C the selective mono-deprotection of ligand **5** of the reaction mixture with **5** and **6** to ligand **6** slowly occurred. With increasing the temperature to 70 °C, the selective mono-deprotection to **6** could be completed within less than one hour by either starting from the mixture **5** and **6** or from the isolated CP $\mathbf{5}^{Zn}$. It was possible to obtain colorless prism-shaped single crystals of $\mathbf{6}^{Zn}$ suitable for SC-XRD upon slow reaction over three weeks at room temperature without stirring. The product $\mathbf{6}^{Zn}$ was not soluble in acetonitrile and a decomposition to **6** was observed when it was dissolved in the strongly coordinating solvent DMSO. The reaction mixture of **5** and **6** was refluxed in presence of $Zn(OTf)_2$ in CH_3CN which also resulted in the complete deprotection and the formation of amine ligand **2** and therefore the previously mentioned coordination polymer $\mathbf{2}^{Zn}$.

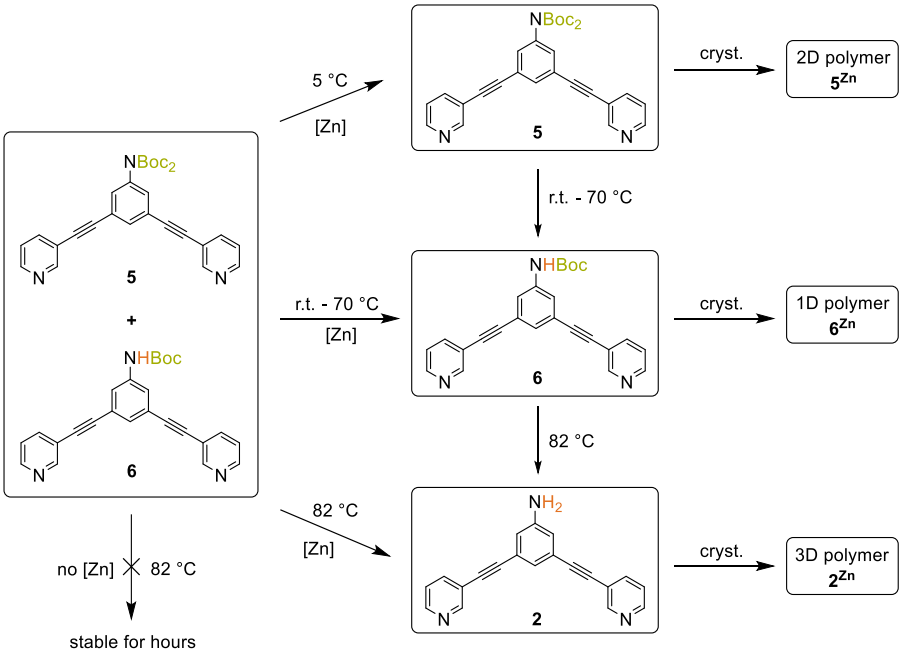

Scheme 3 Different reaction behavior of ligand mixture **5** and **6** in CH_3CN in presence of 0.5 eq. of $Zn(OTf)_2$, ([Zn]), subject to the reaction temperature.[1]

Therefore, the separation of **5** and **6** was realized by temperature dependent conversion with $Zn(OTf)_2$ to selectively receive the di-*boc*-substituted and the mono-*boc*-substituted products $\mathbf{5}^{Zn}$ and $\mathbf{6}^{Zn}$, respectively. Though, an easier separation of the mixture **5** and **6** just by heating the mixture without zinc showed no conversion from **5** to **6**, preventing a simpler method. Product $\mathbf{5}^{Zn}$ could not be dissolved in common organic solvents, except for the strongly coordinating DMSO. However, this resulted in the decomposition of the CP followed by reformation of free ligand **5** as shown by ^{1}H- and ^{13}C-NMR spectroscopy, which revealed a good solubility in CD_3CN (see Figures 12 and 13, chapter I.5.2).

2.4 Single crystal X-ray Analysis

2.4.1 2D Coordination Polymer $\mathbf{5^{Zn}}$

A two-dimensional layer coordination polymer with an unprecedented coordination for Zn(II) in monoclinic space group C 2/c was exhibited for $\mathbf{5^{Zn}}$. A slightly distorted octahedral [ZnN_2O_4] coordination sphere was observed, in which each Zn(II) ion is chelated by two Boc-protecting groups of one **5** molecule and two pyridyl-N-atoms of another ligand molecule. The latter are standing in *cis*-position, while the axial positions are occupied by two monodentate triflate anions. This is so far the first structural report in which an $N(Boc)_2$ moiety acts as a chelator for Zn(II) as well as the first example for an $N(Boc)_2$ group chelating a metal cation within a CP. Table 1 lists selected bond lengths and angles.

Table 1 Selected bond lengths [Å] and angles [°] data for $\mathbf{5^{Zn}}$.[1]

	Bond length [Å]		**Bond angle [°]**
Zn1-O1	2.076(2)	$O1^{\#1}$-Zn1-$O1^{\#2}$	82.4(1)
Zn1-O3	2.142(2)	O1-Zn1-O3	83.96(8)
Zn1-N1	2.094(2)	O1-Zn1-N1	91.55(8)
N2-C8	1.452(2)	N1-Zn1-$O3^{\#1}$	92.0(1)
N2-C12	1.391(3)	N1-Zn1-$O3^{\#2}$	88.3(1)
C12-O2	1.35(1)	$C12^{\#1}$-Zn1-$C12^{\#3}$	123.1(3)
C12-O1	1.224(3)	C8-N2-C12	118.5(2)
O2-C13	1.506(7)		

A planar conformation with a torsion angle of 0 ° is exhibited by the Boc_2-protected N2-atom and the attached C-atoms. This indicates a sp^2-hybridization. It was noticed, that the bond lengths N2-C12 and C12-O2 are in between a single and double bond range, which is attributed to resonance stabilization. Although opposite charges and hence attractive Coulomb interaction are existent, the bond lengths from zinc to the carbonyl-oxygens of the protective group Zn1-O1 are shorter than from the metal cation to the triflate anions Zn1-O3. The formation of a sterically and electronically beneficial 6-membered ring is the reason, why the comparatively strong bond to the chelating ligand is preferred. Additionally, an overlap of the C=O-LUMOs (π*) geometrically enables a π-backbonding from electron rich d^{10}-cation Zn(II) to the boc-carbonyl moiety. Because the *trans*-standing pyridine donors are twisted, a significant backbonding is not allowed. For this reason, they can primarily act as σ-donors, and therefore strengthening the backbonding to the protective group *via trans*-effect (see Figure 2). There is a twist around the C≡C-triple bond by 63.7 ° for the heteroaromatic rings in **5** and therefore the ligand is

arranged in a zig-zag-like manner to chains in which the particular molecules are connected *via* Zn(II) atoms. The $NBoc_2$ moiety is of a planar structure and stands almost perpendicular to the central aromatic ring system. Additionally, the chain is connected to another one sideways, leading to a corrugated two-dimensional layer. The layers are stacked offset in an ABAB-sequence with small, empty channels along the *a*- and *c*-axis.

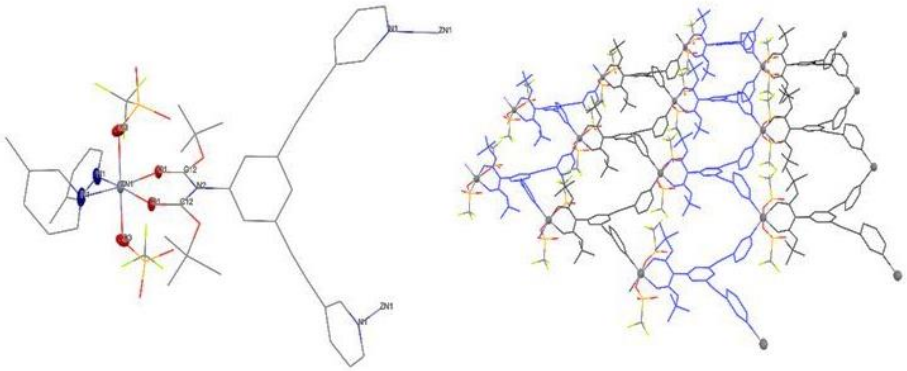

Figure 2 ORTEP-style representation of coordination sphere of Zn(II), all other atoms are represented as wireframe for clarity. Thermal ellipsoids are shown at 50 % probability level (left). Wireframe representation of layer structure of $\mathbf{5}^{Zn}$, molecules colored in blue and black alternating for clarity (right).[1]

2.4.2 1D Coordination Polymer $\mathbf{6}^{Zn}$

During the reaction of ligand mixture **5** and **6** with 0.5 equivalents of $Zn(OTf)_2$ in acetonitrile over a period of three weeks needle-shaped single crystals of the compound $\mathbf{6}^{Zn}$ suitable for SC-XRD were obtained. The single crystal X-ray diffraction analysis revealed that the formation of a chain coordination polymer with an unprecedented layer structure in the triclinic space group *P* -1 (Figure 3) took place. Furthermore, it can be seen that every “chain link” consists of two ligand molecules **6**. These coordinate one Zn(II) ion at a time *via* each pyridyl-N atom equatorially in *cis*-position. In axial positions, each Zn(II)-center is coordinated by two triflate ligands. There are two equatorial positions remaining at the metal ion. These connect the described chain to the next link. A distorted octahedral $[ZnN_4O_2]$ coordination sphere is exhibited for Zn(II). The bond lengths of Zn-N and Zn-O are usually found in a range between 2.12-2.27 Å, the angles between 88 and 92 ° and are thus almost rectangular.

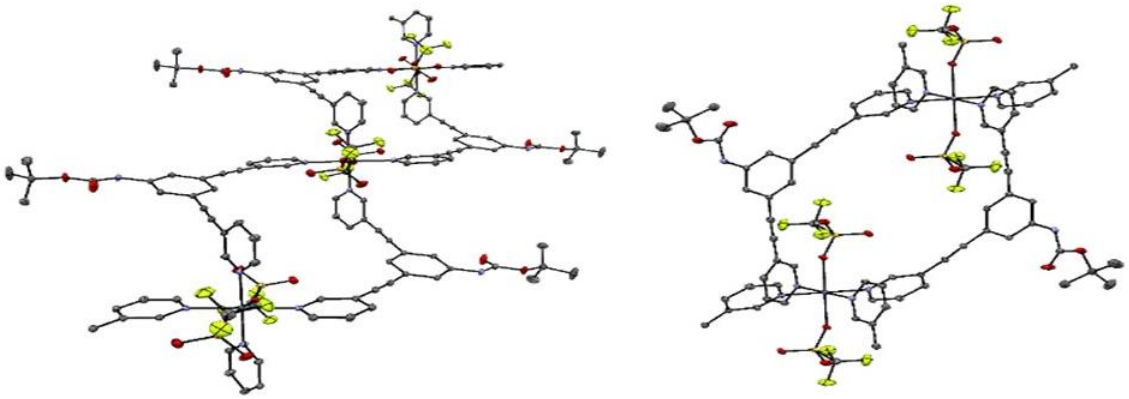

Figure 3 ORTEP-style representation of left: chain-like structure of **6^{Zn}**; right: one isolated "chain link". Ellipsoids shown at a 50 % probability level and hydrogen atoms are omitted for clarity.[1]

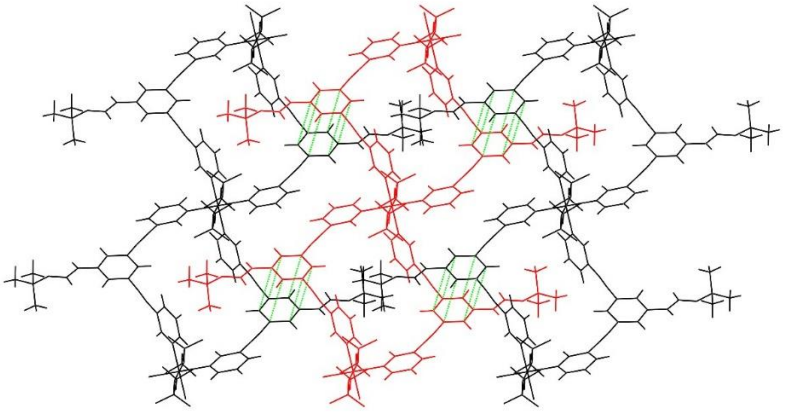

Figure 4 Scale-like accumulation chains in **6^{Zn}**. The chains are colored in black and red alternating for clarity, while their interactions are illustrated using green dashed lines. An enlarged version of this figure can be found in chapter I.5.1.2 as Figure 8.[1]

There is a twist for one of the heteroaromatic rings in **6** around the C≡C-triple bond by 85.6 °, the other one is almost coplanar with the central aniline moiety (the angle was calculated between planes through each aromatic ring). The coordination geometry and the twisted ligand conformation are reasons why the chains exhibit a zig-zag-like structure. The polymers are aligned in a parallel manner and the neighboring aniline aromatic rings are stacked with a distance of 3.25 Å, which imply π-π-interactions (the distance was calculated between planes through each aromatic ring). Because the Boc-moieties point outwards each chain, they are found in the adjacent chain's interstice between the two ligands. Figure 4 shows this intermeshed assembly leading to a yet unprecedented structure. It can be seen that a densely packed coordination polymer follows from the fact that the layers align offset in (*a*+*b*),*c*-orientation (see Figure 5).

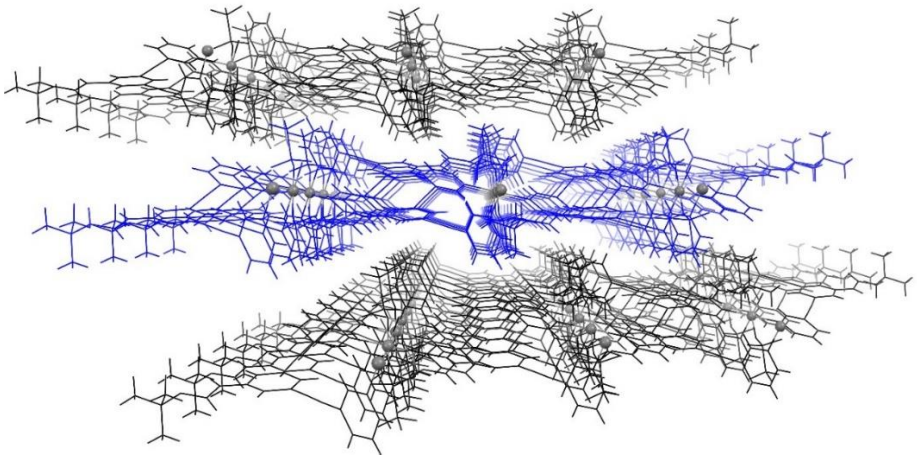

Figure 5 Stacking of the layers in coordination polymer **6^{Zn}**, view in (a+b+c)-direction. The layers of the CP are colored in black and blue alternating for clarity. An enlarged version of this figure can be found in chapter I.5.1.2 as Figure 9.[1]

3. Conclusion and Outlook

In this work the literature known ligands **1**-**4** were reacted with $Zn(OTf)_2$ in acetonitrile in order to get an insight into their reaction behavior towards zinc and to see whether a cage structure or a coordination polymer is formed. The first results showed that only the amine substituted ligand **2** led to a defined structure ($\mathbf{2^{Zn}}$) with a pyridine coordination. The coordination *via* the pyridine moiety was prevented by introducing the sterically demanding protective Boc group at the backbone of the ligand at the NH_2 moiety. The synthesis and characterization of the ligands **5** and **6** beginning with the rigid ligand **2** and Boc_2O in acetonitrile were described, leading to a mixture of the ligands **5** and **6**. The mixture could not be separated by common purification methods. But the separation and isolation of the mono-*boc*-substituted species (**6**) from the di-*boc*-substituted one (**5**) was enabled by the time and especially temperature dependent reaction with $Zn(OTf)_2$ in CH_3CN, yielding the novel coordination polymers $\mathbf{5^{Zn}}$ and $\mathbf{6^{Zn}}$. Single crystal XRD measurements showed for $\mathbf{6^{Zn}}$ a one-dimensional coordination polymer with a layer structure, while $\mathbf{5^{Zn}}$ exhibits a two-dimensional layer structure, with the $NBoc_2$ moiety as a chelator for Zn(II). So far, this is the first structural report about a $NBoc_2$ group chelating a metal within a coordination polymer. Further studies could be conducted concerning a better reaction controllability which is linked to a more selective formation of the di-*boc*-substituted species (**5**). Other properties of these compounds, which would be interesting to further investigate, are for example their behavior towards higher temperatures or pressure. Differential scanning calorimetry or thermogravimetric analysis are important methods to examine the thermal stability of the compounds and in order to see up to which temperature the Boc groups will be firmly bound. Measurements according to the Brunauer-Emmett-Teller theory could give information about the size of the surface of these porous solids and also about the accessibility of the pores and the Lewis acidic zinc centers in particular. These are important parameters for possible applications in the fields of gas storage or heterogeneous catalysis.

4. Experimental Section

4.1 General Remarks

All chemicals were purchased from commercial sources and were used without further purification. The solvents were either distilled prior to use or obtained from a *M. Braun* Solvent Purification System (SPS-800). The *Sonogashira* cross-coupling reaction is carried out under argon atmosphere using standard Schlenk techniques. Unless otherwise stated, chromatographic separations were performed using silica gel (63 – 200 µm). Compounds **1**-**4** were prepared according to previously published methods.[4, 7c, 17b, 18]

NMR spectra were recorded with a *Bruker* Avance Ultrashield 400 MHz and a *Bruker* AV 500C QNP Cryo at a temperature of 298 K unless otherwise stated. All ^{1}H and $^{13}C(^{1}H)$ chemical shifts δ are reported in parts per million (ppm), with the residual solvent peak serving as internal reference. Abbreviations for NMR multiplicities are: singlet (s), doublet (d), triplet (t), and multiplet (m). Coupling constants *J* are given in Hz.

Elemental analysis was measured at the Microanalytical Laboratory of the Catalysis Research Center at the Technical University of Munich. The elements C, H, and N were determined with a combustion analyzer (EURO EA-CHNS, *HEKAtech*) and are given in mass percentages.

Heated electrospray ionization mass spectrometry measurements were conducted with a Dionex Ultimate 3000 UHPLC focused chromatography system, connected with a Thermo Scientific LCQ Fleet mass spectrometer.

4.2 Synthetic Procedures

4.2.1 Synthesis of Ligands **5** and **6**

Di-*tert*-butyldicarbonate (203.21 mg, 930.13 µmol, 2.7 eq), *N,N*-dimethyl-4-aminopyridine (8.27 mg, 67.72 µmol, 0.2 eq) and compound **2** (100.00 mg, 338.95 µmol, 1.0 eq.) are dissolved in 30 mL dry acetonitrile in an argon atmosphere. After stirring the reaction mixture for 24 h at room temperature it is concentrated to small volume under reduced pressure. The crude product is purified by column chromatography (DCM/MeOH = 99:1) leading to a mixture of ligand **5** and **6** as a colorless solid in an approximate ratio of 60:40 (100.00 mg, 201.80 µmol, 60 %).

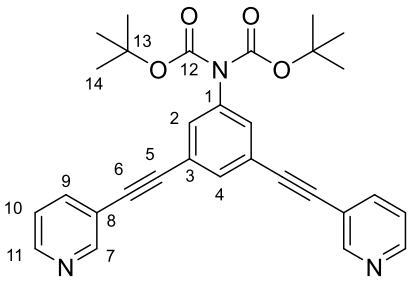

5
M = 495.58 g/mol

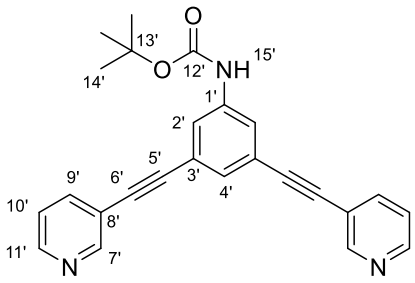

6
M = 395.46 g/mol

4.2.1.1 *N,N*-bis(*tert*-butoxycarbonyl)-3,5-bis[(pyridin-3-yl)-ethinyl]aniline (**5**)

^{1}H-NMR (400 MHz, CD_3CN): δ = 8.76 (s, 2H, H^{7}), 8.58 (d, ^{3}J = 4.8 Hz, 2H, H^{11}), 7.92 (d, ^{3}J = 7.9 Hz, 2H, H^{9}), 7.70 (t, ^{4}J = 1.4 Hz, 1H, H^{4}), 7.45 (d, ^{4}J = 1.4 Hz, 2H, H^{2}), 7.39 (dt, ^{3}J = 3.9 Hz, 2H, H^{10}), 1.43 (s, 18H, H^{14}).

^{13}C-NMR (101 MHz, CD_3CN): δ = 155.7 (C^{12}), 153.0 (C^{7}), 150.3 (C^{11}), 142.1 (C^{1}), 139.5 (C^{9}), 136.5 (C^{4}), 132.7 (C^{2}), 127.5 (C^{3}), 124.4 (C^{10}), 108.8 (C^{8}), 103.0 (C^{5}), 91.0 (C^{6}), 82.1 (C^{13}), 28.1 (C^{14}).

DC: R_f = 0.59 (DCM/MeOH = 7:1).

4.2.1.2 *N*-(*tert*-butoxycarbonyl)-3,5-bis[(pyridin-3-yl)-ethinyl]aniline (**6**)

^{1}H-NMR (400 MHz, CD_3CN): δ = 8.78 (s, 1H, $NH^{15'}$), 8.76 (s, 2H, $H^{7'}$), 8.58 (d, ^{3}J = 4.8 Hz, 2H, $H^{11'}$), 7.92 (d, ^{3}J = 7.9 Hz, 2H, $H^{9'}$), 7.75 (t, ^{4}J = 1.4 Hz, 1H, $H^{4'}$), 7.53 (d, ^{4}J = 1.4 Hz, 2H, $H^{2'}$), 7.39 (dt, ^{3}J = 3.9 Hz, 2H, $H^{10'}$), 1.49 (s, 9H, $H^{14'}$).

^{13}C-NMR (101 MHz, CD_3CN): δ = 155.7 ($C^{12'}$), 153.0 ($C^{7'}$), 150.3 ($C^{11'}$), 144.3 ($C^{1'}$), 139.5 ($C^{9'}$), 136.5 ($C^{4'}$), 132.3 ($C^{2'}$), 127.5 ($C^{3'}$), 124.4 ($C^{10'}$), 108.8 ($C^{8'}$), 103.0 ($C^{5'}$), 91.0 ($C^{6'}$), 85.5 ($C^{13'}$), 28.2 ($C^{14'}$).

4.2.2 Synthesis of the single crystals $\mathbf{2}^{Zn}$, $\mathbf{5}^{Zn}$ and $\mathbf{6}^{Zn}$

4.2.2.1 Synthesis of $\mathbf{2}^{Zn}$

The compounds **2** (2.00 mg, 4.04 µmol, 2.0 eq.) and $Zn(OTf)_2$ (0.73 mg, 2.02 µmol, 1.0 eq.) are dissolved in acetonitrile and the mixture is refluxed for 2 h. Diethyl ether is slowly added at room temperature leading to yellow needle-shaped single crystals after standing for several days. For the composition $[Zn(\mathbf{2})_2(OTf)_2]_n$ a yield of 50 % is obtained.

4.2.2.2 Synthesis of $\mathbf{5}^{Zn}$

A solution of $Zn(OTf)_2$ (0.73 mg, 2.02 µmol, 1.0 eq.) in 0.2 mL CD_3CN is added to a solution of ligand mixture **5** and **6** (2.00 mg, 4.04 µmol, 2.0 eq.) in 0.4 mL CD_3CN at room temperature. After storing the solution at 5 °C overnight the product is obtained as colorless solid. A yield of 45 % is received for $[Zn(\mathbf{5})_2(OTf)_2]_n$.

4.2.2.3 Synthesis of $\mathbf{6}^{Zn}$

A solution of $Zn(OTf)_2$ (0.73 mg, 2.02 µmol, 1.0 eq.) in 0.2 mL CD_3CN is added to a solution of ligand mixture **5** and **6** (2.00 mg, 4.04 µmol, 2.0 eq.) in 0.4 mL CD_3CN at room temperature. The reaction mixture is stored at room temperature. After several weeks, prism-shaped colorless single crystals precipitated. For $[Zn(\mathbf{6})_2(OTf)_2]_n$ a yield of 29 % is received.

5. Supplementary Data

5.1 Single crystal X-ray Structure Determination

5.1.1 General Data

X-ray crystallographic data were collected on different single crystal X-ray diffractometers with the following setups:[20]

1) *Bruker* D8 Kappa APEX II, a fine-focus sealed tube and a *Triumph* monochromator using the APEX2 software package (**5^{Zn}**)
2) a CCD detector (*Bruker* APEX II, κ-CCD), a FR591 rotating anode and a MONTEL mirror optic using the APEX2 software package (**6^{Zn}**)

All measurements used MoK_α radiation (λ = 0.71073 Å). The measurements were performed on single crystals coated with perfluorinated ether. The crystal was fixed on top of a glass fiber or Kapton micro sampler and frozen under a stream of cold nitrogen. A matrix scan was used to determine the initial lattice parameters. Reflections were corrected for Lorentz and polarization effects, scan speed, and background using SAINT.[21] Absorption corrections, including odd and even ordered spherical harminics were performed using SADABS.[21] Space group assignments were based upon systematic absences, E statistics, and successful refinement of the structures. Structures were solved by direct methods (SHELXS) or charge flipping (SHELXT) with the aid of successive difference Fourier maps, and were refined against all data using SHELXL-2014 in conjunction with SHELXLE.[22] Hydrogen atoms were calculated in ideal positions as follows: Methyl hydrogen atoms were refined as part of rigid rotating groups, with a C-H distance of 0.98 Å and $U_{iso(H)} = 1.5 \cdot U_{eq(C)}$. Other H atoms were placed in calculated positions and refined using a riding model, with methylene and aromatic C-H distances of 0.99 Å and 0.95 Å, respectively, other C-H distances of 1.00 Å and $U_{iso(H)} = 1.2 \cdot U_{eq(C)}$. Non-hydrogen atoms were refined with anisotropic displacement parameters. Full matrix least-squares refinements were carried out by minimizing $\Sigma w(F_o^2 - F_c^2)^2$ with SHELXL weighting scheme.[22b] Neutral atom scattering factors for all atoms and anomalous dispersion corrections for the non-hydrogen atoms were taken from *International Tables for Crystallography.*[23] Images of the crystal structures were generated with Mercury.[24] CCDC 1871636 (for **5^{Zn}**) and 1871637 (for **6^{Zn}**) contain the supplementary crystallographic data for this paper. These data can be obtained free of charge *via* www.ccdc.cam.ac.uk/data_request/cif, or by emailing data_request@ccdc.cam.ac.uk, or by contacting The Cambridge Crystallographic Data Centre, 12 Union Road, Cambridge CB2 1EZ, UK; fax: +44 1223 336033.

5.1.2 Detailed crystallographic Data

Table 2 detailed crystallographic data for **5^{Zn}** and **6^{Zn}**.

	Compound 5^{Zn}	**Compound 6^{Zn}**
CCDC	1871636	1871637
Chemical formula	$C_{32}H_{29}F_6N_3O_{10}S_2Zn$	$C_{56}H_{48}F_6N_8O_{10}S_2Zn$
Formula weight [g mol^{-1}]	859.11	1236.55
Temperature [K]	100(2)	100(2)
Wavelength [Å]	0.71073	0.71073
Crystal size [mm^3]	0.074 x 0.114 x 0.293	0.087 x 0.144 x 0.220
Crystal habit	clear colorless fragment	clear colorless fragment
Crystal system	monoclinic	triclinic
Space group	*C* 2/c	*P* -1
a [Å]	12.2927(19)	11.909(3)
b [Å]	25.069(4)	12.217(3)
c [Å]	14.999(3)	12.240(3)
α [°]	90	111.734(11)
β [°]	100.872(9)	117.326(10)
γ [°]	90	91.261(13)
Volume [Å^3]	4539.2(13)	1429.3(7)
Z	4	2
Density calculated [g cm^{-3}]	1.257	1.437
μ [mm^{-1}]	0.705	0.587
F(000)	1752.0	636.0
Θ range for data collection [°]	2.13 to 27.10	1.85 to 33.73
Index ranges (h, k, l)	-15 ≤ h ≤ 15 -32 ≤ k ≤ 32 -19 ≤ l ≤ 19	-18 ≤ h ≤ 18 -19 ≤ k ≤ 19 -19 ≤ l ≤ 19
Reflections collected	27558	59411
Independent reflections	4991 [R(int) = 0.0634]	11400 [R(int) = 0.0414]
Coverage of independent reflections [%]	99.5	99.9
Max. and min. transmission	0.9500 and 0.8200	0.9510 and 0.8820
Data / restraints / parameters	4991 / 112 / 335	11400 / 0 / 380
Goodness-of-fit on F^2	1.062	1.040
Δ/σ$_{max}$	-	0.001
Final R indices (I>2σ(I))	3611data R_1 = 0.0486; wR_2 = 0.1330	9353 data R_1 = 0.0347; wR_2 = 0.0865
Final R indices (all data)	R_1 = 0.0753, wR_2 = 0.1459	R_1 = 0.0469; wR_2 = 0.0918
Largest difference peak and hole [eÅ^{-3}]	0.590 and -0.841	0.611 and -0.404

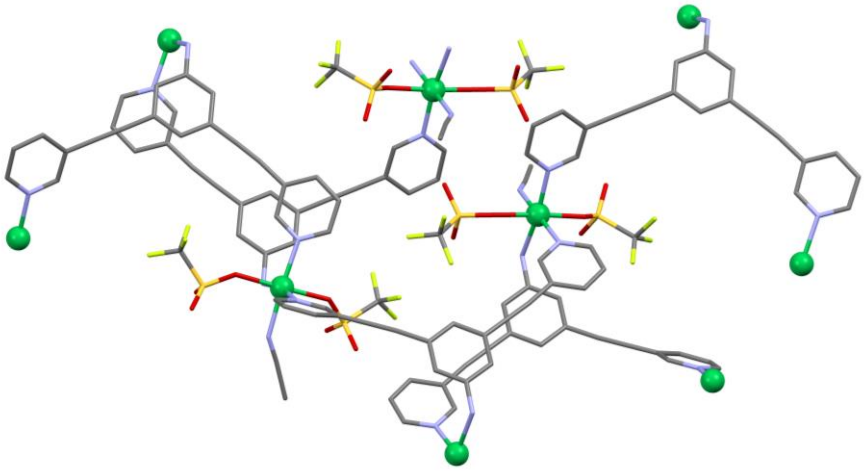

Figure 6 X-ray crystal structure cutout of $\mathbf{2}^{Zn}$. green: Zn; blue: N; yellow: S; red: O; light green: F.[1]

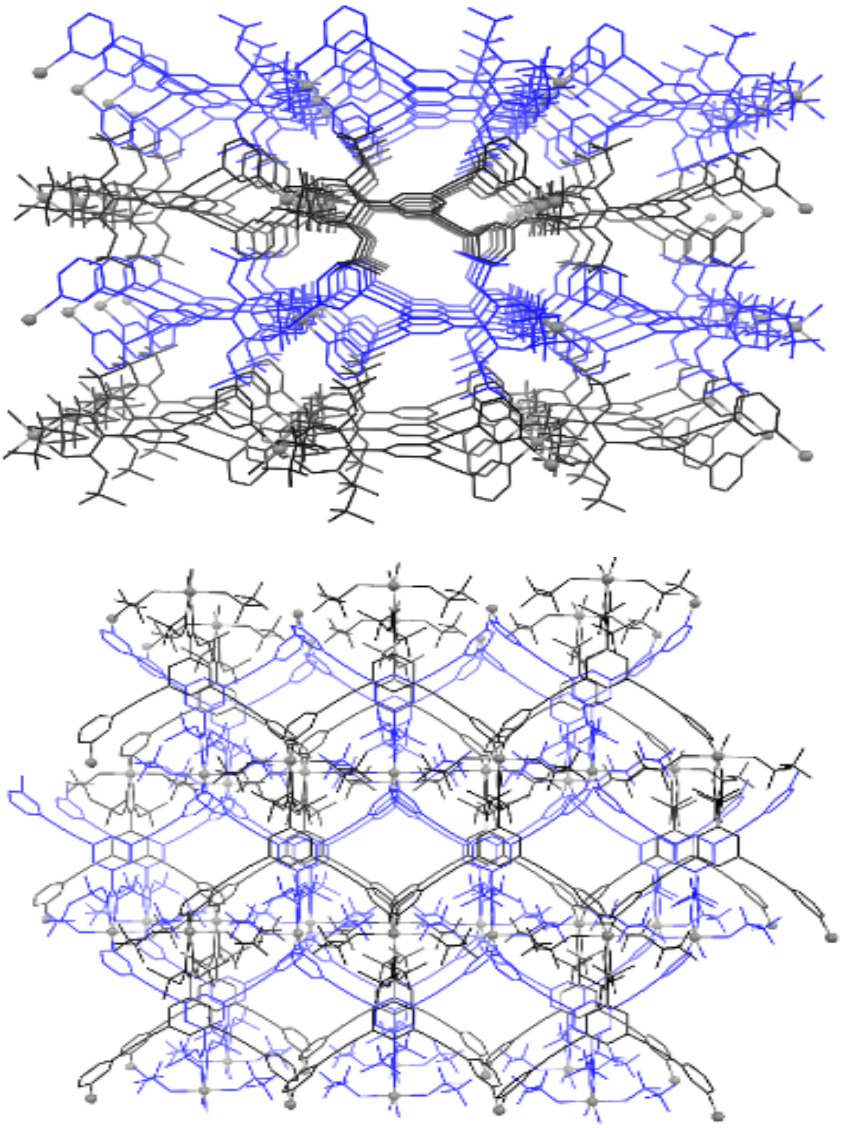

Figure 7 Stacking of the two-dimensional layers in $\mathbf{5}^{Zn}$ along a-axis (top) and c-axis (bottom). The layers are colored black and blue alternating for clarity.[1]

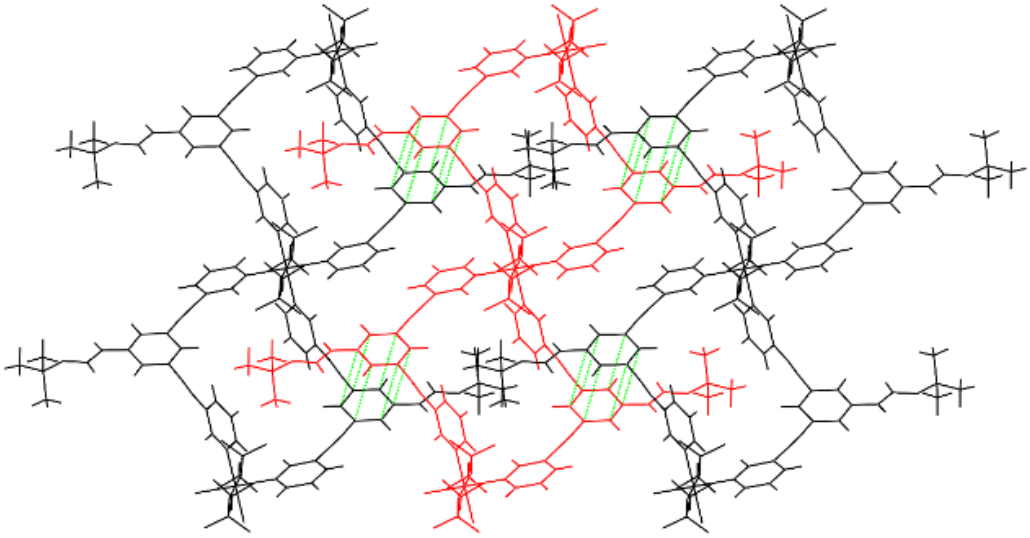

Figure 8 Scale-like accumulation chains in **6^{Zn}**. Chains are colored in black and red alternating for clarity, π π-interactions are illustrated using green dashed lines.[1]

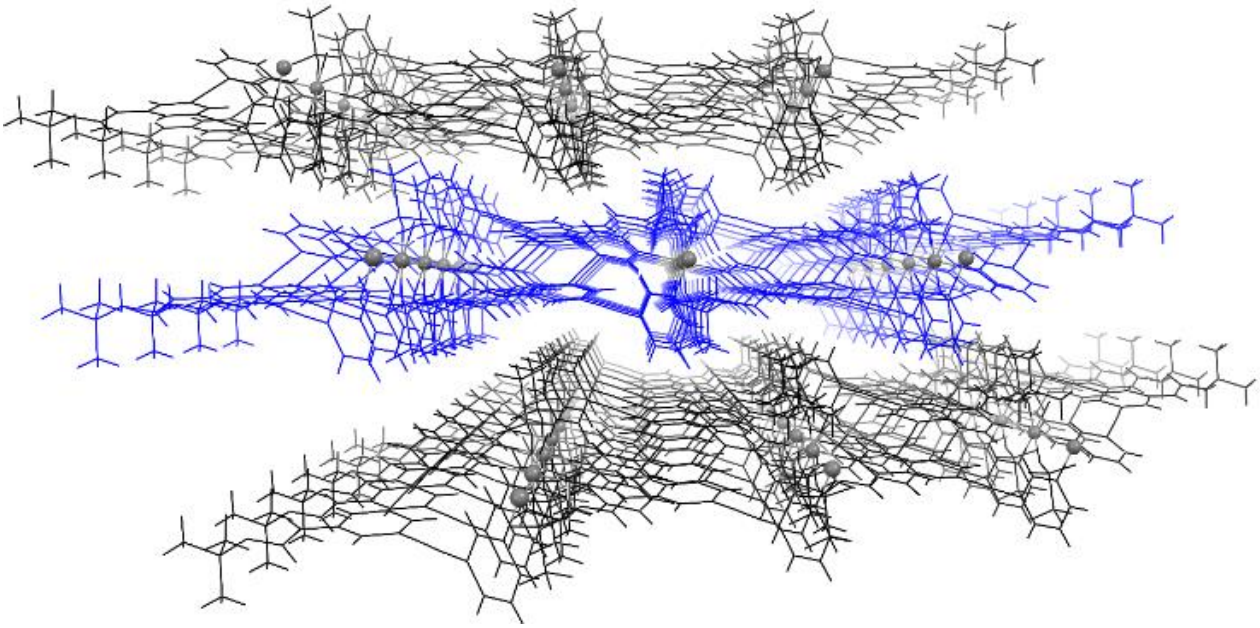

Figure 9 Stacking of the layers in **6^{Zn}**, view in (a+b+c) direction. Layers are colored in black and blue alternating for clarity.[1]

5.2 ^{1}H- and ^{13}C-NMR spectroscopy Data

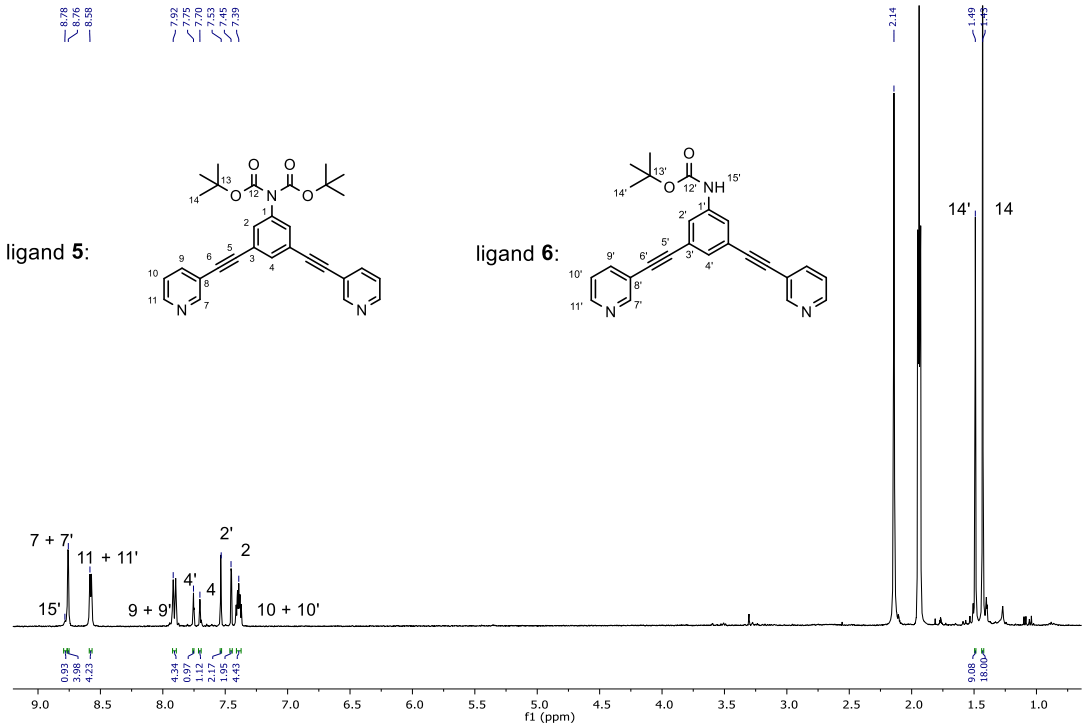

Figure 10 ^{1}H-NMR spectrum of ligand mixture of **5** and **6** in CD_3CN at 298 K.[1]

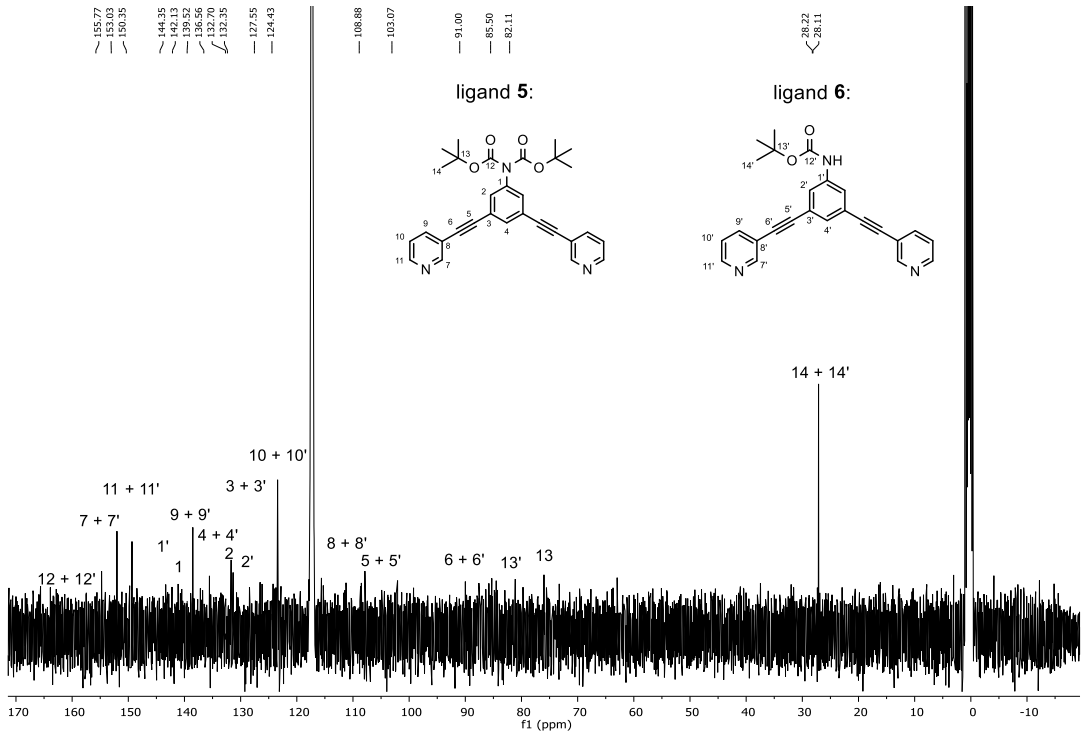

Figure 11 ^{13}C-NMR spectrum of ligand mixture of **5** and **6** in CD_3CN at 298 K.[1]

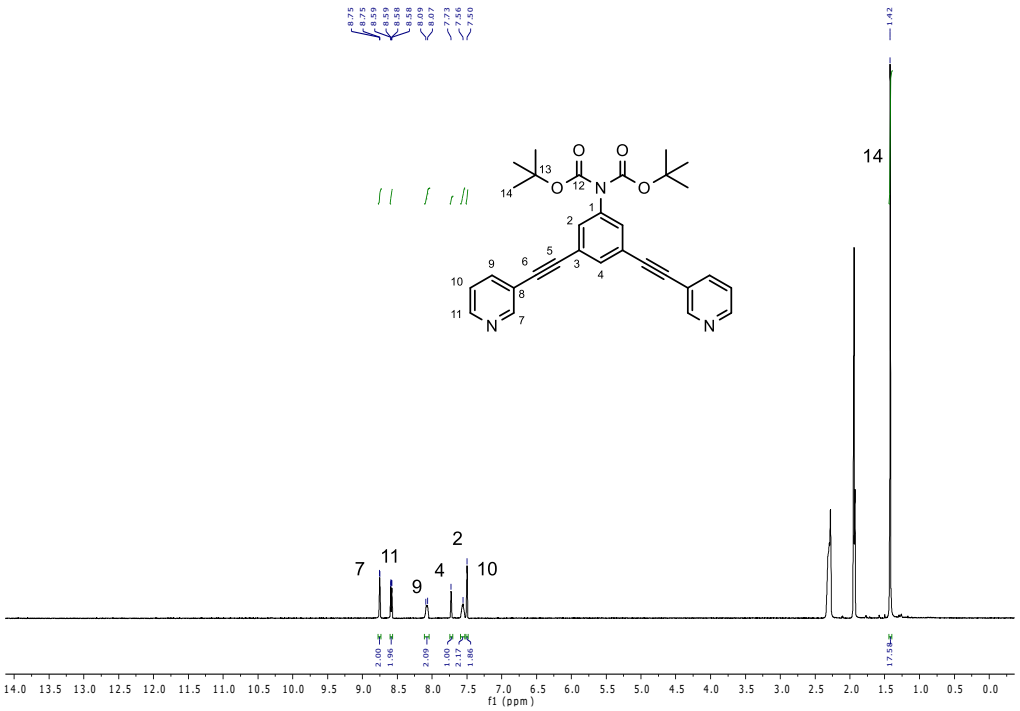

Figure 12 ^{1}H-NMR spectrum of isolated ligand **5** in CD_3CN at 298 K.[1]

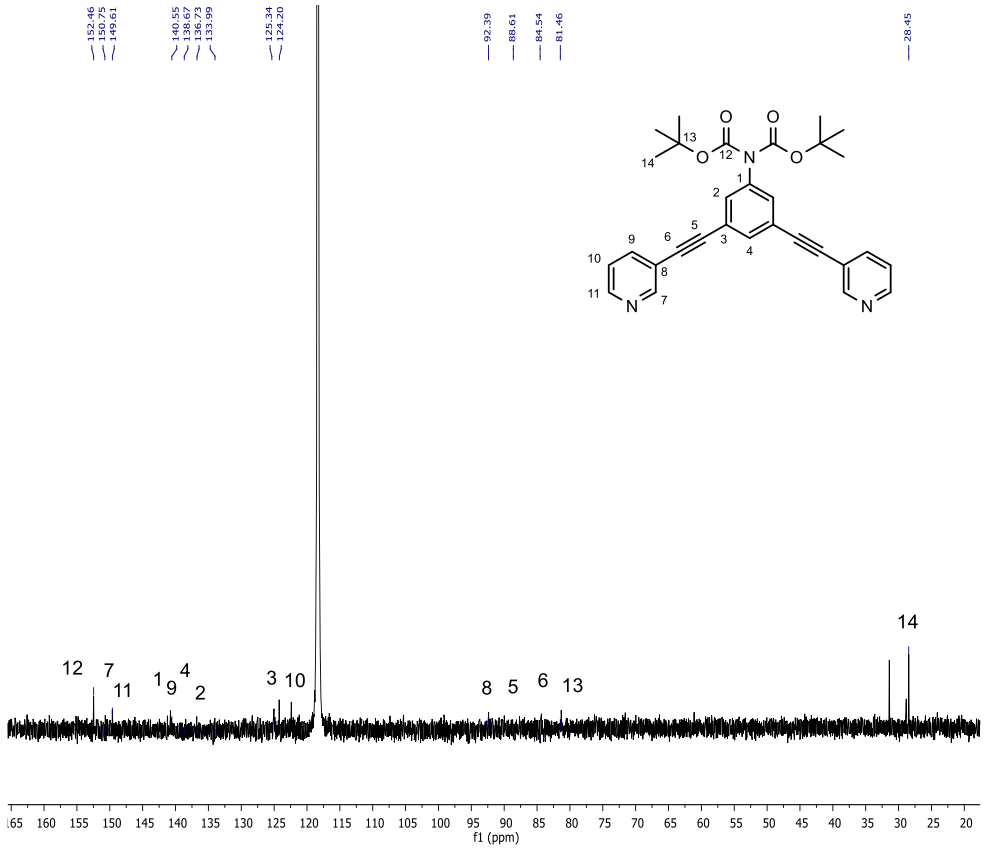

Figure 13 $^{13}C(^{1}H)$ NMR spectrum of isolated ligand **5** in CD_3CN at 298 K.[1]

II. Synthesis and Characterization of new Precursors for the Deposition of Refractory Metals from Ionic Liquids (GALACTIF)

Dieses Kapitel wurde durch das Bundesministerium für Bildung und Forschung (BMBF) finanziell unterstützt.

1. Introduction

1.1 Refractory Metals

There are various definitions concerning the term ‘refractory metal’, but in general, these are ignoble, early transition metals. According to one of the most common definitions five elements belong to this group of metals due to their very high melting point above 2200 °C, namely niobium, tantalum, molybdenum, tungsten and rhenium (Figure 14, dark green shaded metals).[25] A slightly wider definition of this term contains all elements with a melting point above 1850 °C, including amongst others elements like titanium, vanadium and chromium (Figure 14, light green shaded metals). Although the radioactive technetium holds a melting point of 2157 °C, it has never been incorporated into the group of refractory metals.[26] All these definitions list the very high melting point as the only requirement for the metals in order to belong to this group. But there is also a more restrictive definition, which includes the criteria, that the metals must have a body-centered cubic crystal structure and that the ratio of the melting point of the metal oxide to that of the metal itself is less than one.[27] However, the latter properties attract less interest and the very high melting point is listed as the key requirement for the integration of metals to the term ‘refractory metals’ and many applications of refractory metals and their alloys rely on this feature.[27]

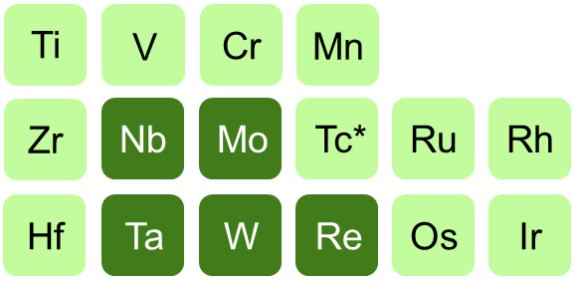

Figure 14 Cutout of the periodic table. dark green: metals with a melting point above 2200 °C (more limiting definition of the term 'refractory metal'); light green shaded: metals with a melting point above 1850 °C (wider definition of the term ‘refractory metal’).

These metals are located in different groups of the periodic table and thus, they exhibit quite different chemical and physical properties. Though there are some characteristics, they have in common. Due to their high melting point, refractory metals have an extremely high thermal stability and a high stability against creep deformation. They show a relatively high density, a high mechanical and tensile strength, a high hardness at room temperature, and a low coefficient of friction. In addition, they possess a particularly good biocompatibility, especially titanium, which makes them remarkably interesting for medical applications. Because refractory metals are chemically nearly inert, they hold a high resistance to corrosion and an elevated persistence against acids and other aggressive chemicals. They are not only extraordinarily resistant to heat but also to water and wear. Since the high melting point is one of the most attractive properties, many applications take advantage of that feature.[27-28]

Many applications in various fields result from the fact, that refractory metals can withstand extreme conditions due to their properties. Their high melting point makes them interesting components for high-temperature applications. For example, tungsten is used in lighting as lamp filaments and molybdenum, as well as tantalum and tungsten, are suitable for vacuum furnace technology. They are also important in industry fields like aerospace, in jet or turbine engines and rocket motors (*e.g*. titanium and niobium), or nuclear industries, *e.g* in fusion reactors because some refractory metals exhibit an excellent resistance to gamma- and neutron radiation. Niobium and some of its alloys with tin or titanium are employed in the physical industry because they exhibit excellent superconducting properties. Refractory metals are also applied in the chemical industry in casting molds, chemical reaction vessels for aggressive environments (*e.g*. tantalum) as tools, in lubricants, or as catalysts. This group of metals also serves very well as alloying additives to improve amongst others the hardenability, the strength, the wear and corrosion resistance and toughness at elevated temperatures of different materials and components. However, it has to be taken into consideration that many applications require a very high quality of the material and this can lead to some difficulties due to the hardness, brittleness and work hardening of refractory metals.[27, 28b-d, 29]

1.2 Electrochemical Deposition

Numerous components can be produced with cheap and good available resources and afterwards they can be functionalized with an appropriate metallic coating. Properties like protection against corrosion or chemical degradation, abrasion or scratch resistance and the electric conductivity can be improved with this functionalization.[30]

Metallic coating of various components can be realized by electrodeposition. During this process, electric current is used to reduce a dissolved metal cation in order to form a coherent metal coating on a surface. The Italian chemist Luigi Brugnatelli established the modern electrochemistry. In 1805, he conducted the first experiments in what is now known as electroplating. But not until the middle of the 20th century important changes arose in the field of electroplating like the use of less toxic plating solutions or an increase in the development of plating for electronic components. The main metals that are deposited commercially are chromium, nickel, gold, silver, cadmium, copper, and zinc together with some alloys of the latter two metals. The whole electroplating industry is based exclusively on aqueous solutions.[28c, 30-31] The metals, which are not listed above, are usually deposited using physical or chemical vapor deposition (PVD or CVD). Many different substrates can be coated with these techniques without being harmful for the environment. But these techniques include high capital investment and it is difficult to prepare uniformly thick coatings, especially for more complicated surfaces.[28c, 31c]

Using aqueous solutions for the electrodeposition holds some advantages, such as the low cost and the non-flammability. The high solubility of electrolytes and metal salts, as well as the high conductivity and the low viscosity are attractive properties. Furthermore, the deposition parameters, *e.g.* the current potential, the composition of the electrolyte, the temperature, or the addition of additives can be adapted and thus, the properties of the materials are modulated easily. But aqueous solutions exhibit some crucial detriments concerning the electrodeposition. One of the major drawbacks, is, that water has a relatively limited potential window. In addition, gas evolution processes can be difficult to manage and can lead to hydrogen embrittlement. With further reaction progress, the metals can form a passivation layer and complexing agents are necessary. Additionally, the generated wastewater might be returned to the water course and many processes are environmentally precarious, like the use of chromic acid for the deposition of chromium.[28c, 30, 31c, 32]

The consequence is that many industrially important metals, like refractory metals and hence resulting materials, cannot be obtained by the electrochemical deposition from aqueous solutions. A change of the reaction medium from aqueous solutions to non-aqueous solutions is necessary in order to gain access to these materials. Polar organic molecules can be used amongst others as non-aqueous solutions. But they tend to strongly coordinate to the metal cations which hinders their reduction. The change to polar organic molecules works for some metals, but these are rather noble metals and there are only few benefits over aqueous solutions. Ionic fluids can be another approach to substitute aqueous solutions. High-temperature molten salts belong to this category, they exhibit most of the advantages aqueous solutions have, and they can overcome most of the limitations of aqueous solutions. But their significant drawback are the high operating temperatures of up to 1000 °C, which are, on the one hand, difficult to realize in an appropriate way and, on the other hand, they restrict the number of applicable substrates. An alternative to high-temperature molten salts are ionic substances that melt at low temperatures, namely ionic liquids. Ionic liquids are molten salts with a melting point below 100 °C and they are composed of organic cations and organic or inorganic anions.[7c, 30, 33] Ionic liquids and the electrochemical deposition from ionic liquids are further described in the chapter 1.3.

1.3 Ionic Liquids

1.3.1 General Aspects of Ionic Liquids

In general, ionic liquids (ILs) are molten salts with a melting point below 100 °C. They are solely composed of organic cations such as substituted imidazolium or tetraalkylammonium ions and organic or inorganic anions, such as $AlCl_4^-$, BF_4^-, PF_6^-, OTf or TFSI. ILs, which are liquid at room temperature, are also called room-temperature ionic liquids (RTILs). The charge on the sterically demanding ions is delocalized which implicates a reduction of the lattice energy and therefore the low melting point compared to conventional salts.[33a]

In 1914, Paul Walden discovered the first room temperature molten salt during the reaction of ethylamine with concentrated nitric acid. The resulting salt, ethylammonium nitrate, exhibits a melting point of 12 °C.[34] In the 1970s and 1980s, Osteryoung *et al.*[35] as well as Hussey *et al.*[36] conducted thorough investigations to room temperature molten salts using the combination of an organic halide and $AlCl_3$. Osteryoung applied *N*-ethylpyridinium bromide/$AlCl_3$ and Hussey used 1-ethyl-3-methylimidazolium chloride/$AlCl_3$ (EMIm Cl/$AlCl_3$). The resulting molten salts based on $AlCl_3$ are now considered as the first generation of ionic liquids. They are rather Lewis acidic and of hygroscopic nature, so these compounds must be prepared and treated under inert gas atmosphere. A technical application is hindered because toxic and corrosive HCl is produced upon occurrent hydrolysis.[32, 35a, 36a] In 1992, Wilkes *et al.* synthesized for the first time molten salts that can be handled under air by combination of organic cations like alkyl-substituted imidazolium cations, *e.g.* EMIm, and anions like tetrafluoroborate (BF_4^-) or hexafluorophosphate (PF_6^-).[37] Subsequent results showed that these anions are subject to decomposition in the presence of water, particularly under elevated temperatures. However, the synthesis results were the basis for further investigations concerning this new field of air- and water-stable compounds and this group is now described as the second generation of ionic liquids.[28c, 38] Kenneth Seddon introduced the term 'ionic liquids' for this new class of molten salts for the first time in 1995.[39] With further progress concerning the synthesis and new insights into this field, other anions were combined with organic cations. Hence, ionic liquids with more hydrophobic anions, *e.g.* trifluoromethane sulphonate (OTf) and bis((trifluoromethyl)sulfonyl)amide (TFSI), were developed. These systems are stable under ambient conditions with only low water uptake and they are described as the third generation of ionic liquids.[40] Due to the manifold combination possibilities of different anions with various substituted cations, there is nearly an unlimited number of ionic liquids. Their physicochemical properties can be selectively adjusted for specific applications by varying their substituents in order to obtain tailor-made ILs. Therefore, it is of particular importance to know a lot about the physical and chemical properties and the structure – properties relationship. There are many various features, which can be differentially strong pronounced for every ionic liquid due to their great spectrum. Though it is necessary to consider, that all of the following properties do not have to be necessarily valid for every ionic liquid.[28c, 32, 41] Some basic properties are summarized in Figure 15.

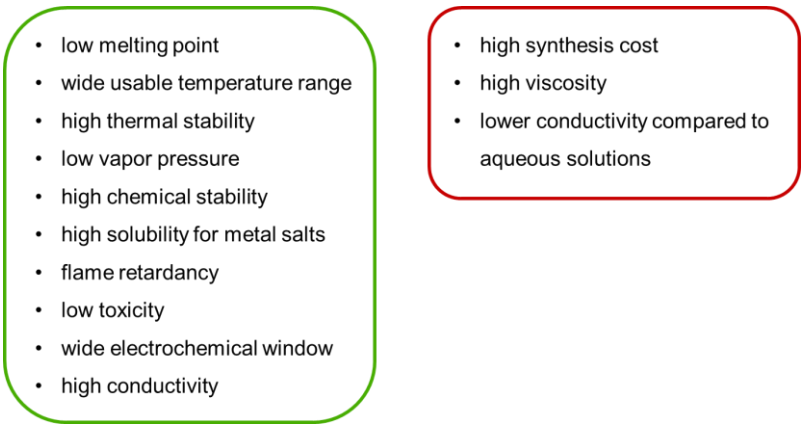

Figure 15 Some basic properties of ionic liquids. Left: advantages of ILs. Right: Drawbacks of ILs.

As aforementioned, ionic liquids are distinct from conventional inorganic salts by their low melting point. It arises because the charge on the large, non-symmetrical cations is delocalized and hence the structural design of the ILs has a direct influence on the electrostatic interactions and weakens the lattice energy resulting in lowering the melting point. But it is still intricate to forecast the melting point of any IL because the complex correlation between structure and phase behavior is not fully understood yet.[28c, 31c] Another important property concerning the temperature is the fact, that they are liquid over a wide temperature range in which work is possible. Many RTILs exhibit a high thermal stability and are in the liquid phase within a range from -50 °C to +250 °C and thus they can be applied properly even at higher temperatures. This is also directly associated with their low vapor pressure. At ambient conditions, their vapor pressure is nearly zero, which is why ILs are considered as non-volatile liquids at normal pressures. But even at higher temperatures, as high as 300 °C, ILs hold an extremely low vapor pressure.[28c, 31c, 32-33, 40b, 42] Further beneficial properties are their high chemical stability and their high solubility for both inorganic and organic materials. Also, ILs are not flammable if they are kept below the thermal decomposition temperature of the organic cations. Ionic liquids are indeed considered as environmentally more friendly solvents due to their lower toxicity compared to some other solvents, but possible long-term toxicities and ecologically damaging impacts are not yet fully evaluated.[28c, 32-33, 40b, 42-43] Key advantages of ionic liquids concerning the electrochemistry are their wide electrochemical window, which can be up to ±5 V vs. NHE and their high conductivity compared to non-aqueous solvents. Although ILs have many beneficial properties, there also are some essential drawbacks. On the one hand they exhibit a relatively high conductivity compared to other non-aqueous solvents, but on the other hand, their conductivity is low compared to conventional aqueous solutions. In addition, most ILs have a viscosity, which is typically 10 to 100 times higher than that of other organic solvents or water as a result of strong electrostatic and other interaction forces. The low conductivity of ILs in comparison to aqueous systems is a direct consequence of the high viscosity. Also, the synthesis of ionic liquids is usually connected with high cost of production.[28c, 31c, 33a, 40b, 42] Some properties, which are key factors for the electrodeposition from ionic liquids, are further exemplified in chapter 1.3.2.

1.3.2 Electrodeposition from Ionic Liquids

The key properties of ionic liquids concerning the electrodeposition from ILs are their low vapor pressure, their high thermal stability, their viscosity, the high solubility of metal salts, the high conductivity compared to non-aqueous solvents and especially their wide potential window. As aforementioned, ILs exhibit an extremely low vapor pressure over a wide temperature range, a high thermal stability, and a non-flammability. Therefore, a deposition process can be safely constructed and ILs can be efficiently applied even at elevated temperatures. In addition, the viscosity and the conductivity are no longer crucial factors at higher temperatures because the viscosity decreases with increasing temperature and therefore the conductivity rises as a direct consequence. The viscosity of ILs usually is in the range of 10 - 500 cP. For most applications low viscosities are favored but it is complex to perfectly design the ionic liquids to that effect because the viscosity is significantly influenced by the structure of both the

cation and the anion, the water content, existing impurities, the chosen synthetic route including starting materials and the measurement method. Ionic liquids based on (substituted) imidazolium cations tend to have a relatively high cation stability and a low viscosity, especially the combination with the bis((trifluoromethyl)sulfonyl)amide anion (TFSI) as well as ILs with trifluoromethane sulphonate anion (OTf). Electrostatic interactions have a big impact on the viscosity which is why ionic liquids are supposed to show a lower viscosity if they consist of larger ions or ions with charge delocalization.[28c, 31c, 32, 41, 44] The possibly most important property of ionic liquids concerning the electrochemical deposition of metals is their wide potential window, which is strongly influenced by different factors, like the water content of the reaction solution, the used electrode material, and the temperature, which makes it difficult to compare different values. Existing impurities, *e.g.* water or halide anions, have to be removed tentatively because they can massively narrow the potential window. The chemical structure of the materials also affects the potential window as well as cathodic and anodic limits of the pure ionic liquids are ascribed to the oxidative decomposition of the anion and the reductive decomposition of the cation, respectively. Most of the ionic liquids with an imidazolium cation and discrete anions have potential windows in the range of 4 – 5 V and are stable against potentials up to -2.2 V. Furthermore, they exhibit an excellent fluidity and conductivity. The cation 1-butyl-3-methylimidazolium (BMIm) is the most favored cation owing to its high conductivity. If imidazolium cations are substituted by an alkyl chain at the carbon atom between the two nitrogen atoms, they will show a wider potential window, but concomitant they show a higher viscosity. ILs with pyrrolidinium based cations have not yet been comprehensively applied in the field of electrochemical deposition, but they are promising cations due to their wide potential window. In addition, piperidinium or aliphatic cations like ammonium or phosphonium, also are very promising cations, because they are very stable to both oxidation and reduction with potential windows of about 5 V. Anions also have an impact on the potential window of ILs. Anions such as BF_4^- and PF_6^- were frequently applied to begin with due to their wide potential window and their stability to reduction, but their slow hydrolysis leads to the release of HF. The avoidance of this severe drawback has led to the rising application of water stable anions such as TFSI. Ionic liquids with the TFSI anion have relatively wide potential windows on different electrodes and they exhibit a high conductivity as well as a low viscosity.[28c, 30, 31c, 32, 33b, 42, 44] Another key property of ionic liquids concerning the electrodeposition is their high solubility for metal salts. This is a beneficial feature as there are many precursors for the electrodeposition of metals which are either not soluble or decompose in water but exhibit a high solubility and stability in ionic liquids. By the avoidance of using aqueous solutions, it is possible to apply water-sensitive substrate materials.[31c, 42]

Thus, using ionic liquids for the electrodeposition instead of aqueous solutions enables to gain access to metals and hence resulting materials, which could not be electrodeposited from aqueous solutions so far. This is especially valid for metals with an extremely negative redox potential, like refractory metals. Moreover, metals which can be deposited from aqueous solutions, can also be electrodeposited from ionic liquids, often with an even better quality, because the metal coatings do not suffer from hydrogen embrittlement using ILs. Hydrogen embrittlement is a severe problem during electrodeposition from aqueous solutions and it is induced by the release of gaseous hydrogen produced during water electrolysis. Since most of the ionic liquids are aprotic, there is only a negligible amount of hydrogen produced during electrodeposition. The application of ionic liquids for the electrochemical deposition

renders possible the easier preparation of alloys and the deposition of new alloys, which have so far been difficult or impossible in water because the redox potentials of metal ions are much closer together in ionic liquids. Despite all the beneficial properties which ionic liquids implicate and all the possibilities which arise from the change of the medium from aqueous solution to ionic liquids, it has to be taken into account, that there are some serious differences between water and ionic liquids. There are differences concerning some basic physical properties like the viscosity, the conductivity, or the potential window. Ionic liquids also are distinct from aqueous systems in the mechanism of the deposition and in the structure of the interface and the elapsing processes at the interface. To some extent, all crucial factors have not yet been identified and fully understood and are the topic of ongoing research in this field of electrochemistry.[28c, 31c, 32, 33b, 40b, 42, 45]

1.4 Electrochemical Deposition of Refractory Metals – State of the Art

Using ionic liquids for the electrochemical deposition enables to gain access to metal coatings with refractory metals which could not be deposited from aqueous solutions. But the change of the medium to ionic liquids works only conditionally for some metals because there are many parameters for all the different metals which have to be considered. The state of the art for the electrodeposition of refractory metals from ionic liquids is described in the following.

1.4.1 Titanium

Coatings with titanium are of great importance due to its many beneficial properties, like the high mechanical and tensile strength, high corrosion resistance, the light weight, and the high compatibility with body tissue, which makes it suitable for medical implants. Furthermore, titanium easily passivates during air contact by forming an oxide layer and the underlying metal layer is well protected against corrosion. Titanium coatings are suitable for different applications in the chemical industry, engineering or for medical implants.[28a, 28b, 29d]

At first, titanium has been deposited from molten salts at temperatures of 450 – 850 °C using melts with mixtures of $TiCl_2$ and $TiCl_3$. But the reaction mixtures with molten salts have been difficult to handle due to the high temperatures and the obtained metal could not have been obtained with high quality owing to occurrent embrittlement.[46] Furthermore, the deposition from aromatic solvents has been conducted using Cu or Ag as additive for facilitated nucleation.[47] Based on these results a change of the medium to ionic liquids has been carried out and deposition experiments have been conducted at room temperature using the air and water stable IL BMIm TFSI and $TiCl_4$ as a source of titanium. But the results could not have been reproduced. Instead of ultrathin titanium layers various polymeric subvalent titanium halide species have been formed. The use of TiO_2 as Ti source and the first generation ionic

liquid BMIm Cl / $AlCl_3$ has led to metallic titanium, but it could not have been characterized sufficiently.[28a, 28c, 38, 48] Also, efforts to obtain thin Ti layers using a different titanium halide as metal source or ILs with other anions than TFSI or other cations have failed.[49] Endres *et al.*[50] investigated the deposition using different titanium halides (F^-, Cl^- and I^-) and varying ionic liquids, namely EMIm TFSI, BMP TFSI and $P_{6,6,6,14}$ TFSI. But instead of elemental titanium non-stoichiometric halides have been formed, amongst others $TiCl_{0.2}$, $TiCl_{0.5}$ and $TiCl_{1.1}$, as evidenced by CV and EQCM measurements. The best result was an ultrathin layer of Ti or $TiCl_x$ with a thickness below 1 nm. The application of an additive such as Li, or (poly)pyrrole[51] did not lead to the desired result either. Au can also be used as an additive and it is an effective nucleating agent for the reduced Ti species, but a stable co-deposit of Ti and Au is formed and the Au cannot be removed from the product afterwards.[52] Applying $Ti(OCH(CH_3)_2)_4$ as titanium source for the deposition from imidazolium based ILs leads to metallic Ti layers, but only the lower lying layers are actually detected as elemental titanium and a bulk deposition could not be obtained.[43] Endres *et al.*[29d] analyzed the changes in the nanostructure at varying Ti-concentrations during the deposition from BMP TFSI. The results show that the concentration of the used titanium precursor, $TiCl_4$, has a strong impact on the interface between electrode and electrolyte. At 0.1 M of $TiCl_4$, there is a multilayered structure at the interface, whereas it is disrupted completely at a concentration of 0.25 M of $TiCl_4$. Furthermore, it is mentioned, that there are different factors which strongly influence the deposition, like the applied potential, the interactions between precursor and IL, the used IL, and the concentration of the precursor. Some of these parameters, such as the interaction between substrate and ionic liquid, the strength of the interactions and their resulting consequences for the other factors, have not yet been fully understood.

In conclusion, the electrodeposition of titanium from ionic liquids is only possible with limitations. Titanium exhibits an overly complex electrochemistry due to the existence of various oxidation states (+2, +3 and +4) in solution. The reduction of the titanium species with possible intermediate steps or stable intermediates has not yet been clearly understood. During the deposition non-stoichiometric subhalides are formed primarily instead of elemental titanium. The obtained layers often have cracks, because the subhalides extremely disturb the formation of homogeneous metal layers. There are also many parameters which interact and influence the deposition, especially the impact on one another is a key point. Some of them, especially the impact on one another, have not yet been fully understood so far. In order to enable a titanium coating, wider electrochemical windows of the ionic liquids are not the only criterion which has to be taken into account.[29d, 50, 52-53]

1.4.2 Vanadium

Vanadium is predominantly used in various industry fields as steel additive. This is based on the fact, that vanadium can form stable carbides and nitrides, and these compounds enhance the strength of the steel and its wear resistance significantly. It is also applied in critical components such as axles or

bicycle frames. There are also some alloys with vanadium which exhibit superconducting properties. Some alloys of vanadium with Al and Ti are used in jet engines or as dental implants.[54]

Although vanadium is an industrial relevant material, there are no published results for its electrochemical deposition from ionic liquids. There is only one work which investigated the electrochemical behavior of V(II) in a first-generation ionic liquid, namely EMIm Cl/$AlCl_3$. It is shown that an Al-V alloy can only be electrodeposited from this melt by addition of the additive EMIm BF_4. Increasing the V content of the alloy was also possible by varying some of deposition parameters.[55]

1.4.3 Niobium

Niobium coatings are often used in electrolytic capacitors, nuclear reactors, or aerospace rocket motors due to its excellent thermal and chemical stability and corrosion resistance. It can be also applied as alloying additive for steel to enhance its strength or in medical implants owing to the good biocompatibility. Niobium and some of its alloys with tin or titanium exhibit very good superconducting properties.[28b, 28c, 29c]

At first, niobium has been deposited from molten salts at temperatures of 550 – 850 °C using different melts such as KF-LiF and KF-NaF[56], LiF-KF-K_2NbF_7[57], or LiCl-KCl and NaCl-KCl[58] and NbF_5 as niobium source. The results have shown, that not until a temperature of 750 °C homogeneous metal layers were deposited and that at temperatures below 650 °C the layers were either not coherent or highly heterogeneous.[58] Although the deposition from molten salts is efficient for Nb, the high operating temperatures and resulting factors such as thermal damage and structural changes of the substrate as well as arising corrosion problems are crucial criteria which have to be taken into consideration. The electrochemical deposition of niobium from BMP TFSI and PMIm TFSI was investigated using NbF_5 as niobium source. Divers characterization methods have shown that the obtained metal layers are rough, cracked and contained residue of the used IL.[59] Giridhar *et al.*[60] examined the deposition from BMP TFSI between room temperature and 170 °C using NbF_5 as niobium source. Besides elemental Nb there were also found oxides of niobium and some non-stoichiometric subhalides. Additives such as LiF or LiTFSI were added to the reaction mixture to improve the quality of the metal layers. Furthermore, the deposition from BMP TFSI has been investigated at temperatures around 125 °C, but in the obtained metal layers was a larger quantity of fluoride.[61] Thin coating of metallic niobium was possible to obtain at 125 °C using BMP TFSI as IL, NbF_5 as niobium source and LiF as additive.[62]

In conclusion, the electrodeposition of niobium from ionic liquids is possible, but the same problems appear as for titanium. Various niobium oxides and oxyhalides are formed during the deposition process, which disturb the formation of homogeneous metal layers. Furthermore, subhalides such as Nb_3Cl_8 can be generated during the deposition. Nb_3Cl_8 can exist in an insoluble form and thus a further reduction of the niobium species to metallic niobium can be prevented.[63]

1.4.4 Tantalum

Tantalum exhibits an extraordinarily high corrosion resistance in a wide range of aggressive media, for which reason it is often applied as material of chemical reaction vessels or pipes where harsh acidic conditions dominate. Coatings with tantalum are also used in various medical fields due to its biocompatibility or in the production of electronic components, especially electrolytic capacitors. Tantalum tends to passivate during air contact by forming an oxide film and the underlying metal layers are well protected against corrosion and other effects.[28c, 29c, 64]

The first results concerning the electrodeposition of tantalum were obtained using various molten salt mixtures, such as LiF-NaF-KF and LiF-NaF-CaF_2, and K_2TaF_7 as tantalum source at temperatures of 650 – 850 °C. As aforementioned, the molten salts have many technical and economic drawbacks and are only hardly appropriate for coating of sensitive materials. Moreover, there are often oxides present in the molten salts which can deteriorate the quality of the coatings significantly due to the formation of oxyfluorotantalates. Their further reduction rather leads to oxides of Ta than to metallic Ta.[64a, 65] The deposition of tantalum from BMP TFSI was investigated using TaF_5 as Ta source on different substrate surfaces and at varying temperatures. Whereas it was possible to deposit ultrathin layers at room temperature, metal layers with a thickness of about 1 µm could be obtained at 200 °C and low electric current. The quality of the deposit could be enhanced by applying LiF as additive and by using temperatures of 150 – 200 °C. But the deposition of tantalum subhalides was observed.[66] Furthermore, fundamental studies towards the deposition of tantalum from BMP TFSI at room temperature were conducted. It was shown that metallic Ta could be obtained at room temperature, if a slow deposition and low potentials are applied. Otherwise, non-stoichiometric subhalides are primarily formed because fluorides are concentrated at the interface. Bulk layers of the deposited Ta still contained traces of the used IL and attempts to deposit thicker metal layers failed.[64b] The electrodeposition from various ionic liquids with a systematic investigation of the different parameters was conducted. It was not successful to deposit good adherent and free of cracks metal layers and most of them still contained residue of the used IL. Elemental Ta layers can be indeed obtained, but they are still rough and there are also oxides and different halide species existent. The uniformity of the layers increased with increasing deposition temperature.[67] A slight improvement for the deposition was observed, when ultrasound was used as additional source of energy.[68]

In conclusion, the electrodeposition of tantalum from ionic liquids is possible, but it is not a straightforward process using ILs, especially at lower temperatures. As already mentioned for titanium and niobium, the formation of oxides and non-stoichiometric subhalides during the deposition process is a major problem and hinders the formation of homogenous metal layers. Under the wrong conditions, mainly subvalent amorphous $[Ta_6Cl_{12}]^{2+}$ species are obtained which can prevent a further reduction to metallic tantalum.[28c, 64b]

1.4.5 Chromium

Chromium is predominantly used in various industry fields such as aircraft industries as alloying material for steel. Using Cr as additive leads to a significant increase in corrosion resistance of the material due to the beneficial properties of chromium. It is also often applied in the surface coating technology because Cr enhances the hardness and the wear resistance of the coated materials. It is also used in the field of decorative coating. Chromium tends to passivate during air contact by forming an oxide film and the underlying metal layers are well protected against corrosion and other external effects.[69]

Initially, chromium coatings are usually electrodeposited from aqueous solutions using a Cr(VI) species. But Cr(VI) exhibits some severe drawbacks like its intense carcinogenicity and toxicity as well as some serious environmental concerns. Therefore, Cr(VI) compounds have to be substituted for less toxic aqueous electrolytes such as Cr(III) species. However, an electrodeposition from aqueous solutions using Cr(III) compounds is hindered or even prevented due to the high stability of Cr(III) complexes in water.[69c, 70] Therefore the reaction medium was changed to molten salts. Chromium was electrodeposited from a eutectic mixture of choline chloride and $CrCl_3 \cdot 6\ H_2O$. The mixture is a deep eutectic solvent with a eutectic composition of 1:2. It was possible to obtain crack-free chromium deposits. The quality of the deposit could be enhanced by using LiCl as additive. Thus, thick, adherent, crack-free and nanocrystalline chromium deposits could be received.[28c, 69b, 71] By changing the eutectic composition to a ratio of 2.5:1 (choline chloride : $CrCl_3 \cdot 6\ H_2O$), there is no need of an additive any more to obtain metallic, crack-free deposits of chromium.[72] The electrodeposition from the ionic liquid BMIm BF_4 was investigated applying $CrCl_3 \cdot 6\ H_2O$ as Cr source. The obtained deposits consisted not only of pure metallic chromium but rather of black chromium, which is a mixture or Cr and chromium oxides with an amorphous or nanocrystalline structure. Some hydroxide species were also formed during the deposition and incorporated into the metal layers. The IL BMIm BF4 seems to be a promising material to replace Cr(VI) baths, due to its high conductivity, relatively low viscosity and wide electrochemical window.[69c, 70, 73] The electrodeposition of a Cr(III) species was also examined from other alkyl-substituted imidazolium ILs with different anions such as Cl^-, Br^- or HSO_4^-. The deposits were nearly amorphous for BMIm Br due to some existing impurities, and a nanocrystalline structure was obtained for the IL BMIm HSO_4. The Cr coatings reveal a better quality if they are conducted at higher potentials. Compact coatings can be obtained using various alkyl-substituted imidazolium ILs with Cl^-, whereby the metal layers from BMIm Cl exhibit a better thickness and hardness.[74]

1.4.6 Molybdenum

Molybdenum is widely used in alloys to improve the creep resistance and the strength at high temperatures. There it is often applied, because Mo is cheaper than superior alloys of its higher homologue tungsten. Furthermore, it is predominantly employed as strengthening alloy of steel to enhance the hardenability, the strength and toughness at elevated temperatures and the wear as well

as the corrosion resistance. Mo can withstand extreme conditions like extremely high temperatures, which makes it suitable for hot metal working tools, as components of high temperature service equipment, as ingredient of heat pipes or electrical contacts or industrial motors.[29b, 29c, 75]

Although molybdenum and its coatings have many important industrial applications, there are only few works concerning its electrodeposition from ionic liquids. The electrodeposition from aqueous solutions has been unsuccessful because molybdenum tends to form oxides rather than elemental Mo.[76] Investigations to deposit Mo from molten salts, like $ZnCl_2$-NaCl-KCl, containing $MoCl_3$ at 250 °C have shown that a dense, adhesive film with a thickness of about 3 µm could only be obtained by using KF as additive.[77] Other molten salts have led to similar results.[78] So far, molybdenum has been deposited in the form of different alloys such as Al-Mo-Ti or Ni-Mo alloys. But these components did not contain more than 49 wt.% of Mo. Different ionic liquids were applied as additive to increase the Mo-content and to improve the quality, but the deposited alloys still exhibited cracks and pits, which reduces their industrial application.[79] The electrodeposition of Mo from BMIm BF_4 was investigated. Amorphous Mo layers could be obtained at temperatures above 150 °C, but they were very brittle. The addition of ethylene glycol enhanced the quality of the deposit significantly and dense, crack-free and more adhesive Mo layers could be obtained at temperatures of 120 – 150 °C.[80]

1.4.7 Tungsten

Tungsten has the highest melting point of all refractory metals and is therefore of great importance for high-temperature applications. It is applied in vacuum furnace technology and as wire filaments in lighting where it increases the efficiency of the lamp. There are many industrial fields in which tungsten and resulting materials are used such as the aerospace or automotive industries or for military applications. Molybdenum and tungsten exhibit an excellent resistance to gamma and neutron radiation which makes them promising materials for fusion reactors. Tungsten can be also used for the production of hard materials like carbides. WC is one of the hardest carbides and is a very efficient electrical conductor and can be also employed to produce wear-resistant abrasives. Alloys of W are used for applications to further improve their high-temperature strength and corrosion resistance such as electric arcs, where a better combustibility can be reached if a W-Th alloy is used.[29e, 32, 81]

Tungsten has been electrodeposited predominantly from molten salts. First investigations used ternary alkalifluoride melts and WF_6 as tungsten source at temperatures of 700 – 850 °C.[82] Then molten salts with other halides such as $ZnBr_2$-NaBr-WBr_5, $ZnCl_2$-NaCl-WCl_6 or $ZnCl_2$-NaCl have been used at 450 °C using different tungsten sources like WO_3, K_2WO_4, WCl_4 or K_2WCl_6 for the latter melt. Deposits of tungsten could be obtained but the formation of various oxochlorotungsten species could be also observed. By using WCl_4 as W source a deposition from $ZnCl_2$-NaCl-KCl melt at 250 °C was possible. The addition of KF improved the quality of the deposit.[83] Furthermore, the deposition from halide-oxide-melts was investigated. Molten salts such as Na_2WO_4-WO_3 or Li_2WO_4-Na_2WO_4-K_2WO_4 were applied at temperatures of 600 – 900 °C. The obtained deposits were partly well-crystallized, compact, and smooth,

but they did not only contain tungsten but also various tungsten oxides. KF as additive could slightly improve the quality of the deposits. The very high temperatures of the deposition are a severe drawback and influence the quality of the substrate negatively.[83c, 84] The electrodeposition from ionic liquids was rather conducted for tungsten containing alloys such as Al-W or Al-W-Mn alloys.[81c, 85] But a first generation like ionic liquid, EMP Cl/$ZnCl_2$, was used to deposit tungsten at 150 °C with WCl_4 as tungsten source and KF as additive. Applying WCl_6 as W source under the same conditions led to a smoother and denser deposit, but the metal layers were still rough and cracked as with WCl_4.[81b]

In conclusion, to date the electrodeposition of refractory metals from ionic liquids is possible, but only for some metals and only with some significant limitations. Some severe drawbacks are the formation of subhalides and oxides and their inclusion in the layers, which deteriorates the adhesion on the surface and the quality of the metal layers. The change of the medium to ILs enabled access to some metals but there are more parameters which influence each other and have to be taken into consideration.

1.5 Nitrile Ligated Transition Metal Complexes

1.5.1 General Aspects

Transition metal organonitrile complexes have been known for a long time and has found some useful applications.[86] This group of complexes serves as precursors for a variety of non-aqueous synthetic usage, such as the synthesis of other complexes, inorganic materials, or catalysts. The broad usefulness of these complexes derives from the lability of the nitrile ligands, which can either be easily replaced by more strongly coordinating ligands or by other substrates or metal cores. Furthermore, applying weakly-coordinating anions as counterions facilitates the formation of vacant coordination sites and thus generating virtually ‘naked’ metal ions. Monomeric complexes bearing WCAs of almost every first-row transition metal and some of the second and third row transition metals are known, as well as some dimeric complexes. However, there are many published synthetic procedures, which lead to impure products or uncertain formulations.[87]

By using very labile nitrile ligands and weakly-coordinating anions, the metal cation should be existent as ‘naked’ metal ion. Therefore, a reduction of the metal cation to the metal should be facilitated and the leaving groups should be soluble to not be incorporated into the formed metal layers.

1.5.2 Synthetic Strategies

Solvent-stabilized metalorganic complexes with weakly coordinating anions of the general formulas $[M(NCR)_{2,4,6}][A]_{1,2,3}$ or $[M_2(NCR)_{8\text{-}10}][A]_4$ (M = transition metal; R = organic fragment; A = counter ion) can be synthesized by several methods.

The first one is the oxidation of zero-valent metals with strong one-electron oxidants of the intended anion. Thereto nitrosonium salts of the respective weakly coordinating anion can be used such as $NOBF_4$. The nitrosonium salts are strong one-electron oxidants and enable the oxidation of almost every first-row transition metal, resulting in a complex of the structure $[M(NCR)_n][A]_2$ with M = V, Mn, Fe, Co, Ni, Cu, Zn; n = 4,6.[86b]

The second method is the protolysis of metal acetates with corresponding acids resulting in a two-step procedure. The first step is the formation of dinuclear tetraacetates, and the second step is their protonation in nitrile containing solvents. Hence, dinuclear complexes $[M_2(NCR)_{8\text{-}10}][A]_4$ can be obtained for M = Mo, Rh, Tc or Re as well as a monomeric complex $[M(NCR)_4][A]_2$ in the case of Cr. The acids of the respective WCAs usually are Brønsted acids and the protons are stabilized by additional water or ether ligands such as $HBF_4 \cdot Et_2O$.[87a, 87b, 88]

The third synthetic procedure is the halide abstraction by salt metathesis. By using metathesis reagents like silver salts weakly coordinating anions can be introduced to organonitrile complexes. The conversion occurs with a stoichiometric amount of the respective silver salt in the corresponding nitrile.[87d]

2. OBJECTIVE

Numerous components can be produced with cheap and good available resources and afterwards they can be functionalized with an appropriate metallic coating. Properties such as protection against corrosion or chemical degradation, abrasion or scratch resistance, and electric conductivity can be enhanced with this functionalization.

Though, for many applications metallic coatings are ideal, which either cannot be produced by today's technology or whose production is connected with extensive cost and some severe ecological detriments. Metallic coating of various components is realized by electrochemical deposition. Since the whole electroplating industry is based solely on aqueous solutions, many metals such as the group of the refractory metals, are not accessible by this method, because they require deposition potentials at which water is decomposed electrolytically. On this account a change of the deposition medium from aqueous solutions to non-aqueous solutions is necessary in order to gain access to coatings with refractory metals.

Due to their wide electrochemical window ionic liquids (ILs) are on principle well suited as medium for the electrodeposition, as it enables the deposition of very ignoble metals from ILs. Thus, by the application of ionic liquids, coatings with refractory metals become accessible, but their electrodeposition is connected with some significant drawbacks. Currently, refractory metals are predominantly electrodeposited from their halides. The consequence is that non-stoichiometric subhalide species are formed during the reduction process to the metal, which are incorporated into the formed metal layers and therefore they can negatively influence the properties of the deposit. Various oxide species or other stable intermediates can also be generated during the reduction process, which can prevent a further reduction to the metal. However, by changing the medium to ILs, it was possible to gain access to coatings with some refractory metals.

But not only the medium has to be changed but also the compounds which are used for the electrodeposition. Fundamental new concepts have to be developed to enable the deposition of refractory metals, to gain further insight into the physicochemical processes at the electrodes and the interface and to provide a sound basis for cheaper and more environmentally friendly coating technology.

In order to avoid the formation of subhalides during the deposition, new precursors have to be synthesized which contain neither halides nor hydrogen atoms at the C_α-position, because this is considered to be a critical step during the deposition process.

Solvent-stabilized metalorganic complexes with weakly-coordinating anions of the general formulas $[M(NCR)_x][A]_y$ or $[M_2(NCR)_x][A]_y$ with M = metal; R = organic residue; x = number of nitrile ligands; A = anion and y = number of anions are of particular interest, since the bond of the ligands should be weak enough to facilitate the reduction to the metal and the leaving groups should be soluble to not be incorporated into the layers. Other important parameters are suitable anions and the solubility in selected ionic liquids. However, it has to be taken into consideration that there are significant differences between aqueous solutions and ionic liquids, and that there are many other interacting parameters.

To date, there is no knowledge about the solubility and the solubility behavior of this group of metalorganic complexes in ionic liquids. Therefore, it is the aim of this work to provide a sound basis for the electrodeposition of refractory metals from ionic liquids with the synthesis of solvent-stabilized complexes, which are suitable for the electrodeposition of refractory metals and with the investigation of their solubility in ionic liquids. The focus is on refractory metals such as vanadium, titanium, niobium, tantalum, chromium, molybdenum, and tungsten (Figure 16).

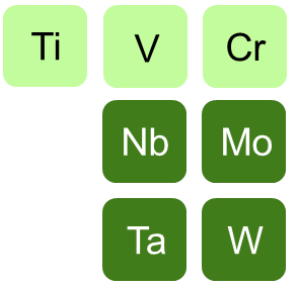

Figure 16 Cutout of the periodic table with the emphasized refractory metals.

3. Results and Discussion

In order to realize the electrochemical deposition of refractory metals from ionic liquids, other precursors than halides have to be used because the deposition of halides is connected with some severe drawbacks as aforementioned. The approach to overcome these detriments is the use of solvent-stabilized metalorganic complexes with weakly coordinating anions with the general formulas $[M(NCR)_x][A]_y$ or $[M_2(NCR)_x][A]_y$ with M = transition metal; R = organic residue; x = number of nitrile ligands; A = anion and y = number of anions. The broad usefulness of these complexes derives from the lability of the nitrile ligands, which can either be easily replaced by more strongly coordinating ligands or by other substrates or metal cores. Furthermore, applying weakly-coordinating anions as counterions facilitates the formation of vacant coordination sites and thus generating virtually 'naked' metal ions.[87] By using very labile nitrile ligands and weakly-coordinating anions, the metal cation should be existent as 'naked' metal ion. Therefore, a reduction of the metal cation to the metal should be facilitated and the leaving groups should be soluble to not be incorporated into the formed metal layers. The results concerning the synthesis of such precursors, the investigation of their solubility in ionic liquids and some electrochemical studies are presented in the following.

For the solvent stabilized transition metal complexes four different nitriles are used, acetonitrile (CH_3CN), benzonitrile (C_6H_5CN), *tert*-butylnitrile ($(CH_3)_3CCN$) and propionitrile (C_2H_5CN).

3.1 Synthesis of the Precursors

3.1.1 Synthesis of $[Cr(NCR)_{3\text{-}4}][BF_4]_2$ (**8**-**11**)

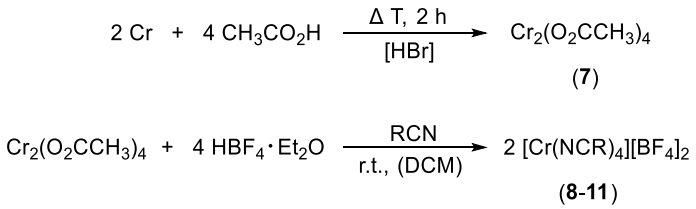

Scheme 4 Schematic representation of the synthesis of $Cr_2(O_2CCH_3)_4$ (**7**) and the organonitrile complexes $[Cr(NCR)_4][BF_4]_2$ (**8**-**11**).

The general synthetic procedure of this group of solvent stabilized metalorganic complexes occured in two steps (Scheme 4). The first step was the formation of dichromium tetraacetate (**7**) by refluxing chromium powder in a 4:1 mixture of acetic acid and acetic anhydride with a catalytic amount of HBr for 2 h according to a literature procedure.[89] Upon cooling the reaction mixture in an ice bath, $Cr_2(O_2CCH_3)_4$ precipitated and was washed with acetone and pentane after filtration. After drying the product under reduced pressure, $Cr_2(O_2CCH_3)_4$ was obtained as brownish red powder with a yield of about 55 %. Conspicuously, this reaction could be conducted without the exclusion of air and water, and the product

could be handled under air for a short period of time without decomposition. The second step was the preparation of the nitrile complexes[87b] by dissolving $Cr_2(O_2CCH_3)_4$ in a solvent mixture of dichloromethane (DCM) and the respective nitrile and $HBF_4 \cdot Et_2O$ was slowly added dropwise. An immediate color change from a brownish red solution to turquois took place showing that there were no indications of the formation of any intermediate. The solution was stirred for 45 min at room temperature to complete the reaction. After removing the solvent, the remaining oil was washed with diethyl ether and *n*-pentane and the product precipitated and was dried *in vacuo*. The products **8**-**11** were obtained as fine blueish powders with a yield of about 75 %. During the course of the reaction the Cr-Cr quadruple bond of $Cr_2(O_2CCH_3)_4$ breaks and leads to a monomeric chromium containing complex. This accentuates the decreased stability of the Cr-Cr quadruple bond in comparison to the Mo-Mo quadruple bond, which is mentioned in chapter 3.1.4 and the higher air- and water-sensitivity of the products compared to the starting material $Cr_2(O_2CCH_3)_4$. The monomeric organonitrile complexes usually have four nitrile molecules as ligands. However, since the solvent ligands are very labile, even a slightly prolonged time of drying them under reduced pressure can lead to a reduction of the number of ligands. The method of choice to suggest the number of ligands is elemental analysis. The results show that the compound $[Cr(NCCH_3)_3][BF_4]_2$ (**8**), which is obtained as fine, blue powder, exhibits three acetonitrile ligands. Slight deviations can be attributed to residues of other solvents or traces of oxidation products due to the lability of Cr(II) species. $[Cr(NCC_6H_5)_3][BF_4]_2$ (**9**) is received in two fractions, as dark blue powder, and as blue crystals, with a combined yield of 69 %. The results from the EA show, that the complex holds three benzonitrile ligands as well as **8**. Small aberrancies can be traced back to measurement techniques. $[Cr(NCC(CH_3)_3)_4][BF_4]_2$ (**10**) was obtained as fine turquois powder and elemental analysis reveals four *tert*-butylnitrile ligands only slight deviations which can be attributed to measurement techniques. The propionitrile ligated complex $[Cr(NCC_2H_5)_4][BF_4]_2$ (**11**), which is received as turquois powder with a yield of 73 %, obtained four nitrile ligands with only small aberrancy in the elemental analysis. All complexes are extremely sensitive to air and water and the aberrancies in the elemental analysis can be attributed to the fact, that the compounds are exposed to air during the preparation for the measurement. Unfortunately, the recorded NMR spectra could not be assigned due to the strong paramagnetic properties.

Paramagnetic compounds exhibit unpaired electrons. These can be radicals, or, as in this case, transition metal complexes whose metal cation possesses unpaired electrons. The magnetic properties of the complexes are strongly controlled by that resulting in paramagnetic NMR spectra. There are several theoretical and experimental factors, which have to be taken into account.[90] One relevant parameter for the interpretation of paramagnetic ^1H NMR spectra is the concentration of the complex. The higher the concentration the better is the resolution of the spectra. In terms of the complexes **8**-**11** the solubility in deuterated solvents is problematic if higher concentrations are required. Another important effect is, that paramagnetic NMR signals tend to be overly broad, which can make it difficult to differentiate between the signal and the baseline in some cases. But broad signals can be intensified by increasing the temperature and hence, they might be detected at higher temperatures. Furthermore, paramagnetic signals tend to have a higher sensitivity towards temperature changes than diamagnetic signals. There is a distinct signal shift can be observed if measurements are conducted at varying temperatures and a difference between paramagnetic and diamagnetic signals becomes possible. With

increasing temperature, the signal is shifted to the region it would appear, if an analog diamagnetic compound existed. The last relevant fact, which is pointed out here, is, that paramagnetic signals can arise outside the regular measurement range, which is from -3 ppm up to 16 ppm. In order to forecast a signal shift, theoretical calculations had to be conducted, but these are beyond the scope of this work.[90]

3.1.2 Synthesis of $[Cr(NCR)_2][CF_3SO_3]_2$ (**12**-**15**)

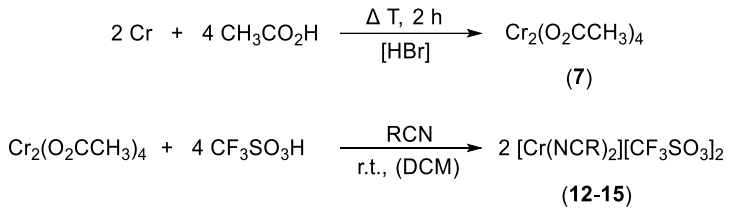

Scheme 5 Schematic representation of the synthesis of $Cr_2(O_2CCH_3)_4$ (**7**) and the organonitrile complexes $[Cr(NCR)_2][CF_3SO_3]_2$ (**12**-**15**).

The general synthetic procedure for this group of complexes is also a two-step procedure as already mentioned in section 3.1.1. The first step is the formation of the dichromium(II) tetraacetate and the second step is its conversion to the solvent-stabilized complex (Scheme 5). $Cr_2(O_2CCH_3)_4$ is dissolved in a mixture of dichloromethane and the corresponding nitrile. Trifluoromethanesulfonic acid is slowly added dropwise resulting in an immediate color change of the solution from brownish red to dark green showing that there are no indications of the formation of any intermediate. The solution is stirred for 45 min at room temperature to complete the reaction. It can be observed that a small amount of the product already starts to precipitate. After removing the solvents, the product is washed with diethyl ether and *n*-pentane and dried *in vacuo*. The products **12**-**15** are obtained as exceptionally fine light green powders with a yield of 65 - 70 %. In comparison with the complexes $[Cr(NCR)_{3\text{-}4}][BF_4]_2$ (**8**-**11**) the group of $[Cr(NCR)_2][CF_3SO_3]_2$ exhibits an even higher air- and water-sensitivity. Strikingly, they only have two nitrile ligands and not three or four as the compounds **8**-**11**. This can be explained with the stronger coordination of the $CF_3SO_3^-$ anion than of the BF_4^- anion, resulting in less free coordination sites for the nitrile ligands. Unfortunately, attempts to crystallize these compounds were not successful. The method of choice to see the exact number of ligands is elemental analysis. The results show that the compound $[Cr(NCCH_3)_2][CF_3SO_3]_2$ (**12**) has two acetonitrile ligands and could be obtained with high purity. Small deviations can be attributed to the measurement technique. $[Cr(NCC_6H_5)_2][CF_3SO_3]_2$ (**13**) as well as $[Cr(NCC(CH_3)_3)_2][CF_3SO_3]_2$ (**14**) are received with high purity and hold two benzonitrile, respectively *tert*-butylnitrile as ligands. The last complex of this group is $[Cr(NCC_2H_5)_2][CF_3SO_3]_2$ (**15**) is obtained with two propionitrile ligands and the found values for the weight percentages are in good accordance with the calculated values. Although this group of complexes is extremely sensitive towards air and moisture, the obtained results from the elemental analysis are in very good accordance with the calculated values.

Attempts to record NMR spectra were not successful due to the paramagnetic properties of the Cr(II) species.

3.1.3 Synthesis of $[Cr(O_2CCH_3)(NCCH_3)_2][TFSI]$ (**16**)

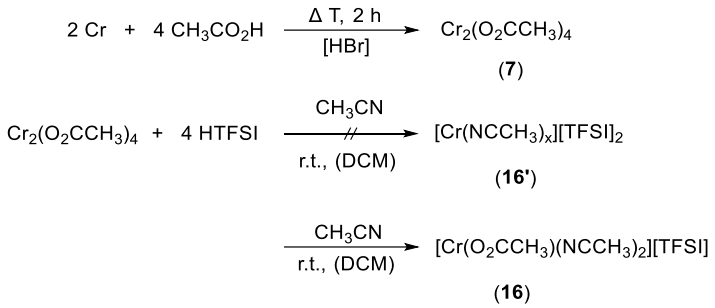

Scheme 6 Schematic presentation of the synthesis of $Cr_2(O_2CCH_3)_4$ (**7**) and $[Cr(O_2CCH_3)(NCCH_3)_2][TFSI]$ (**16**).

Following the synthetic procedure of the already mentioned groups of complexes **8**-**11** and **12**-**15**, the acid triflimide (HTFSI) was used to incorporate another weakly coordinating anion into nitrile stabilized complexes. The first step was, as aforementioned, the formation of $Cr_2(O_2CCH_3)_4$ and the second step is its conversion with HTFSI in a solvent mixture of dichloromethane and acetonitrile (Scheme 6). For the synthesis, $Cr_2(O_2CCH_3)_4$ was dissolved in DCM and since HTFSI is a solid, it was dissolved in acetonitrile for a better addition. The acid solution was added dropwise to the solution of $Cr_2(O_2CCH_3)_4$ resulting in an immediate color change from brownish red to green. The solution was stirred for an additional hour at room temperature to complete the reaction. After removing the solvents, the product is washed with diethyl ether and *n*-pentane and dried under reduced pressure. A fine green powder was obtained with an extremely low yield of about 4 %. The results from the elemental analysis reveal, that rather a compound with a composition of $[Cr(O_2CCH_3)(NCCH_3)_2][TFSI]$ was obtained than an all acetonitrile stabilized complex. This implies that a complete replacement of the acetate anions was not possible by the acid HTFSI. In the next attempt to overcome this fact, the acid is added in a bigger excess, but the same result was obtained. The next trials were to prolong the reaction time and to increase the reaction temperature. But both factors led to the already received result, that the replacement of the acetate anions could not be completed. Since the observations during this reaction such as the immediate color change with the addition of the acid and the green color of the reaction solution were very similar to the observations of the other chromium containing complexes, it was assumed that some reaction has to take place and at least some replacement of the acetate ligands is conducted, as seen in the result from the elemental analysis above. Another approach to complete the replacement of the anions is the addition of another acid. This acid must be able to protonate acetate anions in order to exchange of the acetate anions and its anion must not coordinate stronger than the TFSI anion. Therefore, a stoichiometric amount of $HBF_4 \cdot Et_2O$ is added to the reaction solution. During this reaction, the same observations such as the immediate color change to green and a fine green

powder as product could be made. In order to see if this attempt was successful, a ^{19}F-NMR spectrum was recorded. Therein, it should be seen if an anion exchange took place during the reaction and which fluorine containing anion coordinated, since BF_4^- and TFSI have different chemical shifts. The spectrum shows one singlet at -80.12 ppm, which can be assigned to the TFSI anion. The BF_4^- anion can be excluded because its chemical shift is usually located around -150 ppm, whereas the TFSI anion has a chemical shift of around -85 ppm to -75 ppm.[91] This result showed, that the use of the acid $HBF_4 \cdot Et_2O$ was successful to that effect that neither only the BF_4^- anion was incorporated into the chromium complex nor that a mixture of BF_4^- and TFSI anions occurred because in this case, the ^{19}F-NMR spectrum would show two signals in the respective region. But it still cannot be said if the complete replacement of the acetates took place. Therefore, another elemental analysis measurement was conducted. However, the results were very similar to the already mentioned analysis, indicating that this attempt did not lead to a complete replacement of the acetate anions of $Cr_2(O_2CCH_3)_4$ either. Unfortunately, attempts to grow crystals of this compound suitable for SC-XRD was not successful due to the limited solubility and stability in various solvents such as acetonitrile, acetone, dichloromethane, toluene and tetrahydrofurane.

3.1.4 Synthesis of $[Mo_2(NCR)_{8\text{-}10}][BF_4]_4$ (**18**-**21**)

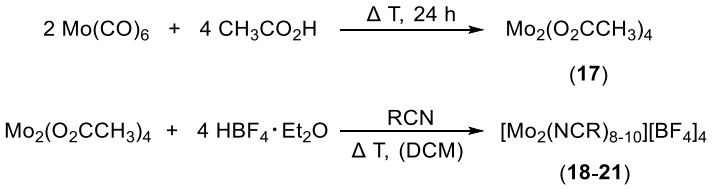

Scheme 7 Schematic representation of the synthesis of $Mo_2(O_2CCH_3)_4$ (**17**) and the organonitrile complexes $[Mo_2(NCR)_{8\text{-}10}][BF_4]_4$ (**18**-**21**).

The general synthetic procedure of this group of solvent stabilized metalorganic complexes occured in two steps (Scheme 7). The first step was the formation of dimolybdenum tetraacetate (**17**) by refluxing molybdenum hexacarbonyl in a 10:7 mixture of acetic acid and acetic anhydride for 24 h according to a literature procedure.[92] By cooling the reaction mixture in an ice bath and concentrating it to about 50 % of its original volume, $Mo_2(O_2CCH_3)_4$ precipitated and was washed with dichloromethane and diethyl ether after filtration. After drying the product under reduced pressure, $Mo_2(O_2CCH_3)_4$ was obtained as bright yellow powder with a yield of about 57 %. To ensure a high solubility of $Mo(CO)_6$ during the whole reaction time, a small amount of toluene was added. The second step is the preparation of the nitrile stabilized complexes[93] by dissolving $Mo_2(O_2CCH_3)_4$ in a solvent mixture of dichloromethane and the respective nitrile. The acid $HBF_4 \cdot Et_2O$ was slowly added dropwise resulting in an immediate color change from bright yellow *via* dark red and purple to dark blue within less than five minutes. The different colors indicate the stepwise exchange of the acetate anions, from $Mo_2(O_2CCH_3)_4$ via $[Mo_2(\mu\text{-}O_2CCH_3)_2(NCR)_6][BF_4]_2$ and $[Mo_2(\mu\text{-}O_2CCH_3)(NCR)_8][BF_4]_3$ to $[Mo_2(NCR)_{8\text{-}10}][BF_4]_4$.[87b, 94] The solution

is stirred at room temperature first and then heated to reflux for about 3 h to complete the reaction. Upon cooling the solution in an ice bath, the dark blue solid, precipitates and after filtering off the solvents, the product was washed with diethyl ether and *n*-pentane and dried *in vacuo*. The products **18**-**21** are obtained as fine blue or violet powders with a yield of about 85 %. In contrast to the reaction of the chromium containing nitrile stabilized complexes in which the Cr-Cr quadruple bond breaks, the Mo-Mo quadruple bond is preserved in the final product as a Mo_2^{4+} core. The binuclear organonitrile complexes can have up to ten nitrile molecules as ligands. However, since the solvent ligands are very labile, even a slightly prolonged time of drying them under reduced pressure can lead to a reduction of the number of ligands. $[Mo_2(NCCH_3)_8][BF_4]_4$ (**18**) was obtained as fine deep blue powder an exhibits eight acetonitrile ligands due to the results of the elemental analysis. Small deviations can be traced back to measurement techniques. There are slight changes in the procedure for the benzonitrile derivative, $[Mo_2(NCC_6H_5)_8][BF_4]_4$ (**19**). After cooling down the reaction mixture to room temperature, the solution was concentrated to about 50 % of its original volume. During cooling the reaction mixture in an ice bath, diethyl ether (10 x 15 mL) was added inducing the precipitation of the product. The solution was stored at -32 °C for several days to complete the precipitation. The solvents were filtered off and the product was washed as described above and dried *in vacuo*. $[Mo_2(NCC_6H_5)_8][BF_4]_4$ (**19**) was received as dark violet solid and elemental analysis reveals eight benzonitrile ligands. $[Mo_2(NCC(CH_3)_3)_{10}][BF_4]_4$ (**20**) as well as $[Mo_2(NCC_2H_5)_{10}][BF_4]_4$ (**21**) were obtained as fine dark blue powders and they hold ten nitrile ligands, respectively.

3.1.5 Synthesis of $[Mo_2(NCR)_{8\text{-}10}][CF_3SO_3]_4$ (**22**-**25**)

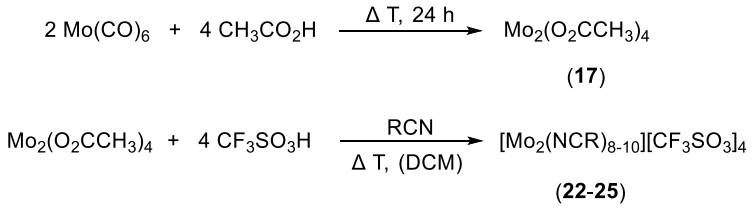

Scheme 8 Schematic representation of the synthesis of $Mo_2(O_2CCH_3)_4$ (**17**) and the organonitrile complexes $[Mo_2(NCR)_{7\text{-}10}][CF_3SO_3]_4$ (**22**-**25**).

The general synthetic procedure for this group of complexes is also a two-step procedure as already mentioned in section 3.1.4. The first step is the formation of the dimolybdenum(II) tetraacetate (**17**) and the second step is its conversion to the solvent-stabilized complex (Scheme 8). $Mo_2(O_2CCH_3)_4$ was dissolved in a mixture of dichloromethane and the corresponding nitrile. Trifluoromethanesulfonic acid was slowly added dropwise resulting in an immediate color change of the solution from bright yellow *via* dark red and purple to dark blue within less than five minutes. The different colors indicate the stepwise exchange of the acetate anions, from $Mo_2(O_2CCH_3)_4$ via $[Mo_2(\mu\text{-}O_2CCH_3)_2(NCR)_6][CF_3SO_3]_2$ and $[Mo_2(\mu\text{-}O_2CCH_3)(NCR)_8][CF_3SO_3]_3$ to $[Mo_2(NCR)_{8\text{-}10}][CF_3SO_3]_4$.[87b, 94] The solution is stirred at room temperature first and then heated to reflux for about 3 h to complete the reaction. Upon cooling the solution in an ice

bath, the dark blue solid, precipitated and after filtering off the solvents, the product was washed with diethyl ether and *n*-pentane and dried *in vacuo*. The products **22**-**25** were obtained as fine dark blue or dark violet powders with a yield of about 90 %. However, since the solvent ligands are very labile, even a slightly prolonged time of drying them under reduced pressure can lead to a reduction of the number of ligands. The method of choice to suggest the number of ligands is elemental analysis. The results show that the compound $[Mo_2(NCCH_3)_7][CF_3SO_3]_4$ (**22**) as well as $[Mo_2(NCC_6H_5)_7][CF_3SO_3]_4$ (**23**), which were received as fine dark blue and dark purple powder, exhibit seven acetonitrile, respectively benzonitrile, ligands. Slight deviations can be attributed to measurement techniques or some residues of other incorporated solvents. $[Mo_2(NCC(CH_3)_3)_{10}][CF_3SO_3]_4$ (**24**) was obtained as dark blue solid and exhibited ten *tert*-butylnitrile ligands. Due to a slightly prolonged drying time and the lability of the nitrile ligands, $[Mo_2(NCC_2H_5)_8][CF_3SO_3]_4$ (**25**) was received as dark blue solid with eight propionitrile ligands.

3.1.6 Synthesis of $[Mo_2(NCCH_3)_8][TFSI]_4$ (**26**)

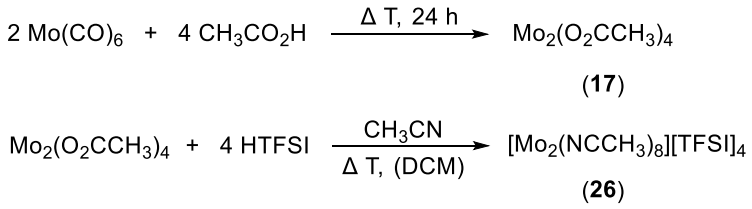

Scheme 9 Schematic representation of the synthesis of $Mo_2(O_2CCH_3)_4$ (**17**) and the organonitrile complex $[Mo_2(NCCH_3)_8][TFSI]_4$ (**26**).

Following the synthetic procedure of the already mentioned groups of complexes **18**-**21** and **22**-**25**, the acid triflimide (HTFSI) was used to incorporate another weakly coordinating anion into molybdenum containing nitrile stabilized complexes. The first step was, as aforementioned, the formation of $Mo_2(O_2CCH_3)_4$ and the second step was its conversion with HTFSI in a solvent mixture of dichloromethane and acetonitrile (Scheme 9). For the synthesis, $Mo_2(O_2CCH_3)_4$ was dissolved in DCM and since HTFSI is a solid, it was dissolved in acetonitrile for a better addition. The acid solution was added dropwise *via* cannula to the solution of $Mo_2(O_2CCH_3)_4$ resulting in an immediate color change from bright yellow *via* dark red and purple to blue within less than ten minutes. As observed for the complexes **18**-**21** and **22**-**25**, the color changes indicated the stepwise exchange of the acetate anions, from $Mo_2(O_2CCH_3)_4$ *via* $[Mo_2(\mu\text{-}O_2CCH_3)_2(NCR)_6][TFSI]_2$ and $[Mo_2(\mu\text{-}O_2CCH_3)(NCR)_8][TFSI]_3$ to $[Mo_2(NCR)_{8\text{-}10}][TFSI]_4$.[87b, 94] The solution was stirred at room temperature first and then heated to reflux for about 3 h to complete the reaction. Upon cooling the solution in an ice bath, the dark blue solid, precipitated and after filtering off the solvents, the product was washed with diethyl ether and *n*-pentane and dried *in vacuo*. The product $[Mo_2(NCR)_{8\text{-}10}][TFSI]_4$ (**26**) was received as fine deep blue powder with a yield of about 30 %. Strikingly, the yield for compound **26** is much lower as for the comparable complexes **18**-**21** and **22**-**25** although the reaction was conducted under the same conditions and the same observations have been made. The extremely lower yield by applying the acid HTFSI was already

noticed for the synthesis of the corresponding Cr containing complex $[Cr(O_2CCH_3)(NCCH_3)_2][TFSI]$ (**16**). The results from the elemental analysis revealed that the compound $[Mo_2(NCR)_8][TFSI]_4$ contained eight acetonitrile ligands. This corresponds with the result from the SC-XRD, which showed, that four acetonitrile molecules coordinated to one molybdenum cation each (see Figure 17). Small deviations of the result from the elemental analysis can be attributed to the fact, that one additional acetonitrile molecule is located between two cations of the complex and these two cations 'share' this acetonitrile molecule (see Figure 30, chapter II.6.1.2). The single crystals which were suitable for SC-XRD were grown by slow diffusion of diethyl ether in a solution of **26** in acetonitrile. The crystals are extremely sensitive to air and moisture, which is why a crystal was chosen directly from the Schlenk tube. The structure of $[Mo_2(NCR)_{8\text{-}10}][TFSI]_4$ (**26**) is composed of a discrete, centrosymmetric $[Mo_2(NCCH_3)_8]^{4+}$ core as shown in Figure 17. The dimolybdenum core resides on an inversion center and the molybdenum atoms are bonded to each other with a quadruple bond of Mo(1)-Mo(1a) = 2.1938(12) Å. On each molybdenum of the Mo_2^{4+} entity four nitrogen atoms of the four equatorial acetonitrile molecules are bonded with an bond length of Mo(1)-N(1) = 2.129(6) Å and Mo(1)-N(2) = 2.128(6) Å, respectively. The TFSI counterions refined nicely with no apparent disorder. All angles of C-N-Mo are between 170.7 (5)° and 172.8 (6)°, which is close to 180 ° as expected. In comparison with the crystal structure of compound **8**[94b], $[Mo_2(NCCH_3)_{10}][BF_4]_4$, it can be seen that the Mo-Mo quadruple bond is with 2.187(1) Å slightly shorter than that of **26**, and that there are bigger differences in the Mo-N bond lengths. All Mo-N bonds of **26** have nearly the same bond length, whereas for **8**, the Mo-N bond length are in a range of 2.113(10) – 2.141(9) Å. Both cores exhibit the same structure and therefore they have nearly the same bond angles for Mo(1)-Mo(1a)-N, N(1)-Mo(1)-N(1b) and N(1)-Mo(1)-N(2). More relevant crystallographic information is given in chapter 6.1.2.

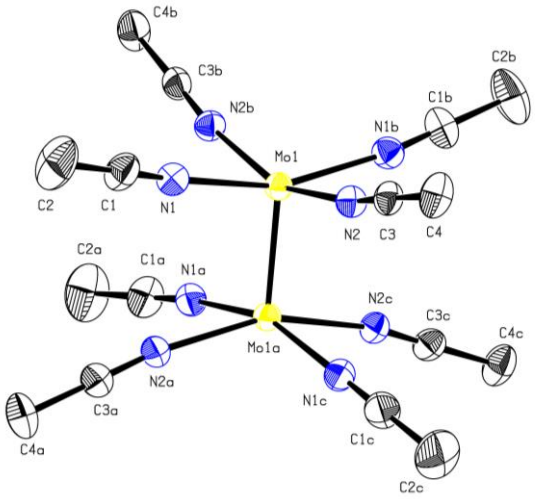

Figure 17 ORTEP style representation of the $[Mo_2(NCCH_3)_8]^{4+}$ core of the complex **26** with ellipsoids shown at a 50 % probability level. Hydrogen atoms and TFSI counterions are omitted for clarity. Color scheme: yellow, molybdenum; blue, nitrogen. Selected bond lengths [Å]: Mo(1)-Mo(1a) 2.1938(12), Mo(1)-N(1) 2.129(6), Mo(1)-N(1b) 2.129(6), Mo(1)-N(2) 2.128(6) and Mo(1)-N(2b) 2.128(6).

3.1.7 Synthesis of $[Mo_2(\mu\text{-}O_2CCH_3)_2(NCC(CH_3)_3)_4][TFSI]_2$ (**27**)

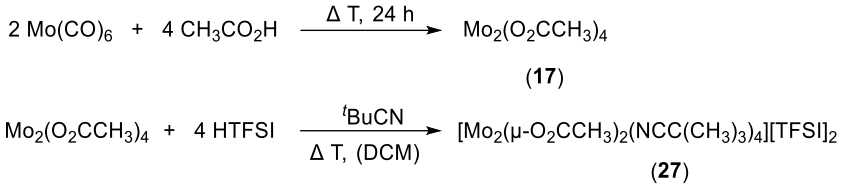

Scheme 10 Schematic representation of the synthesis of $Mo_2(O_2CCH_3)_4$ (**17**) and the organonitrile complex $[Mo_2(\mu\text{-}O_2CCH_3)_2(NCC(CH_3)_3)_4][TFSI]_2$ (**27**).

Following the synthetic procedure of the already mentioned complex **26** with the TFSI anion, the synthesis was conducted with another nitrile, *tert*-butylnitrile. The first step was, as aforementioned, the formation of $Mo_2(O_2CCH_3)_4$ and the second step was its conversion with HTFSI in a solvent mixture of dichloromethane and *tert*-butylnitrile (Scheme 10). For the synthesis, $Mo_2(O_2CCH_3)_4$ was dissolved in DCM and since HTFSI is a solid, it was dissolved in *tert*-butylnitrile for a better addition. The acid solution was added dropwise *via* cannula to the solution of $Mo_2(O_2CCH_3)_4$ resulting in an immediate color change from bright yellow *via* red to purple. As observed for the previously mentioned molybdenum containing complexes, the color changes indicated the stepwise exchange of the acetate anions.[87b, 94] The solution was stirred at room temperature first and then heated to reflux for about 2 h to complete the reaction. In contrast to the other compounds **18**-**26**, cooling the solution in an ice bath did not lead to the precipitation of the product. Instead, the reaction solution was concentrated to 50 % of its original volume and afterwards diethyl ether was added. The solution was filtered off from the resulting oil. Both fractions were stored over night at -32 °C leading to the precipitation of fine pink needles from the second fraction. The oil from the first fraction was also washed with diethyl ether and *n*-pentane. The obtained bright pink powder was dried in vacuo. SC-XRD of the pink needles revealed that the exchange of the acetate anions for TFSI anions did not take place completely and that therefore two acetate anions are still coordinated to the dimolybdenum core (Figure 18). Single crystals were grown from the first fraction by slow diffusion of diethyl ether into a solution of the product in *tert*-butylnitrile. These crystals were also obtained as fine pink needles and led to the same result (cf. Figure 18). The molybdenum atoms are bonded to each other with a quadruple bond of Mo(1)-Mo(2) = 2.1417(3) Å. The Mo-Mo bond distance is significantly shorter than for **26** (2.1938(12) Å), but longer than for $Mo_2(O_2CCH_3)_4$ (2.093(1) Å). Therefore, the number of bridging acetate ligands influences the Mo-Mo bond distance: the higher the number of acetate ligands the shorter the Mo-Mo bond length.[95] On each molybdenum of the Mo_2^{4+} entity two nitrogen atoms of the two equatorial *tert*-butylnitrile molecules are bonded with a bond length of Mo(1)-N(av.) 2.1663 Å and Mo(2)-N(av.) 2.1621 Å, respectively. The structure exhibits *cis* geometry of the bridging carboxylate ligands and the Mo-O bonds have nearly the same bond distances (2.0666(10) Å – 2.0827(10) Å). The TFSI counterions refined nicely with no apparent disorder. The acetate ligands are nearly perpendicular to the Mo-Mo quadruple bond (cf. O(3)-Mo(1)-Mo(2) 91.17(3) °) and also to the other acetate ligand (cf. O(3)-Mo(1)-O(1) 91.77(4) °) and to the adjacent nitrile ligand (cf. O(3)-Mo(1)-N(2) 91.88(4) °). All angles of C-N-Mo are between 153.79(12) ° and 176.99(12) °, whereat the upper two *tert*-butylnitrile ligands are more bent than the lower two *tert*-butylnitrile ligands. More relevant crystallographic information is given in chapter 6.1.2. The results from the elemental analysis

confirmed the results from the crystal structure, that exchange of the acetate anions for TFSI anions did not take place completely. Various attempts were conducted to overcome this fact in order to obtain an all *tert*-butylnitrile stabilized complex such as the addition of the acid in a higher excess. The next trial was to prolong the reaction time during refluxing. But both factors led to the already received result, that the replacement of the acetate anions could not be completed. Another possible reason for the only partial exchange of acetate ligands might be that the nitrile molecules are sterically more demanding due to the *tert*-butyl groups than acetonitrile and that therefore a complete replacement is hindered. The use of another acid which could protonate the acetate anions on the one hand but whose anion does not coordinate stronger than the TFSI anion on the other hand was tested, as already mentioned in chapter 3.1.3. Therefore, a stoichiometric amount of $HBF_4 \cdot Et_2O$ was added to the reaction solution. However, the results were very similar to the already mentioned analysis, indicating that this attempt did not lead to a complete replacement of the acetate anions of $Cr_2(O_2CCH_3)_4$ either.

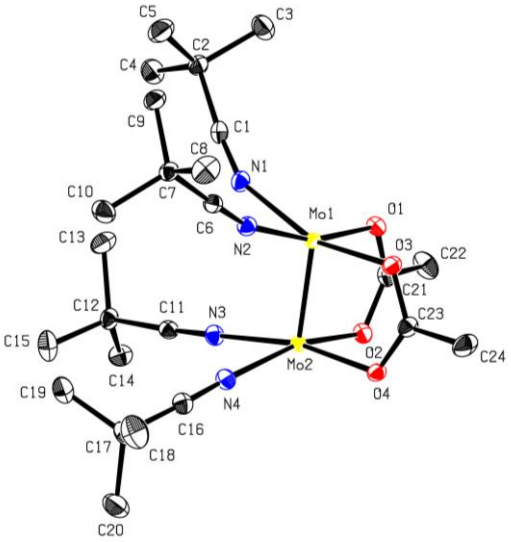

Figure 18 ORTEP style representation of the $[Mo_2(\mu\text{-}O_2CCH_3)_2(NCC(CH_3)_3)_4]^{2+}$ core of the complex **27** with ellipsoids shown at a 50 % probability level. Hydrogen atoms and TFSI counterions are omitted for clarity. Color scheme: yellow, molybdenum; blue, nitrogen; red, oxygen. Selected bond lengths [Å]: Mo(1)-Mo(2) 2.1417(3), Mo(1)-N(1) 2.1735(13), Mo(1)-N(2) 2.1591(13), Mo(1)-O(1) 2.0814(11) and Mo(1)-O(3) 2.0666(10).

3.1.8 Synthesis of $[W(NO)_2(NCR)_{3\text{-}4}][BF_4]_2$ (**28**-**29**)

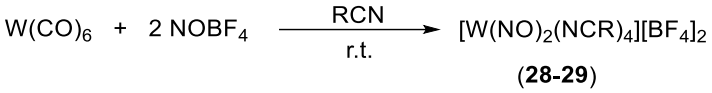

Scheme 11 Schematic representation of the synthesis of the nitrile complexes $[W(NO)_2(NCR)_{3\text{-}4}][BF_4]_2$ (**28**-**29**).

This group of complexes was synthesized according to a literature procedure[96] with slight modifications. $W(CO)_6$ was dissolved in the respective nitrile at room temperature and $NOBF_4$ was added to the solution resulting in an immediate color change from yellow *via* orange to dark green within few minutes. To ensure a high solubility of $W(CO)_6$ during the whole reaction time, a small amount of toluene was added. The reaction mixture was stirred at room temperature overnight and was concentrated to about 50 % of its original volume and cooled in an ice bath to induce the precipitation of the product. The addition of diethyl ether completed the precipitation. After filtering off the solvents the remaining solid was washed with diethyl ether and *n*-pentane and dried *in vacuo* for about 45 min. The products were obtained with a yield of about 85 %. $[W(NO)_2(NCCH_3)_4][BF_4]_2$ (**28**) was received as dark green solid and elemental analysis revealed that there are four acetonitrile ligands coordinating to the metal, while for $[W(NO)_2(NCC(CH_3)_3)_3][BF_4]_2$ (**29**) there are only three *tert*-butylnitrile ligands. This can be attributed to a slightly prolonged drying time. **29** was obtained as light green powder.

3.2 Solubility in Ionic Liquids

In order to realize the electrochemical deposition of refractory metals, other precursors than halides have to be used since the deposition of halides is connected with some severe drawbacks as already mentioned. The approach to overcome these detriments is the use of nitrile stabilized metalorganic complexes with weakly coordinating anions. Thereto the obtained results for the synthesis of such precursors were presented in chapter 3.1. To date, the whole electroplating industry is based solely on aqueous solutions. The consequence is that many industrially relevant metals and hence resulting materials cannot be obtained by the electrochemical deposition from aqueous solutions due to some crucial restrictions of aqueous solution concerning the electrodeposition such as the relatively limited potential window or gas evolution processes during the deposition which can be difficult to handle. Therefore, not only a change of the applied precursors is necessary but also a change of the reaction medium from aqueous solutions to non-aqueous solutions in order to gain access to these materials. Thus, ionic liquids are applied as reaction medium owing to their many beneficial properties like the wider electrochemical window, the wider usable temperature range, the high chemical stability, and the low vapor pressure. Other properties of ionic liquids are further described in section 1.3.

The ionic liquids 1-butyl-1-methylpyrrolidinium triflate (BMP OTf), 1-butyl-1-methylpyrrolidinium bis((trifluoromethyl)sulfonyl)amide (BMP TFSI), Trihexyl(tetradecyl)phosphonium chloride ($P_{6,6,6,14}$ Cl) and Trihexyl(tetradecyl)phosphonium bis((trifluoromethyl)sulfonyl)amide ($P_{6,6,6,14}$ TFSI) were purchased from commercial sources. All other mentioned ionic liquids were synthesized according to previously published procedures.[97] The synthesis of ionic liquids generally requires two steps. The first step is the formation of the desired cation by the quaternization of a (substituted) imidazole, pyridine, a trialkylamine or a trialkylphosphine with a (functionalized) alkylhalide. After several purification steps the quaternary halides are obtained as white to off white solids. The second step is the exchange of the halide for the desired anion by reaction with a metal salt. In this case, metal salts such as NaOTf, LiFSI, but mainly LiTFSI are used. The anion exchange is always conducted in aqueous solution. Therefore, a solution of the metal salt in water was added to a solution of the quaternary halide in water. The resulting suspension was stirred over night at room temperature. After removal of the aqueous phase and several washing steps, the ILs were dried at 70 – 100 °C for several hours to reduce the water content. The RTILs were obtained as colorless to light yellow viscous liquids.

To date, there is no knowledge about the solubility in general and the solubility behavior of this group of metalorganic complexes in ionic liquids. Because there is nearly an unlimited number of ionic liquids, due to the manifold combination possibilities of different anions with various substituted cations, it is not possible to investigate the solubility in all ionic liquids. Thus, a selection of several anions such as Cl^-, OTf, FSI and mainly TFSI, as well as various groups of cations such as imidazolium, ammonium, and phosphonium cations, was made. The aim was to cover different groups of cations and anions in order to provide a sound basis for the investigation of the solubility of nitrile stabilized metalorganic complexes in ionic liquids, especially room temperature ionic liquids. Figure 19 shows a summary of the different selected anions and groups of cations, which were applied in this context. The obtained results concerning the solubility of nitrile stabilized complexes in ionic liquids are presented in the following.

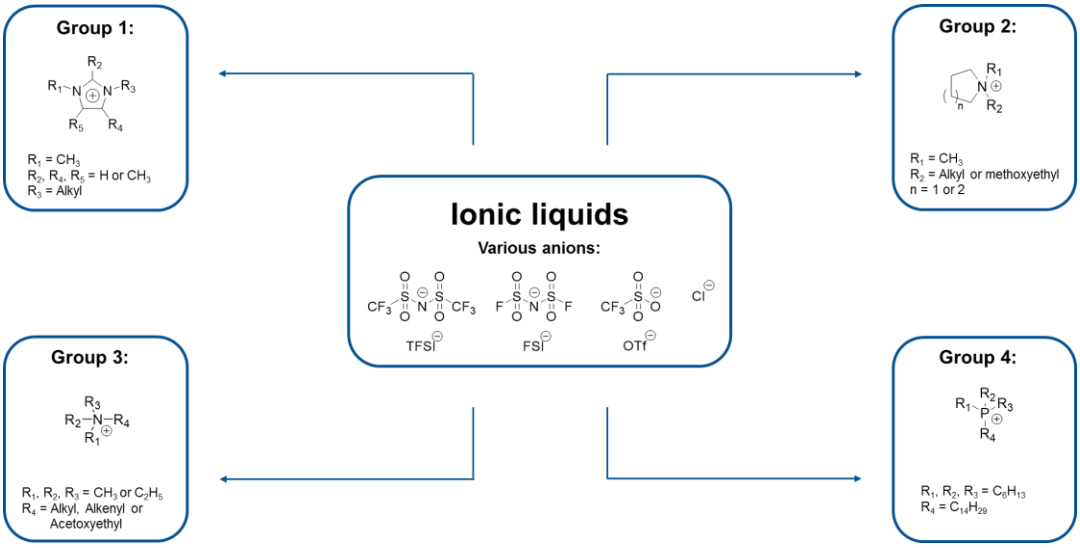

Figure 19 Summary of the different applied anions and groups of cations of the used RTILs.

All nitrile stabilized metalorganic complexes exhibit a very high sensitivity towards air and moisture, why all solubility tests were carried out under argon atmosphere. Furthermore, it is important to note, that all ionic liquids have to be dried extensively in order to keep the water content as low as possible. The investigations concerning the solubility were all conducted at room temperature. At the beginning, a concentration of 0.01 M and a volume of the ionic liquid of 0.1 mL were chosen to analyze if the different compounds are generally soluble in ionic liquids. Afterwards, the concentration was increased in steps of 0.01 M and the volume was raised to 0.5 mL in order to see better if the complexes are dissolved since 0.1 mL is a too small volume. In the following, the concentrations are always given in M = mol/L.

3.2.1 Solubility of $[Cr(NCR)_{3\text{-}4}][BF_4]_2$ (**8**-**11**) in RTILs

At the beginning a concentration of 0.01 M and a volume of the ionic liquid of 0.1 mL was chosen to analyze if the compounds $[Cr(NCR)_{3\text{-}4}][BF_4]_2$ (**8**-**11**) are generally soluble in ionic liquids. To this, ionic liquids were chosen with an alkyl-substituted imidazolium cation with different alkyl chain lengths and the TFSI anion, namely 1-ethyl-3-methylimidazolium TFSI (EMIm TFSI), 1-butyl-3-methylimidazolium TFSI (BMIm TFSI) and 1-octyl-3-methylimidazolium TFSI (OMIm TFSI). By dissolving the compounds **8**-**11** in these three ILs, it could be seen that all compounds were completely dissolved in all ILs after about 1 h at room temperature for a concentration of 0.01 M and a volume of 0.1 mL. Therefore, the concentration was increased stepwise and the solutions were always stirred for at least three hours before the concentration was raised. After seeing that the compounds are generally soluble in the ILs, the volume was also increased to 0.5 mL. $[Cr(NCCH_3)_3][BF_4]_2$ (**8**) could be dissolved completely in all three ionic liquids, though with different concentrations. Whereas it was completely dissolved after a time of about 60 min for BMIm TFSI and OMIm TFSI for every step of increasing the concentration, it took more than three hours for each step until it was completely dissolved in EMIm TFSI. In addition, an already saturated solution of **8** in EMIm TFSI was determined for a concentration of 0.05 M, whereas the concentration could be further increased to 0.07 M for BMIm TFSI and OMIm TFSI until a saturated solution was existent. A very similar behavior could be observed for $[Cr(NCC_6H_5)_3][BF_4]_2$ (**9**), whereat the complex was completely dissolved after about 30 min for every step, which is quite faster than **8**. However, it was not possible to obtain a higher concentration and the least solubility was also reached for EMIm TFSI. $[Cr(NCC(CH_3)_3)_4][BF_4]_2$ (**10**) showed the best solubility behavior of this group of complexes. **10** was already completely dissolved in all three ionic liquids after a few minutes for every step. Although only a maximal concentration of 0.07 M in every IL was obtained as well, it was possible to increase the concentration to 0.07 M for EMIm TFSI. Contrary to **10**, $[Cr(NCC_2H_5)_4][BF_4]_2$ (**11**) showed the least solubility. It took more than 6 hours until the complex was completely dissolved in the ILs for every step and a saturated solution was already reached for a concentration of 0.05 M for all three ILs. The color of all solutions corresponded to the color of the respective complex. After several months, the color of the solution did not change, which shows the long-term stability of these complexes in these ionic liquids. The obtained concentrations for $[Cr(NCR)_{3\text{-}4}][BF_4]_2$ (**8**-**11**) in EMIm TFSI, BMIm TFSI and OMIm TFSI are summarized in table 3.

Table 3 Solubility of $[Cr(NCR)_{3\text{-}4}][BF_4]_2$ (**8**-**11**) in the ILs EMIm TFSI, BMIm TFSI and OMIm TFSI. Concentrations are given in [M].

Number	Compound	EMIm TFSI	BMIm TFSI	OMIm TFSI
8	$[Cr(NCCH_3)_3][BF_4]_2$	0.05	0.07	0.07
9	$[Cr(NCC_6H_5)_3][BF_4]_2$	0.05	0.07	0.07
10	$[Cr(NCC(CH_3)_3)_4][BF_4]_2$	0.07	0.07	0.07
11	$[Cr(NCC_2H_5)_4][BF_4]_2$	0.05	0.05	0.05

A possibility to enhance the solubility of this group of complexes for the alkyl-substituted imidazolium ILs is the substitution of the acidic proton of the imidazolium core, –N-C(H)-N–, for a methyl group. Therefore, the ILs 1-ethyl-2,3-dimethylimidazolium TFSI (EMMIm TFSI), 1-butyl-2,3-dimethylimidazolium TFSI (BMMIm TFSI) and 1-octyl-2,3-dimethylimidazolium TFSI (OMMIm TFSI) were synthesized. In addition, this series was continued with the complete alkylation of the imidazolium core by applying 1,2,4,5-tetramethylimidazole as starting material for the ILs. But since 1-ethyl-2,3,4,5-tetramelthylimidazolium TFSI and 1-butyl-2,3,4,5-tetramethlimidazolium TFSI exhibit a melting point below or close to room temperature, only the octyl derivative of this group could be used, namely 1-octyl-2,3,4,5-tetramethylimidazolium TFSI (OTMIm TFSI). After seeing that the compounds **8**-**11** were generally soluble in these higher substituted ILs, the volume was also increased to 0.5 mL. **8** could be dissolved completely in all four ionic liquids, though with different concentrations. Whereas it was completely dissolved after a time of about 30 min for every step of increasing the concentration in BMMIm TFSI, OMMIm TFSI and OTMIm TFSI, it took about 1 h for the IL EMMIm TFSI. This corresponds with the results from above, that the compound has an inferior solubility in the ethyl-substituted IL to the other ones. An already saturated solution of **8** in EMMIm TFSI was determined for a concentration of 0.06 M, whereas the concentration could be further increased to 0.07 M for BMIm TFSI, OMMIm TFSI and OTMIm TFSI until a saturated solution was existent. The compound **9** showed a very similar behavior. It was completely dissolved after about 20 min for every step in every IL, however the same values for the concentration were obtained as for complex **8**. **10** was thoroughly dissolved in all four ILs of this group after 15 min for every step. Although only a maximal concentration of 0.07 M in every IL was obtained as well, it was possible to increase the concentration to 0.07 M for EMMIm TFSI. As for the ILs of table 3, **11** showed the least solubility in these four ILs. It took a few hours until the complex was completely dissolved for every step and a saturated solution was already obtained for a concentration of 0.05 M, respectively 0.06 M for BMMIm TFSI. The use of higher substituted alkylimidazolium cations was only conditionally successful. The color of all solutions corresponded to the color of the respective complex. After several months, the color of the solution did not change indicating the long-term stability of these complexes in these ILs. The concentrations for the group $[Cr(NCR)_{3\text{-}4}][BF_4]_2$ (**8**-**11**) in EMMIm TFSI, BMMIm TFSI, OMMIm TFSI and OTMIm TFSI are summarized in table 4.

Table 4 Solubility of $[Cr(NCR)_{3\text{-}4}][BF_4]_2$ (**8**-**11**) in the ILs EMMIm TFSI, BMMIm TFSI, OMMIm TFSI and OTMIm TFSI. Concentrations are given in [M].

Number	Compound	EMMIm TFSI	BMMIm TFSI	OMMIm TFSI	OTMIm TFSI
8	$[Cr(NCCH_3)_3][BF_4]_2$	0.06	0.07	0.07	0.07
9	$[Cr(NCC_6H_5)_3][BF_4]_2$	0.06	0.07	0.07	0.07
10	$[Cr(NCC(CH_3)_3)_4][BF_4]_2$	0.07	0.07	0.07	0.07
11	$[Cr(NCC_2H_5)_4][BF_4]_2$	0.05	0.06	0.05	0.05

To broaden the spectrum of ionic liquids in which the metalorganic complexes are soluble, not only imidazolium based ionic liquids were used, but also alkylammonium, respectively functionalized alkylammonium cations were used in combination with the TFSI anion (cf. Figure 19, Group 3). Therefore, two alkylammonium cations with different alkyl chain length in one position were chosen, namely *N*-hexyl-*N*,*N*,*N*-trimethylammonium TFSI (HTMA TFSI) and *N*-decyl-*N*,*N*,*N*-trimethylammonium TFSI (DTMA TFSI), and one ester-functionalized IL, acetylcholine TFSI (ACh TFSI). The starting concentration for these ILs was 0.01 M and the starting volume was 0.1 mL. The concentration was increased in steps of 0.01 M and the solutions were always stirred for at least three hours before the concentration was raised. It was shown that all complexes **8**-**11** have nearly the solubility in HTMA TFSI and DTMA TFSI and that for a concentration of 0.05 M a saturated solution was obtained. Slight differences could be observed, so that for example the benzonitrile and the *tert*-butylnitrile derivatives **9** and **10** were faster dissolved than the other ones and that the dissolving took longer (about 2 h) in the more hydrophobic DTMA TFSI. However, the compounds showed a better solubility in ACh TFSI. All four complexes were dissolved quite fast in this IL and a concentration of 0.07 M could be reached. The same observations could be made as for HTMA TFSI and DTMA TFSI. As already mentioned, the color of the solutions corresponded to the color of the respective complex. Even after several months, there could not be observed any changes, indicating the long-term stability of these compounds in the ILs. The obtained concentrations for $[Cr(NCR)_{3\text{-}4}][BF_4]_2$ (**8**-**11**) in HTMA TFSI, DTMA TFSI, and ACh TFSI are summarized in table 5.

Table 5 Solubility of $[Cr(NCR)_{3\text{-}4}][BF_4]_2$ (**8**-**11**) in the ILs HTMA TFSI, DTMA TFSI and ACh TFSI. Concentrations are given in [M].

Number	Compound	HTMA TFSI	DTMA TFSI	ACh TFSI
8	$[Cr(NCCH_3)_3][BF_4]_2$	0.05	0.05	0.07
9	$[Cr(NCC_6H_5)_3][BF_4]_2$	0.05	0.05	0.07
10	$[Cr(NCC(CH_3)_3)_4][BF_4]_2$	0.05	0.05	0.07
11	$[Cr(NCC_2H_5)_4][BF_4]_2$	0.05	0.05	0.07

There were not only linear alkylammonium ionic liquids used but also some cyclic ammonium ILs, namely *N*-butyl-*N*-methylpyrrolidinium triflate (BMP OTf), *N*-butyl-*N*-methylpyrrolidinium TFSI (BMP TFSI) and *N*-butyl-*N*-methylpiperidinium TFSI (BMPip TFSI). In addition, the latter two cations were also functionalized with a methoxyethyl group resulting in 1-(2-methoxyethyl)-1-methylpyrrolidinium TFSI (MEMP TFSI) and 1-(2-methoxyethyl)-1-methylpiperidinium TFSI (MEMPip TFSI). In this context, the commercially available ILs Trihexyl(tetradecyl)phosphonium chloride ($P_{6,6,6,14}$ Cl) and Trihexyl(tetradecyl)phosphonium bis((trifluoromethyl)sulfonyl)amide ($P_{6,6,6,14}$ TFSI) were also applied for solubility tests. As mentioned above, the starting concentration for these ILs was also 0.01 M and the starting volume was 0.1 mL. The concentration was increased in steps of 0.01 M and the solutions were always stirred for at least three hours before the concentration was raised. After seeing that the compounds **8**-**11** were generally soluble in these group of ILs as well, the volume was also increased to 0.5 mL. $[Cr(NCCH_3)_3][BF_4]_2$ (**8**) could be generally dissolved completely for all ionic liquids for a concentration up to 0.04 M. For the ILs BMP OTf, BMP TFSI and BMPip TFSI a concentration of 0.05 M was obtained. Whereat it could be observed, that the compound was dissolved completely quite faster in BMP TFSI than in BMP OTf. This could be attributed to the impact of the anion of the ionic liquid and also, that **8** could be dissolved a little bit better in BMP TFSI than in BMPip TFSI, which could be traced back to the slightly higher hydrophobic character of BMPip than BMP. By introducing the functionalized methoxyethyl groups into the ILs resulting in MEMP TFSI and MEMPip TFSI, a higher concentration of 0.07 M for **8** could be received. The observations for these ILs were very similar to those of BMP TFSI and BMPip TFSI. The compounds **9** and **10** showed a very analog behavior to **8** for all the ILs. There were only slight differences such as a concentration of 0.06 M could be obtained for BMP TFSI and BMPip TFSI before a saturated solution was existent and the complexes dissolved quite faster than **8**, which corresponds with the previously mentioned results. As for the previous applied ionic liquids, $[Cr(NCC_2H_5)_4][BF_4]_2$ (**11**) revealed the worst solubility and solubility behavior. It was thoroughly dissolved in BMP OTf, BMP TFSI and BMPip TFSI up to a concentration of 0.05 M before a saturated solution was existent. In the more polar ILs MEMP TFSI and MEMPip TFSI, a slightly better solubility could be reached with 0.06 M, but this value is still lower compared to the other compounds. By far the worst solubility for all compounds of this group was obtained for $P_{6,6,6,14}$ Cl and $P_{6,6,6,14}$ TFSI. This can be attributed to the extremely high hydrophobic character of these ILs. It took more than 20 h until **8**-**11** were completely dissolved and the concentration could be increased. As already mentioned, the color of the solutions corresponded to the color of the respective complex. Even after several months, there could not be observed any changes, indicating the long-term stability of these compounds in the ionic liquids. The obtained concentrations for $[Cr(NCR)_{3\text{-}4}][BF_4]_2$ (**8**-**11**) in BMP OTf, BMP TFSI, BMPip TFSI, MEMP TFSI, MEMPip TFSI, $P_{6,6,6,14}$ Cl and $P_{6,6,6,14}$ TFSI are summarized in tables 6 and 7.

Table 6 Solubility of $[Cr(NCR)_{3\text{-}4}][BF_4]_2$ (**8**-**11**) in the ILs BMP OTf, BMP TFSI and BMPip TFSI. Concentrations are given in [M].

Number	Compound	BMP OTf	BMP TFSI	BMPip TFSI
8	$[Cr(NCCH_3)_3][BF_4]_2$	0.05	0.05	0.05
9	$[Cr(NCC_6H_5)_3][BF_4]_2$	0.05	0.06	0.06
10	$[Cr(NCC(CH_3)_3)_4][BF_4]_2$	0.05	0.06	0.06
11	$[Cr(NCC_2H_5)_4][BF_4]_2$	0.05	0.05	0.05

Table 7 Solubility of $[Cr(NCR)_{3\text{-}4}][BF_4]_2$ (**8**-**11**) in the ILs MEMP TFSI, MEMPip TFSI, $P_{6,6,6,14}$ Cl and $P_{6,6,6,14}$ TFSI. Concentrations are given in [M].

Number	Compound	MEMP TFSI	MEMPip TFSI	$P_{6,6,6,14}$ Cl	$P_{6,6,6,14}$ TFSI
8	$[Cr(NCCH_3)_3][BF_4]_2$	0.07	0.07	0.04	0.04
9	$[Cr(NCC_6H_5)_3][BF_4]_2$	0.07	0.07	0.04	0.04
10	$[Cr(NCC(CH_3)_3)_4][BF_4]_2$	0.07	0.07	0.04	0.04
11	$[Cr(NCC_2H_5)_4][BF_4]_2$	0.06	0.06	0.03	0.03

In conclusion, the complexes **8**-**11** of the group $[Cr(NCR)_{3\text{-}4}][BF_4]_2$ could be dissolved in different ionic liquids such as differently substituted alkylimidazolium, linear or cyclic alkylammonium or phosphonium cations with various anions. Furthermore, they show a high long-term stability in the ILs and a small impact of the different nitrile ligands can be observed. Unfortunately, the highest possible concentrations are only in a range 0.07 M before a saturated solution is obtained.

3.2.2 Solubility of $[Cr(NCR)_2][CF_3SO_3]_2$ (**12**-**15**) in RTILs

After it was shown that the complexes of the group $[Cr(NCR)_{3\text{-}4}][BF_4]_2$ (**8**-**11**) were generally soluble in various ionic liquids, the solubility of the next group of chromium containing complexes, $[Cr(NCR)_2][CF_3SO_3]_2$ (**12**-**15**), was investigated. It was started with a concentration of 0.01 M and a volume of the ionic liquid of 0.1 mL to analyze if the compounds $[Cr(NCR)_2][CF_3SO_3]_2$ (**12**-**15**) were generally soluble in ionic liquids. Just like for $[Cr(NCR)_{3\text{-}4}][BF_4]_2$ (**8**-**11**) it was begun with the alkyl-substituted imidazolium TFSI ILs EMIm TFSI, BMIm TFSI and OMIm TFSI for $[Cr(NCR)_2][CF_3SO_3]_2$ (**12**-**15**). By dissolving the compounds **12**-**15** in these three ionic liquids, it could be seen that all of them were generally soluble in these ILs and they were completely dissolved in all ILs after about one hour

at room temperature for a concentration of 0.01 M and a volume of 0.1 mL. Thus, the concentration was increased stepwise and the solutions were always stirred for at least three hours before the concentration was further raised. $[Cr(NCCH_3)_2][\ CF_3SO_3]_2$ (**12**) could be thoroughly dissolved in all three ionic liquids for a concentration of at least 0.05 M. Whereas it was completely dissolved after about 30 min for BMIm TFSI and OMIm TFSI for each step of increasing the concentration, it took more than two hours for each step for EMIm TFSI. Additionally, a saturated solution of **12** was received for EMIm TFSI at a concentration of 0.05 M. For the other two ionic liquids the concentration could be further increased to 0.07 M until a saturated solution was existent. These results corresponded with the results from chapter 3.2.1 for EMIm TFSI. A very similar behavior could be observed for the compounds **13** and **14**. The complexes were completely dissolved after about 15 min for every step, which is quite faster than **12**. However, it was not possible to obtain a higher concentration and the least solubility was also reached for EMIm TFSI, although it was possible to increase the concentration to 0.06 M for this IL. Contrary to $[Cr(NCC_2H_5)_4][BF_4]_2$ (**11**) which showed the least solubility in these three ILs, $[Cr(NCC_2H_5)_2][\ CF_3SO_3]_2$ (**15**) only showed a lower solubility for EMIm TFSI. It took a few hours until the complex was thoroughly dissolved in the ILs for every step and a saturated solution was already reached for 0.05 M for EMIm TFSI. A higher concentration of 0.07 M could be obtained for BMIm TFSI and OMIm TFSI. The color of all solutions corresponded to the color of the respective complex. After several months, there could not be observed any changes, indicating the long-term stability of these compounds in the ionic liquids. The obtained concentrations for $[Cr(NCR)_2][CF_3SO_3]_2$ (**12**-**15**) in EMIm TFSI, BMIm TFSI and OMIm TFSI are summarized in table 8.

Table 8 Solubility of $[Cr(NCR)_2][CF_3SO_3]_2$ (**12**-**15**) in the ILs EMIm TFSI, BMIm TFSI and OMIm TFSI. Concentrations are given in [M].

Number	Compound	EMIm TFSI	BMIm TFSI	OMIm TFSI
12	$[Cr(NCCH_3)_2][CF_3SO_3]_2$	0.05	0.07	0.07
13	$[Cr(NCC_6H_5)_2][CF_3SO_3]_2$	0.06	0.07	0.07
14	$[Cr(NCC(CH_3)_3)_2][CF_3SO_3]_2$	0.06	0.07	0.07
15	$[Cr(NCC_2H_5)_2][CF_3SO_3]_2$	0.05	0.07	0.07

An attempt to improve the solubility of this group of complexes for the alkyl-substituted imidazolium ILs is the substitution of the acidic proton of the imidazolium core, –N-C(H)-N–, for a methyl group. Therefore, the ILs EMMIm TFSI, BMMIm TFSI and OMMIm TFSI were synthesized. In addition, this series was continued with the complete alkylation of the imidazolium core by applying 1,2,4,5-tetramethylimidazole as starting material for the ILs. But since 1-ethyl-2,3,4,5-tetramelthylimidazolium TFSI and 1-butyl-2,3,4,5-tetramethlimidazolium TFSI exhibit a melting point below or close to room temperature, only the octyl derivative of this group could be used, namely 1-octyl-2,3,4,5-tetramethylimidazolium TFSI (OTMIm TFSI). The concentration was increased in steps of 0.01 M and the solutions were always

stirred for at least three hours before the concentration was raised. After seeing that the compounds **12**-**15** were generally soluble in these higher substituted ILs, the volume was also increased to 0.5 mL. **12** could be dissolved thoroughly in all four ionic liquids, though with different concentrations. Whereas it was completely dissolved after a time of about 20 min for every step of increasing the concentration in BMMIm TFSI, OMMIm TFSI and OTMIm TFSI, it took about 1 h for the IL EMMIm TFSI. This corresponds with the results from above, that the compound has an inferior solubility in the ethyl-substituted IL to the other ones. An already saturated solution of **12** in EMMIm TFSI was determined for a concentration of 0.05 M, whereas the concentration could be further increased to 0.07 M for BMIm TFSI, OMMIm TFSI and OTMIm TFSI until a saturated solution was existent. The compounds **13** and **14** showed a very similar behavior. They were completely dissolved after about 30 min for every step in every IL, however the same values for the concentration were obtained as for complex **12**. Just like for the other ionic liquids, the propionitrile derivative **15** showed the least solubility in these four ILs. It took longer than for the other complexes until it was completely dissolved for every step and a saturated solution was obtained for a concentration of 0.05 M for EMMIm TFSI and OTMIm TFSI, respectively 0.06 M for BMMIm TFSI and OMMIm TFSI. The color of all solutions corresponded to the color of the respective complex. After several months, the color of the solution did not change, which indicates the long-term stability of these complexes in these ILs. In conclusion, the use of higher substituted alkylimidazolium cations was only conditionally successful. The obtained concentrations for $[Cr(NCR)_2][CF_3SO_3]_2$ (**12**-**15**) in EMMIm TFSI, BMMIm TFSI, OMMIm TFSI and OTMIm TFSI are summarized in table 9.

Table 9 Solubility of $[Cr(NCR)_2][CF_3SO_3]_2$ (**12**-**15**) in the ILs EMMIm TFSI, BMMIm TFSI, OMMIm TFSI and OTMIm TFSI. Concentrations are given in [M].

Number	Compound	EMMIm TFSI	BMMIm TFSI	OMMIm TFSI	OTMIm TFSI
12	$[Cr(NCCH_3)_2][CF_3SO_3]_2$	0.05	0.07	0.07	0.07
13	$[Cr(NCC_6H_5)_2][CF_3SO_3]_2$	0.05	0.07	0.07	0.07
14	$[Cr(NCC(CH_3)_3)_2][CF_3SO_3]_2$	0.05	0.07	0.07	0.07
15	$[Cr(NCC_2H_5)_2][CF_3SO_3]_2$	0.05	0.06	0.06	0.05

To broaden the spectrum of ionic liquids in which the metalorganic complexes are soluble, not only imidazolium based ionic liquids were used, but also alkylammonium, respectively functionalized alkylammonium cations were used in combination with the TFSI anion (cf. Figure 19, Group 3). Therefore, HTMA TFSI and DTMA TFSI with a different alkyl chain length in one position were chosen and the ester-functionalized IL, acetylcholine TFSI (ACh TFSI). The starting concentration for these ILs was 0.01 M and the starting volume was 0.1 mL. The concentration was increased in steps of 0.01 M and the solutions were always stirred for at least three hours before the concentration was raised. It was shown that indeed all complexes **12**-**15** were generally soluble in this group of ILs, but they exhibit an

inferior solubility compared to the compounds **8**-**11** in these ILs. It could be observed that the complexes **12**-**14** were soluble in HTMA TFSI up to a concentration of 0.05 M until a saturated solution was existent, whereas **15** showed, as expected, the least concentration with 0.04 M. The solubility deteriorated by the use of the more hydrophobic IL DTMA TFSI for **12**, **14** and **15**. Merely the benzonitrile derivative **13** showed the same highest possible concentration of 0.05 M. The other compounds had a highest possible concentration of 0.04 M, respectively 0.03 M as in the case the propionitrile derivative **15**. However, slight differences could be observed such as that the benzonitrile and the *tert*-butylnitrile derivatives **13** and **14** were faster dissolved in both ILs than the other ones and that for all complexes the dissolving took longer in the more hydrophobic DTMA TFSI. Certainly, the compounds showed a better solubility in the more polar IL ACh TFSI. All four complexes were dissolved quite fast in this IL and a concentration of 0.07 M could be reached, respectively 0.06 M for **15**. As already mentioned, the color of the solutions corresponded to the color of the respective complex. Even after several months, there could not be observed any changes, indicating the long-term stability of these compounds in the ILs. The obtained concentrations for $[Cr(NCR)_2][CF_3SO_3]_2$ (**12**-**15**) in HTMA TFSI, DTMA TFSI, and ACh TFSI are summarized in table 10.

Table 10 Solubility of $[Cr(NCR)_2][CF_3SO_3]_2$ (**12**-**15**) in the ILs HTMA TFSI, DTMA TFSI, and ACh TFSI. Concentrations are given in [M].

Number	Compound	HTMA TFSI	DTMA TFSI	ACh TFSI
12	$[Cr(NCCH_3)_2][CF_3SO_3]_2$	0.05	0.04	0.07
13	$[Cr(NCC_6H_5)_2][CF_3SO_3]_2$	0.05	0.05	0.07
14	$[Cr(NCC(CH_3)_3)_2][CF_3SO_3]_2$	0.05	0.04	0.07
15	$[Cr(NCC_2H_5)_2][CF_3SO_3]_2$	0.04	0.03	0.06

With the ILs BMP OTf, BMP TFSI and BMPip TFSI not only linear alkylammonium ionic liquids used but also some cyclic ammonium ILs. In addition, the latter two cations were also functionalized with a methoxyethyl group resulting in MEMP TFSI and MEMPip TFSI. In this context, the commercially available ILs $P_{6,6,6,14}$ Cl and $P_{6,6,6,14}$ TFSI were also applied for solubility tests. As mentioned above, the starting concentration for these ILs was also 0.01 M and the starting volume was 0.1 mL. After seeing that the compounds **12**-**15** were generally soluble in these group of ILs as well, the volume was also increased to 0.5 mL. All compounds revealed a quite good solubility in BMP OTf and a concentration of 0.06 M could be obtained, which is slightly higher than for the compounds **8**-**11**. Also, the complexes dissolved a little bit faster than the corresponding derivatives **8**-**11**. This could be associated with the fact, that the ionic liquid has the same anion as the complexes and that therefore a slightly better solubility could be enabled. As mentioned above for BMP TFSI and BMPip TFSI, a similar behavior could be observed for the compounds **12**-**15**. All complexes were soluble in BMP TFSI and BMPip TFSI, whereat a concentration of 0.06 M was obtained for **13** and **14** and a slightly lower one of 0.05 M for **12**

and **15** as expected due to the so far received results of the general solubility of propionitrile derivatives. There were small differences between BMP TFSI and BMPip TFSI such as that the compounds were dissolved completely a little bit faster in BMP TFSI than in BMPip TFSI, which could be attributed to the slightly higher hydrophobic character of BMPip than BMP. By introducing the functionalized methoxyethyl groups into the ILs resulting in MEMP TFSI and MEMPip TFSI, a higher concentration of 0.07 M for **12**-**14** could be received. The observations for these two ILs corresponded with those of BMP TFSI and BMPip TFSI. As for the previous ionic liquids, **15** revealed a worse solubility and solubility behavior. It could be thoroughly dissolved in MEMP TFSI and MEMPip TFSI up to a concentration of 0.06 M before a saturated solution was existent. By far the worst solubility for all compounds of this group was obtained for $P_{6,6,6,14}$ Cl and $P_{6,6,6,14}$ TFSI. This can be attributed to the extremely high hydrophobic character of these ILs. It took more than 48 h until **12**-**15** were completely dissolved and the concentration could be increased. **13** and **14** showed a little better solubility with 0.05 M than **12** and **15** with 0.04 M as the highest possible concentration. As already mentioned, the color of the solutions corresponded to the color of the respective complex. Even after several months, there could not be observed any changes, indicating the long-term stability of these compounds in the ionic liquids. The obtained concentrations for $[Cr(NCR)_2][CF_3SO_3]_2$ (**12**-**15**) in BMP OTf, BMP TFSI, BMPip TFSI, MEMP TFSI, MEMPip TFSI, $P_{6,6,6,14}$ Cl and $P_{6,6,6,14}$ TFSI are summarized in tables 11 and 12.

In conclusion, the complexes **12**-**15** of the group $[Cr(NCR)_2][CF_3SO_3]_2$ could be dissolved in different ionic liquids such as differently substituted alkylimidazolium, linear or cyclic alkylammonium or phosphonium cations with various anions. Furthermore, they all show a high long-term stability in the ILs and a small impact of the different nitrile ligands can be observed. For some combinations of compound and ionic liquid a higher concentration could be obtained in comparison to the corresponding derivative of the compounds **8**-**11**. Unfortunately, the highest possible concentrations are only in a range 0.07 M before a saturated solution is obtained.

Table 11 Solubility of $[Cr(NCR)_2][CF_3SO_3]_2$ (**12**-**15**) in the ILs BMP OTf, BMP TFSI, and BMPip TFSI. Concentrations are given in [M].

Number	Compound	BMP OTf	BMP TFSI	BMPip TFSI
12	$[Cr(NCCH_3)_2][CF_3SO_3]_2$	0.06	0.05	0.05
13	$[Cr(NCC_6H_5)_2][\ CF_3SO_3]_2$	0.06	0.06	0.06
14	$[Cr(NCC(CH_3)_3)_2][CF_3SO_3]_2$	0.06	0.06	0.06
15	$[Cr(NCC_2H_5)_2][CF_3SO_3]_2$	0.06	0.05	0.05

Table 12 Solubility of $[Cr(NCR)_2][CF_3SO_3]_2$ (**12**-**15**) in the ILs MEMP TFSI, MEMPip TFSI, $P_{6,6,6,14}$ Cl and $P_{6,6,6,14}$ TFSI. Concentrations are given in [M].

Number	Compound	MEMP TFSI	MEMPip TFSI	$P_{6,6,6,14}$ Cl	$P_{6,6,6,14}$ TFSI
12	$[Cr(NCCH_3)_2][CF_3SO_3]_2$	0.07	0.07	0.04	0.04
13	$[Cr(NCC_6H_5)_2][CF_3SO_3]_2$	0.07	0.07	0.05	0.05
14	$[Cr(NCC(CH_3)_3)_2][CF_3SO_3]_2$	0.07	0.07	0.05	0.05
15	$[Cr(NCC_2H_5)_2][CF_3SO_3]_2$	0.06	0.06	0.04	0.04

3.2.3 Solubility of $[Cr(O_2CCH_3)(NCCH_3)_2][TFSI]$ (**16**) in RTILs

Due to the poor yield of $[Cr(O_2CCH_3)(NCCH_3)_2][TFSI]$ (**16**) which could unfortunately not be further improved as discussed in chapter 3.1.3, it was not possible to conduct thorough solubility tests determining a concentration. However, a small amount of **16** was dissolved in some selected ionic liquids in order to show if the complex was generally soluble in these ILs. It could be seen that the compound is soluble in some ionic liquids and should be further investigated once a better yield is obtained. The received results are summarized in table 13.

Table 13 Solubility of $[Cr(O_2CCH_3)(NCCH_3)_2][TFSI]$ (**16**) in some selected ionic liquids. Concentrations are given in [M].

Number	Compound	BMIm TFSI	BMMIm TFSI	BMP TFSI
		✓	✓	✓
16	$[Cr(O_2CCH_3)(NCCH_3)_2][TFSI]$	**HTMA TFSI**	**ACh TFSI**	**MEMP TFSI**
		✓	✓	✓

3.2.4 Solubility of $[Mo_2(NCR)_{8\text{-}10}][BF_4]_4$ (**18**-**21**) in RTILs

It was shown in the chapters 3.2.1 – 3.2.3 that several chromium containing complexes can be dissolved in various ionic liquids. In the next step, not only the solubility of the chromium compounds **8**-**16** was investigated, but also the solubility and the solubility behavior of several molybdenum containing complexes were examined. For the beginning, a concentration of 0.01 M and a volume of the ionic liquid of 0.1 mL were chosen to analyze if the compounds $[Mo_2(NCR)_{8\text{-}10}][BF_4]_4$ (**18**-**21**) are generally soluble in ionic liquids. Just like for $[Cr(NCR)_{3\text{-}4}][BF_4]_2$ (**8**-**11**), ionic liquids were chosen with an alkyl-substituted imidazolium cation with different alkyl chain lengths and the TFSI anion, EMIm TFSI, BMIm TFSI and OMIm TFSI. By dissolving the compounds **18**-**21** in these three ILs, it could be seen that all compounds

were completely dissolved in all ILs after about 1 h at room temperature for a concentration of 0.01 M and a volume of 0.1 mL. Therefore, the concentration was increased stepwise and the solutions were always stirred for at least three hours before the concentration was raised. After seeing that the compounds are generally soluble in the ILs, the volume was also increased to 0.5 mL. **18** could be dissolved completely in all three ionic liquids, though with different concentrations. Whereas it was completely dissolved after a time of about two hours for BMIm TFSI and OMIm TFSI for every step of increasing the concentration, it took more than four hours for each step until it was completely dissolved in EMIm TFSI. In addition, an already saturated solution of **18** in EMIm TFSI was determined for a concentration of 0.05 M, while a concentration of 0.07 M was possible to reach for BMIm TFSI and OMIm TFSI. A very similar behavior could be observed for the compounds **19** and **20**. Both could be thoroughly dissolved after about 1 h in all three ILs, which was a little bit faster than for **18**. However, it was not possible to obtain a higher concentration than 0.07 M in BMIm TFSI and OMIm TFSI. Both compounds showed a lower solubility for EMIm TFSI, which was already expected due to the so far obtained results concerning this ionic liquid. As already seen for the other propionitrile derivatives **11** and **15**, $[Mo_2(NCC_2H_5)_{10}][BF_4]_4$ also showed the least solubility in the ILs. It took almost 24 h until the complex was completely dissolved for every step and a saturated solution was already reached for a concentration of 0.05 M in EMIm TFSI, respectively 0.06 M for BMIm TFSI and OMIm TFSI. The color of all solutions corresponded to the color of the respective complex. After several months, the color of the solution did not change, which indicates the long-term stability of these complexes in these ionic liquids. The obtained concentrations for $[Mo_2(NCR)_{8\text{-}10}][BF_4]_4$ (**18**-**21**) in EMIm TFSI, BMIm TFSI and OMIm TFSI are summarized in table 14.

Table 14 Solubility of $[Mo_2(NCR)_{8\text{-}10}][BF_4]_4$ (**18**-**21**) in the ILs EMIm TFSI, BMIm TFSI and OMIm TFSI. Concentrations are given in [M].

Number	Compound	EMIm TFSI	BMIm TFSI	OMIm TFSI
18	$[Mo_2(NCCH_3)_8][BF_4]_4$	0.05	0.07	0.07
19	$[Mo_2(NCC_6H_5)_8][BF_4]_4$	0.05	0.07	0.07
20	$[Mo_2(NCC(CH_3)_3)_{10}][BF_4]_4$	0.05	0.07	0.07
21	$[Mo_2(NCC_2H_5)_{10}][BF_4]_4$	0.05	0.06	0.06

A possibility to enhance the solubility of this group of complexes for the alkyl-substituted imidazolium ILs is the substitution of the acidic proton of the imidazolium core, –N-C(H)-N–, for a methyl group. Therefore, the ILs EMMIm TFSI, BMMIm TFSI and OMMIm TFSI were synthesized. In addition, this series was continued with the complete alkylation of the imidazolium core by applying 1,2,4,5-tetramethylimidazole as starting material for the ILs. But since 1-ethyl-2,3,4,5-tetramelthylimidazolium TFSI and 1-butyl-2,3,4,5-tetramethlimidazolium TFSI exhibit a melting point below or close to room temperature, only the octyl derivative of this group could be used, OTMIm TFSI. The concentration was

increased in steps of 0.01 M and the solutions were always stirred for at least three hours before the concentration was raised. After seeing that the compounds **18**-**21** were generally soluble in these higher substituted ILs, the volume was also increased to 0.5 mL. **18** could be dissolved thoroughly in all four ionic liquids, though with different concentrations. Whereas it was completely dissolved after a time of about one hour for every step of increasing the concentration in BMMIm TFSI, OMMIm TFSI and OTMIm TFSI, it took about 3 h for the IL EMMIm TFSI. This corresponds with the results from above, that the compound has an inferior solubility in the ethyl-substituted IL to the other ones. An already saturated solution of **18** in EMMIm TFSI was determined for a concentration of 0.05 M, whereas the concentration could be further increased to 0.07 M for BMMIm TFSI, OMMIm TFSI and OTMIm TFSI until a saturated solution was existent. As expected, the compounds **19** and **20** showed an analog behavior. The only difference was that the complexes were completely dissolved a little bit faster than **18**. Despite their beneficial solubility behavior, it was not possible to get a higher concentration than 0.07 M for BMMIm TFSI, OMMIm TFSI and OTMIm TFSI. Just like for **18**, a concentration of 0.05 M was obtained for **19** and **20** in EMMIm TFSI. As for the other ionic liquids, the propionitrile derivative **21** showed the least solubility in these four ILs. It took longer than for the other complexes until it was thoroughly dissolved for every step and a saturated solution was obtained for a concentration of 0.05 M for EMMIm TFSI., respectively 0.06 M for OMMIm TFSI and OTMIm TFSI. Merely for the IL BMMIm TFSI a concentration of 0.07 M could be received, which is the highest concentration of a propionitrile derivative in an ionic liquid. The color of all solutions corresponded to the color of the respective complex. After several months, the color of the solution did not change, which indicates the long-term stability of these complexes in these ILs. In conclusion, the use of higher substituted alkylimidazolium cations was insofar successful as a concentration of 0.07 M for a propionitrile derivative could be obtained. The received concentrations for $[Mo_2(NCR)_{8\text{-}10}][BF_4]_4$ (**18**-**21**) in EMMIm TFSI, BMMIm TFSI, OMMIm TFSI and OTMIm TFSI are summarized in table 15.

Table 15 Solubility of $[Mo_2(NCR)_{8\text{-}10}][BF_4]_4$ (**18**-**21**) in the ILs EMMIm TFSI, BMMIm TFSI, OMMIm TFSI and OTMIm TFSI. Concentrations are given in [M].

Number	Compound	EMMIm TFSI	BMMIm TFSI	OMMIm TFSI	OTMIm TFSI
18	$[Mo_2(NCCH_3)_8][BF_4]_4$	0.05	0.07	0.07	0.07
19	$[Mo_2(NCC_6H_5)_8][BF_4]_4$	0.05	0.07	0.07	0.07
20	$[Mo_2(NCC(CH_3)_3)_{10}][BF_4]_4$	0.05	0.07	0.07	0.07
21	$[Mo_2(NCC_2H_5)_{10}][BF_4]_4$	0.05	0.07	0.06	0.06

To broaden the spectrum of ionic liquids in which the complexes $[Mo_2(NCR)_{8\text{-}10}][BF_4]_4$ (**18**-**21**) are soluble, not only imidazolium based ionic liquids were used, but also alkylammonium, respectively functionalized alkylammonium cations were used in combination with the TFSI anion (cf. Figure 19, Group 3). Therefore, HTMA TFSI and DTMA TFSI with a different alkyl chain length in one position were selected

and the ester-functionalized IL, acetylcholine TFSI (ACh TFSI). The starting concentration for these ILs was 0.01 M and the starting volume was 0.1 mL. The compounds were generally soluble in this group of ionic liquids. It could be observed for HTMA TFSI that **18** could be dissolved up to a concentration of 0.04 M while **19** and **20** showed, as expected, a slightly higher solubility and 0.05 M could be reached. However, for **21** it took the longest for every step of increasing the concentration, until the compound was thoroughly dissolved and already at 0.03 M a saturated solution was existent. The solubility deteriorated by the use of the more hydrophobic IL DTMA TFSI for **19** and **20**. The acetonitrile derivative **18** and propionitrile compound **21** showed the same highest possible concentration of 0.04 M, respectively 0.03 M. In addition, it took somewhat longer until the complexes dissolved in DTMA TFSI. Certainly, the compounds showed a better solubility in the more polar IL ACh TFSI. All four complexes were dissolved quite fast in this IL and a concentration of 0.05 M could be reached, respectively 0.04 M for **21**. As already mentioned, the color of the solutions corresponded to the color of the respective complex. Even after several months, there could not be observed any changes, indicating the long-term stability of these compounds in the ILs. The obtained concentrations for $[Mo_2(NCR)_{8\text{-}10}][BF_4]_4$ (**18**-**21**) in HTMA TFSI, DTMA TFSI, and ACh TFSI are summarized in table 16.

Table 16 Solubility of $[Mo_2(NCR)_{8\text{-}10}][BF_4]_4$ (**18**-**21**) in the ILs HTMA TFSI, DTMA TFSI, and ACh TFSI. Concentrations are given in [M].

Number	Compound	HTMA TFSI	DTMA TFSI	ACh TFSI
18	$[Mo_2(NCCH_3)_8][BF_4]_4$	0.04	0.04	0.05
19	$[Mo_2(NCC_6H_5)_8][BF_4]_4$	0.05	0.04	0.05
20	$[Mo_2(NCC(CH_3)_3)_{10}][BF_4]_4$	0.05	0.04	0.05
21	$[Mo_2(NCC_2H_5)_{10}][BF_4]_4$	0.03	0.03	0.04

The solubility of the complexes of the group $[Mo_2(NCR)_{8\text{-}10}][BF_4]_4$ was not only investigated in linear alkylammonium ionic liquids but also in some cyclic ammonium ILs such as BMP OTf, BMP TFSI and BMPip TFSI. In addition, the latter two cations were also functionalized with a methoxyethyl group resulting in MEMP TFSI and MEMPip TFSI. In this context, the commercially available ILs $P_{6,6,6,14}$ Cl and $P_{6,6,6,14}$ TFSI were also applied for solubility tests. As mentioned above, the starting concentration for these ILs was also 0.01 M and the starting volume was 0.1 mL. After seeing that the compounds **18**-**21** were generally soluble in these group of ILs as well, the volume was also increased to 0.5 mL. Starting with the IL BMP OTf, **19** and **20** could be dissolved up to a concentration of 0.05 M, whereat it took about two hours until both compounds were completely dissolved for every step. Contrary, for **18** and **21** it took almost 5 hours until they were thoroughly dissolved, and a concentration of 0.04 M could be obtained. As mentioned above for BMP TFSI and BMPip TFSI, a similar behavior could be observed for the compounds **18**-**21**. All complexes were soluble in BMP TFSI and BMPip TFSI, whereat a concentration of 0.05 M was obtained for **18**-**21** in BMP TFSI and BMPip TFSI. Merely, **21** showed a

lower concentration of 0.04 M in BMPip TFSI, but this corresponded with the so far received results of the general solubility of propionitrile derivatives. There were only small differences between BMP TFSI and BMPip TFSI which could be observed, such as that the compounds were dissolved completely a little bit faster in BMP TFSI than in BMPip TFSI, which could be attributed to the slightly higher hydrophobic character of BMPip than BMP. By introducing the functionalized methoxyethyl groups into the ILs resulting in MEMP TFSI and MEMPip TFSI, a higher concentration of 0.06 M for **18**-**20** could be received. The observations for these two ILs corresponded with those of BMP TFSI and BMPip TFSI. As for the previous ionic liquids, **21** revealed a worse solubility and solubility behavior. It was possible to dissolve it thoroughly in MEMP TFSI and MEMPip TFSI up to a concentration of 0.05 M before a saturated solution was existent. By far the worst solubility for all compounds of this group was shown for $P_{6,6,6,14}$ Cl and $P_{6,6,6,14}$ TFSI. This can be attributed to the extremely high hydrophobic character of these ILs. It took almost four days until **18**-**21** were completely dissolved and the concentration could be increased. **19** and **20** showed a little better solubility with 0.04 M than **18** and **21** with only 0.03 M as the highest possible concentration. As already mentioned, the color of the solutions corresponded to the color of the respective complex. Even after several months, there could not be observed any changes, indicating the long-term stability of these compounds in the ionic liquids. The obtained concentrations for $[Mo_2(NCR)_{8\text{-}10}][BF_4]_4$ (**18**-**21**) in BMP OTf, BMP TFSI, BMPip TFSI, MEMP TFSI, MEMPip TFSI, $P_{6,6,6,14}$ Cl and $P_{6,6,6,14}$ TFSI are summarized in tables 17 and 18.

In conclusion, the complexes **18**-**21** of the group $[Mo_2(NCR)_{8\text{-}10}][BF_4]_4$ could be dissolved in different ionic liquids such as differently substituted alkylimidazolium, linear or cyclic alkylammonium or phosphonium cations with various anions. Furthermore, they all show a high long-term stability in the ILs and a small impact of the different nitrile ligands can be observed. Unfortunately, the highest possible concentrations are only in a range 0.06 M before a saturated solution is obtained.

Table 17 Solubility of $[Mo_2(NCR)_{8\text{-}10}][BF_4]_4$ (**18**-**21**) in the ILs BMP OTf, BMP TFSI, and BMPip TFSI. Concentrations are given in [M].

Number	Compound	BMP OTf	BMP TFSI	BMPip TFSI
18	$[Mo_2(NCCH_3)_8][BF_4]_4$	0.04	0.05	0.05
19	$[Mo_2(NCC_6H_5)_8][BF_4]_4$	0.05	0.05	0.05
20	$[Mo_2(NCC(CH_3)_3)_{10}][BF_4]_4$	0.05	0.05	0.05
21	$[Mo_2(NCC_2H_5)_{10}][BF_4]_4$	0.04	0.05	0.04

Table 18 Solubility of $[Mo_2(NCR)_{8\text{-}10}][BF_4]_4$ (**18**-**21**) in the ILs MEMP TFSI, MEMPip TFSI, $P_{6,6,6,14}Cl$ and $P_{6,6,6,14}$ TFSI. Concentrations are given in [M].

Number	Compound	MEMP TFSI	MEMPip TFSI	$P_{6,6,6,14}Cl$	$P_{6,6,6,14}$ TFSI
18	$[Mo_2(NCCH_3)_8][BF_4]_4$	0.06	0.06	0.03	0.03
19	$[Mo_2(NCC_6H_5)_8][BF_4]_4$	0.06	0.06	0.04	0.04
20	$[Mo_2(NCC(CH_3)_3)_{10}][BF_4]_4$	0.06	0.06	0.04	0.04
21	$[Mo_2(NCC_2H_5)_{10}][BF_4]_4$	0.05	0.05	0.03	0.03

3.2.5 Solubility of $[Mo_2(NCR)_{7\text{-}10}][CF_3SO_3]_4$ (**22**-**25**) in RTILs

It was shown in chapter 3.2.4 that the molybdenum containing complexes $[Mo_2(NCR)_{7\text{-}10}][CF_3SO_3]_4$ (**22**-**25**) can be dissolved in various ionic liquids. In the next step, the solubility and the solubility behavior of their triflate derivatives $[Mo_2(NCR)_{7\text{-}10}][CF_3SO_3]_4$ were investigated. For the beginning, a concentration of 0.01 M and a volume of the ionic liquid of 0.1 mL were chosen to analyze if the compounds of the group $[Mo_2(NCR)_{7\text{-}10}][CF_3SO_3]_4$ (**22**-**25**) are generally soluble in ionic liquids. ILs were used with an alkyl-substituted imidazolium cation with different alkyl chain lengths and the TFSI anion, EMIm TFSI, BMIm TFSI and OMIm TFSI. By dissolving **22**-**25** in these three ILs, it could be observed, that all compounds were thoroughly dissolved in all ILs after about two hours at room temperature for a concentration of 0.01 M and a volume of 0.1 mL. Therefore, the volume was increased to 0.5 mL and the solutions were always stirred for at least three hours before the concentration was raised in steps of 0.01 M. **22** could be dissolved completely in all three ionic liquids, though with different concentrations. Whereas it was thoroughly dissolved after a time of about two hours for BMIm TFSI and OMIm TFSI for every step of increasing the concentration, it took more than four hours for each step until it was completely dissolved in EMIm TFSI. In addition, an already saturated solution of **22** in EMIm TFSI was determined for a concentration of 0.05 M, while a concentration of 0.07 M was possible to reach for BMIm TFSI and 0.06 M for OMIm TFSI. **23** and **24** showed a very similar behavior. They were both completely dissolved in all three ILs after about one hour, which is somewhat faster than for **22**. However, it was not possible to obtain a higher concentration than 0.07 M in BMIm TFSI and OMIm TFSI. Both compounds showed a lower solubility for EMIm TFSI, which was already expected due to the so far obtained results concerning this ionic liquid. As already seen for the other propionitrile derivatives with molybdenum **21** and also with chromium **11** and **15**, $[Mo_2(NCC_2H_5)_8][CF_3SO_3]_4$ also showed the least solubility in the ILs. It took almost 18 h until the complex was completely dissolved for every step and a saturated solution was already reached for a concentration of 0.05 M in all three ILs. The color of all solutions corresponded to the color of the respective complex. After several months, the color of the solution did not change, which indicates the long-term stability of these complexes in these ionic liquids. The obtained concentrations for $[Mo_2(NCR)_{7\text{-}10}][CF_3SO_3]_4$ (**22**-**25**) in EMIm TFSI, BMIm TFSI and OMIm TFSI are summarized in table 19.

Table 19 Solubility of $[Mo_2(NCR)_{7\text{-}10}][CF_3SO_3]_4$ (**22**-**25**) in the ILs EMIm TFSI, BMIm TFSI, and OMIm TFSI. Concentrations are given in [M].

Number	Compound	EMIm TFSI	BMIm TFSI	OMIm TFSI
22	$[Mo_2(NCCH_3)_7][CF_3SO_3]_4$	0.05	0.07	0.06
23	$[Mo_2(NCC_6H_5)_7][CF_3SO_3]_4$	0.06	0.07	0.07
24	$[Mo_2(NCC(CH_3)_3)_{10}][CF_3SO_3]_4$	0.06	0.07	0.07
25	$[Mo_2(NCC_2H_5)_8][CF_3SO_3]_4$	0.05	0.05	0.05

The substitution of the acidic proton of the imidazolium core of the alkyl-substituted imidazolium ILs for a methyl group leads to a further group of ILs, which can be used to test the solubility of the compounds $[Mo_2(NCR)_{7\text{-}10}][CF_3SO_3]_4$ (**22**-**25**). Therefore, the ILs EMMIm TFSI, BMMIm TFSI and OMMIm TFSI were synthesized. In addition, this series was continued with the complete alkylation of the imidazolium core by applying 1,2,4,5-tetramethylimidazole as starting material for the ILs. But since 1-ethyl-2,3,4,5-tetramelthylimidazolium TFSI and 1-butyl-2,3,4,5-tetramethlimidazolium TFSI exhibit a melting point below or close to room temperature, only the octyl derivative of this group could be used, OTMIm TFSI. It could be observed that all compounds were generally soluble in these higher substituted ILs. **22** showed a very similar behavior to the previous mentioned ILs and also in comparison with compound **18** in these ILs. It could be dissolved thoroughly in all the ILs, but the lowest concentration was obtained for the ethyl-substituted ionic liquid. A saturated solution was already existent at a concentration of 0.05 M. Furthermore, it took longer until the compound was dissolved than for the other complexes of this group. For the ILs with longer alkyl chains, BMMIm TFSI, OMMIm TFSI and OTMIm TFSI, a higher concentration of 0.07 M could be obtained. This corresponds with the results from above, that the compound has an inferior solubility in the ethyl-substituted IL compared to the other ones. As expected, the compounds **23** and **24** showed an analog behavior. The only difference was that the complexes were completely dissolved a little bit faster than **22**. Despite their beneficial solubility behavior, it was not possible to get a higher concentration than 0.07 M for BMMIm TFSI, OMMIm TFSI and OTMIm TFSI. Just like for **18** and **22**, a concentration of 0.05 M was obtained for **23** and **24** in EMMIm TFSI. As for the other ionic liquids, the propionitrile derivative **25** showed the least solubility in these four ILs. It took longer than for the other complexes until it was completely dissolved for every step and a saturated solution was obtained for a concentration of 0.05 M for EMMIm TFSI and OTMIm TFSI, respectively 0.06 M for OMMIm TFSI. Merely for the IL BMMIm TFSI a concentration of 0.07 M could be received, which is one of the highest concentrations of a propionitrile derivative in an ionic liquid. The color of all solutions corresponded to the color of the respective complex. After several months, the color of the solution did not change, which indicates the long-term stability of these complexes in these ILs. In conclusion, the use of higher substituted alkylimidazolium cations was insofar successful as a concentration of 0.07 M for a propionitrile derivative could be obtained. The received concentrations for $[Mo_2(NCR)_{7\text{-}10}][CF_3SO_3]_4$ (**22**-**25**) in EMMIm TFSI, BMMIm TFSI, OMMIm TFSI and OTMIm TFSI are summarized in table 20.

Table 20 Solubility of $[Mo_2(NCR)_{7\text{-}10}][CF_3SO_3]_4$ (**22**-**25**) in the ILs EMMIm TFSI, BMMIm TFSI, OMMIm TFSI and OTMIm TFSI. Concentrations are given in [M].

Number	Compound	EMMIm TFSI	BMMIm TFSI	OMMIm TFSI	OTMIm TFSI
22	$[Mo_2(NCCH_3)_7][CF_3SO_3]_4$	0.05	0.07	0.07	0.07
23	$[Mo_2(NCC_6H_5)_7][CF_3SO_3]_4$	0.06	0.07	0.07	0.07
24	$[Mo_2(NCC(CH_3)_3)_{10}][CF_3SO_3]_4$	0.06	0.07	0.07	0.07
25	$[Mo_2(NCC_2H_5)_8][CF_3SO_3]_4$	0.05	0.07	0.06	0.05

Besides the various alky-substituted imidazolium ionic liquids, some alkylammonium, respectively functionalized alkylammonium cations were used in combination with the TFSI anion in order to investigate the solubility of $[Mo_2(NCR)_{7\text{-}10}][CF_3SO_3]_4$ (**22**-**25**). Therefore, HTMA TFSI and DTMA TFSI with a different alkyl chain length in one position were selected and the ester-functionalized IL, acetylcholine TFSI (ACh TFSI). The starting concentration for these ILs was 0.01 M and the starting volume was 0.1 mL. The compounds were generally soluble in this group of ionic liquids. It could be observed for HTMA TFSI that all compounds could be dissolved up to a concentration of 0.04 M. At this point a saturated solution for **25** was existent, while it was possible to increase the concentration to 0.05 M for **22**-**24**. Furthermore, it took longer for **25** to be dissolved completely than for the other ones. The solubility deteriorated by the use of the more hydrophobic IL DTMA TFSI for **22** ad **25**. In addition, it took somewhat longer until the complexes dissolved in DTMA TFSI due to its slightly higher hydrophobic character. The benzonitrile and *tert*-buylnitrile derivatives showed a better solubility behavior in general, which is probably why the same concentration of 0.05 M could be obtained as in HTMA TFSI. Certainly, the compounds showed a better solubility in the more polar IL ACh TFSI. All four complexes were dissolved quite fast in this IL and a concentration of 0.06 M could be reached for **22**-**25**. As already mentioned, the color of the solutions corresponded to the color of the respective complex. Even after several months, there could not be observed any changes, indicating the long-term stability of these compounds in the ILs. The obtained concentrations for $[Mo_2(NCR)_{7\text{-}10}][CF_3SO_3]_4$ (**22**-**25**) in HTMA TFSI, DTMA TFSI, and ACh TFSI are summarized in table 21.

Table 21 Solubility of $[Mo_2(NCR)_{7\text{-}10}][CF_3SO_3]_4$ (**22**-**25**) in the ILs HTMA TFSI, DTMA TFSI, and ACh TFSI. Concentrations are given in [M].

Number	Compound	HTMA TFSI	DTMA TFSI	ACh TFSI
22	$[Mo_2(NCCH_3)_7][CF_3SO_3]_4$	0.05	0.04	0.06
23	$[Mo_2(NCC_6H_5)_7][CF_3SO_3]_4$	0.05	0.05	0.06
24	$[Mo_2(NCC(CH_3)_3)_{10}][CF_3SO_3]_4$	0.05	0.05	0.06
25	$[Mo_2(NCC_2H_5)_8][CF_3SO_3]_4$	0.04	0.04	0.06

The solubility of the complexes of the group $[Mo_2(NCR)_{7\text{-}10}][CF_3SO_3]_4$ was also investigated in some cyclic ammonium ILs such as BMP OTf, BMP TFSI and BMPip TFSI. In addition, the latter two cations were also functionalized with a methoxyethyl group resulting in MEMP TFSI and MEMPip TFSI. In this context, the commercially available ILs $P_{6,6,6,14}$ Cl and $P_{6,6,6,14}$ TFSI were also applied for solubility tests. As mentioned above, the starting concentration for these ILs was also 0.01 M and the starting volume was 0.1 mL. After seeing that the compounds **22**-**25** were generally soluble in these group of ILs as well, the volume was also increased to 0.5 mL. All compounds revealed a quite good solubility in BMP OTf and a concentration of 0.06 M could be obtained, which is slightly higher than for the compounds **18**-**21** in this IL. Also, the complexes dissolved a little bit faster than the corresponding derivatives. This could be associated with the fact, that the ionic liquid contains the same anion as the complexes and that therefore a slightly better solubility could be enabled. This property could also already be observed for the chromium containing complexes $[Cr(NCR)_2][CF_3SO_3]_2$ (**12**-**15**). In comparison with **18**-**21**, a similar behavior could be noticed for **22**-**25** in BMP TFSI and BMPip TFSI. All complexes were soluble in BMP TFSI and BMPip TFSI, whereat a concentration of 0.05 M was obtained for **22** and **25** in BMP TFSI and BMPip TFSI. **23** and **24** could be dissolved up to a concentration of 0.06 M in BMP TFSI, and their solubility degraded a little bit to 0.05 M by using BMPip TFSI. There were only small differences between BMP TFSI and BMPip TFSI which could be observed, such as that the compounds were dissolved completely a little bit faster in BMP TFSI than in BMPip TFSI, which could be attributed to the slightly higher hydrophobic character of BMPip than BMP. By introducing the functionalized methoxyethyl group into the ILs resulting in MEMP TFSI and MEMPip TFSI, a higher concentration was received for most of the complexes of this group. The observations for these two ILs corresponded with those of BMP TFSI and BMPip TFSI. A concentration of 0.06 M in MEMP TFSI, respectively 0.07 M, was obtained for **22**-**24**, which is slightly higher than in the more hydrophobic BMP TFSI. Merely **25** had the same concentration which was already expected due to the inferior solubility of the propionitrile containing complexes in the ionic liquids. By applying MEMPip TFSI instead of MEMP TFSI, the highest possible concentration deteriorated a little bit, which was already observed for BMP TFSI and BMPip TFSI. By far the worst solubility for all compounds of this group was shown for $P_{6,6,6,14}$ Cl and $P_{6,6,6,14}$ TFSI. This can be attributed to the extremely high hydrophobic character of these ILs. It took almost seven days until **22**-**25** were completely dissolved and the concentration could be increased. **23** and **24** showed a little better solubility with 0.04 M than **22** and **25** with only 0.03 M as the highest possible concentration. The color of the solutions corresponded to the color of the respective complex. Even after several months, there could not be observed any changes, indicating the long-term stability of these compounds in the ionic liquids. The obtained concentrations for $[Mo_2(NCR)_{7\text{-}10}][CF_3SO_3]_4$ (**22**-**25**) in BMP OTf, BMP TFSI, BMPip TFSI, MEMP TFSI, MEMPip TFSI, $P_{6,6,6,14}$ Cl and $P_{6,6,6,14}$ TFSI are summarized in tables 22 and 23.

In conclusion, the complexes **22**-**25** of the group $[Mo_2(NCR)_{7\text{-}10}][CF_3SO_3]_4$ could be dissolved in different ionic liquids such as differently substituted alkylimidazolium, linear or cyclic alkylammonium or phosphonium cations with various anions. In addition, they all show a high long-term stability in all applied ionic liquids and a small impact of the different nitrile ligands can be observed such as the lower solubility of the propionitrile derivatives. Unfortunately, the highest possible concentrations are only in a range 0.07 M before a saturated solution is obtained.

Table 22 Solubility of $[Mo_2(NCR)_{7\text{-}10}][CF_3SO_3]_4$ (**22**-**25**) in the ILs BMP OTf, BMP TFSI, and BMPip TFSI. Concentrations are given in [M].

Number	Compound	BMP OTf	BMP TFSI	BMPip TFSI
22	$[Mo_2(NCCH_3)_7][CF_3SO_3]_4$	0.06	0.05	0.05
23	$[Mo_2(NCC_6H_5)_7][CF_3SO_3]_4$	0.06	0.06	0.05
24	$[Mo_2(NCC(CH_3)_3)_{10}][CF_3SO_3]_4$	0.06	0.06	0.05
25	$[Mo_2(NCC_2H_5)_8][CF_3SO_3]_4$	0.06	0.05	0.05

Table 23 Solubility of $[Mo_2(NCR)_{7\text{-}10}][CF_3SO_3]_4$ (**22**-**25**) in the ILs MEMP TFSI, MEMPip TFSI, $P_{6,6,6,14}$ Cl and $P_{6,6,6,14}$ TFSI. Concentrations are given in [M].

Number	Compound	MEMP TFSI	MEMPip TFSI	$P_{6,6,6,14}$ Cl	$P_{6,6,6,14}$ TFSI
22	$[Mo_2(NCCH_3)_7][CF_3SO_3]_4$	0.06	0.05	0.03	0.03
23	$[Mo_2(NCC_6H_5)_7][CF_3SO_3]_4$	0.07	0.06	0.04	0.04
24	$[Mo_2(NCC(CH_3)_3)_{10}][CF_3SO_3]_4$	0.07	0.06	0.04	0.04
25	$[Mo_2(NCC_2H_5)_8][CF_3SO_3]_4$	0.05	0.04	0.03	0.03

3.2.6 Solubility of the complexes **26**, **27** and **30** in RTILs

In the previous chapters the solubility and the solubility behavior of various chromium and molybdenum containing complexes were investigated. For both metals, nitrile stabilized complexes were synthesized with either BF_4^- or $CF_3SO_3^-$ anions. It was shown that all of these complexes were generally soluble in various ionic liquids and highly stable, but unfortunately their concentration was very low compared to the concentrations which are required in order to enable a electrochemical deposition from ionic liquids (cf. chapters 1.3 and 1.4). The aim of this work was to not only dissolve the compounds in ionic liquids but also to improve their solubility. Since it could be seen that the complexes which contain the same anion as the ionic liquid exhibit a slightly better solubility, the weakly coordinating anion TFSI was incorporated into the nitrile stabilized metalorganic complex (cf. chapters 3.1.3, 3.1.6 and 3.1.7). The results concerning the solubility and the solubility behavior of the synthesized complexes $[Mo_2(NCCH_3)_{8.5}][TFSI]_4$ (**26**) and $[Mo_2(\mu\text{-}O_2CCH_3)_2(NC^tBu)_4][TFSI]_2$ (**27**) are presented in the following. Due to the obtained results for **27**, the compound $[Mo_2(\mu\text{-}O_2CCH_3)_2(NCMe)_6][BF_4]_2$ (**30**) was synthesized according to a literature procedure[94a] for comparison.

At the beginning, the alkyl-substituted imidazolium ionic liquids EMIm TFSI, BMIm TFSI and OMIm TFSI were applied. A concentration of 0.01 M and a volume of the IL of 0.1 mL were chosen to analyze if the compounds are generally soluble in ionic liquids. By dissolving **26** and **27** in these three ILs, it was observed, that they were thoroughly dissolved in all ILs for a concentration of 0.01 M and a volume of 0.1 mL. Therefore, the volume was increased to 0.5 mL and the solutions were always stirred for at least three hours before the concentration was raised in steps of 0.01 M. **27** was dissolved completely after about 30 min in all ILs, whereas it took about 2 h for **26** for every step of increasing the concentration. It was possible to obtain a concentration of 0.05 M for both compounds in EMIm TFSI. Higher concentrations of 0.06 M for **26** in BMIm TFSI and OMIm TFSI and of 0.07 M for **27** in BMIm TFSI and OMIm TFSI were received. Solubility tests with the higher substituted imidazolium ionic liquids showed a similar behavior. **27** was thoroughly dissolved faster than **26**. Both compounds could be dissolved in EMMIm TFSI up to 0.05 M until a saturated solution was existent. A higher concentration of 0.06 M respectively 0.07 M was possible for both complexes in BMMIm TFSI, OMMIm TFSI and OTMIm TFSI. These results corresponded well with the other obtained outcomes for these ionic liquids.

Besides the various alky-substituted imidazolium ionic liquids, some alkylammonium, respectively functionalized alkylammonium cations were used in combination with the TFSI anion in order to investigate the solubility of **26** and **27**. Therefore, HTMA TFSI and DTMA TFSI with a different alkyl chain length in one position were selected and the ester-functionalized IL, acetylcholine TFSI (ACh TFSI). The starting concentration for these ILs was 0.01 M and the starting volume was 0.1 mL. The compounds were generally soluble in this group of ionic liquids. While for all other tested complexes the highest concentration was 0.05 M in both HTMA TFSI and DTMA TFSI, **26** could be dissolved in HTMA TFSI up to 0.06 M and for **27** even a concentration of 0.07 M was possible. The solubility deteriorated by the use of the more hydrophobic IL DTMA TFSI for **26** ad **27**. In addition, it took somewhat longer until the complexes dissolved in DTMA TFSI due to its slightly higher hydrophobic character. Nevertheless, concentrations of 0.06 M for **26**, respectively 0.07 M for **27**, were still obtained. Strikingly, the compounds showed a far better solubility in the more polar ionic liquid ACh TFSI.

$[Mo_2(NCCH_3)_{8.5}][TFSI]_4$ (**26**) could be dissolved up to a concentration of 0.10 M, and for $[Mo_2(\mu\text{-}OAc)_2(NC^tBu)_4][TFSI]_2$ (**27**) even a concentration of 0.15 M was possible to obtain. These both values are the highest concentrations which were so far received. Another beneficial observation was, that **27** was dissolved in under 30 min for every step of increasing the concentration in ACh TFSI.

The solubility of the complexes **26** and **27** was also investigated in some cyclic ammonium ILs such as BMP OTf, BMP TFSI and BMPip TFSI. In addition, the latter two cations were also functionalized with a methoxyethyl group resulting in MEMP TFSI and MEMPip TFSI. In this context, the commercially available ILs $P_{6,6,6,14}$ Cl and $P_{6,6,6,14}$ TFSI were also applied for solubility tests. As mentioned above, the starting concentration for these ILs was also 0.01 M and the starting volume was 0.1 mL. After seeing that the compounds **26** and **27** were generally soluble in these group of ILs as well, the volume was also increased to 0.5 mL. It was observed, that for BMP OTf very similar concentrations were obtained with 0.06 M, respectively 0.05 M. But **26** and **27** showed a better solubility in BMP TFSI and BMPip TFSI, especially **27** in BMPip TFSI. Contrary to all other compounds which showed an inferior solubility in BMPip TFSI to BMP TFSI, **27** exhibited in both ILs a concentration of 0.07 M. The functionalization to MEMP TFSI and MEMPip TFSI once again caused an improvement of the solubility. **26** could be thoroughly dissolved in both ILs up to a concentration of 0.08 M. For **27** even a concentration of 0.10 M was obtained in MEMP TFSI and MEMPip TFSI. By far the worst solubility was again received for $P_{6,6,6,14}$ Cl and $P_{6,6,6,14}$ TFSI with the highest concentration of 0.04 M for both compounds. It took more than one week until the complexes were completely dissolved in both ILs. This can be attributed to their extremely high hydrophobic character.

Due to the superior solubility of compound **27**, the complex $[Mo_2(\mu\text{-}OAc)_2(NCMe)_6][BF_4]_2$ (**30**) was synthesized in order to see if the enhanced solubility of **27** can be attributed to the two acetate anions. Compound **30** was not dissolved in every ionic liquid, but in some selected ILs, in which **27** showed an improved solubility. It was observed that for ACh TFSI, which exhibited the highest concentration for **27**, a concentration of 0.13 M is possible for **30**, which is nearly as high as that for **27**. Furthermore, in the other tested ionic liquids, BMP TFSI, BMPip TFSI, MEMP TFSI and MEMPip TFSI, the same concentrations were received. Just like **27**, **30** was dissolved faster in the ILs than **26**. All in all, the additional acetate anions in the complex highly improved the solubility.

The color of all solutions corresponded to the color of the respective complex. After several months, the color of the solution did not change, which indicates the long-term stability of these complexes in these ionic liquids. The obtained concentrations for $[Mo_2(NCCH_3)_{8.5}][TFSI]_4$ (**26**), $[Mo_2(\mu\text{-}OAc)_2(NC^tBu)_4][TFSI]_2$ (**27**) and $[Mo_2(\mu\text{-}OAc)_2(NCMe)_6][BF_4]_2$ (**30**) in all tested ionic liquids are summarized in table 24. The highest concentrations are highlighted in green.

In conclusion, the compounds **26** and **27** are generally soluble in various ionic liquids and exhibit a better solubility due to the fact, that they contain the same anion as the IL. Especially **27** possesses a superior solubility, which might be attributed to the additional acetate anions. Compound **30** also has additional acetate anions and holds a similar solubility to **27**.

Table 24 Solubility of compounds **26**, **27** and **30** in several ionic liquids. Concentrations are given in [M]. The highest concentrations are highlighted in green.

	Compound		
	26	**27**	**30**
	$[Mo_2(NCCH_3)_{8.5}][TFSI]_4$	$[Mo_2(\mu\text{-}OAc)_2(NC^tBu)_4][TFSI]_2$	$[Mo_2(\mu\text{-}OAc)_2(NCMe)_6][BF_4]_2$
EMIm TFSI	0.05	0.05	
BMIm TFSI	0.06	0.07	
OMIm TFSI	0.06	0.07	
EMMIm TFSI	0.05	0.05	
BMMIm TFSI	0.07	0.06	
OMMIm TFSI	0.07	0.06	
OTMIm TFSI	0.06	0.06	
HTMA TFSI	0.06	0.07	
DTMA TFSI	0.05	0.06	
ACh TFSI	**0.10**	**0.15**	**0.13**
BMP OTf	0.06	0.05	
BMP TFSI	0.07	0.07	0.07
MEMP TFSI	**0.08**	**0.10**	**0.10**
BMPip TFSI	0.06	0.07	0.07
MEMPip TFSI	**0.08**	**0.10**	**0.10**
$P_{6,6,6,14}$ Cl	0.03	0.04	
$P_{6,6,6,14}$ TFSI	0.04	0.04	

3.2.7 Solubility of $[W(NO)_2(NCR)_{3\text{-}4}][BF_4]_2$ (**28**-**29**) in RTILs

The tungsten containing complexes $[W(NO)_2(NCCH_3)_4][BF_4]_2$ (**28**) and $[W(NO)_2(NCC(CH_3)_3)_3][BF_4]_2$ (**29**) have been synthesized to investigate their solubility in various ionic liquids. Strikingly, both compounds do not only hold nitrile ligands but also incorporated NO ligands. It is interesting to get to know if these additional ligands influence the solubility in ionic liquids and if so, to what effect. As in the last section could be seen, additional acetate ligands improve the solubility. The results concerning the solubility and the solubility behavior of the compounds **28** and **29** are presented in the following.

At the beginning, the alkyl-substituted imidazolium ionic liquids EMIm TFSI, BMIm TFSI and OMIm TFSI were applied. A concentration of 0.01 M and a volume of 0.1 mL were chosen to analyze if the compounds are generally soluble in ionic liquids. By dissolving **28** and **29** in these three ILs, it was observed that that they were thoroughly dissolved in all ILs for a concentration of 0.01 M and a volume of 0.1 mL. Therefore, the volume was increased to 0.5 mL and the solutions were always stirred for at least three hours before the concentration was raised in steps of 0.01 M. Both compounds were dissolved completely after about 1 hour in all ILs for every step of increasing the concentration. It was possible to obtain a concentration of 0.13 M for **28** in EMIm TFSI and even of 0.15 M for **29**. These are by far the highest concentrations, which are received for a compound and for the IL EMIm TFSI. As already noticed for the other groups of complexes, the *tert*-butylnitrile derivative always showed a better solubility behavior as compounds with the other nitriles. Even higher concentrations of 0.15 M and 0.17 M were obtained for BMIm TFSI and OMIm TFSI. Solubility tests with the higher substituted imidazolium ionic liquids showed a very similar behavior. Both **28** and **29** dissolved completely after about 90 min in all four ILs for every step of increasing the concentration. Concentrations of 0.15 M were received for both compounds in EMMIm TFSI and OMMIm TFSI. **28** and **29** exhibited a better solubility in OTMIm TFSI with 0.16 M, respectively 0.17 M, but especially in BMMIm TFSI in which concentrations of 0.17 and 0.18 were possible until a saturated solution was existent. These values are the highest which were received for the group of the substituted imidazolium ionic liquids.

Besides the various alky-substituted imidazolium ionic liquids, some alkylammonium, respectively functionalized alkylammonium cations were used in combination with the FSI and TFSI anions in order to investigate the solubility of **28** and **29**. Therefore, HTMA TFSI, DTMA TFSI and *N*,*N*,*N*-triethylbut-2-enammonium bis(fluorosulfonyl)amide (TEBA FSI) with a different alkyl chain lengths in one position were selected and the ester-functionalized IL, acetylcholine TFSI (ACh TFSI). The starting concentration for these ILs was 0.01 M and the starting volume was 0.1 mL. The compounds were generally soluble in this group of ionic liquids. Although these ILs exhibit a hydrophobic character and most of the examined complexes showed an inferior solubility in HTMA TFSI and DTMA TFSI to the other ILs, **28** and **29** could be very well dissolved. The highest concentrations were observed for HTMA TFSI which are 0.17 M for **28** and even 0.20 M for **29**. The solubility deteriorated a little bit by the use of the more hydrophobic IL DTMA TFSI for **28** and **29**. In addition, it took somewhat longer until the complexes dissolved in DTMA TFSI due to its slightly higher hydrophobic character. Nevertheless, concentrations of 0.15 M for **28**, respectively 0.18 M for **29**, were still obtained. So far, the lowest concentrations were received for TEBA FSI with 0.10 M for **28**, respectively 0.12 M for **29**. At the beginning, both complexes could be thoroughly dissolved resulting in bright green solutions, but after a few weeks the color changed to dark brown for **28**. A precipitate could not be observed. Attempts to crystallize possible decomposition products were unsuccessful. A possible reason could be that the complex **28** might exhibit a sensitivity to light. The compounds showed a far better solubility in the more polar ionic liquid ACh TFSI. **28** could be dissolved up to a concentration of 0.17 M, and for **29** even a concentration of 0.25 M was possible to obtain. The latter is the highest concentration which was so far received. Another beneficial observation was, that both complexes were dissolved in under 30 min for every step of increasing the concentration in ACh TFSI.

The solubility of the complexes **28** and **29** was also investigated in some cyclic ammonium ionic liquids such as BMP TFSI and BMPip TFSI. In addition, these cations were also functionalized with a methoxyethyl group resulting in MEMP TFSI and MEMPip TFSI. In this context, the commercially available ILs $P_{6,6,6,14}$ Cl and $P_{6,6,6,14}$ TFSI were also applied for solubility tests. As for all other solubility tests, the starting concentration for these ILs was also 0.01 M and the starting volume was 0.1 mL. After seeing that the compounds **28** and **29** were generally soluble in these group of ILs as well, the volume was also increased to 0.5 mL. It was observed that both **28** and **29** were thoroughly dissolved in BMP TFSI and BMPip TFSI, whereas a slightly higher concentration of 0.15 M for **28**, respectively 0.17 M for **29**, was obtained for both compounds in BMP TFSI. The functionalization to MEMP TFSI and MEMPip TFSI caused an improvement of the solubility, especially for **29**. Both complexes were completely dissolved in about 1 h in the ILs for every step of increasing the concentration. **29** again showed the higher possible concentration of 0.20 M for MEMP TFSI and 0.19 M for MEMPip TFSI. As expected, the worst solubility was again received for $P_{6,6,6,14}$ Cl and $P_{6,6,6,14}$ TFSI with the highest concentration of 0.05 M for both compounds. These concentrations are considerably lower than for the other ionic liquids and it took more than one week until the complexes were completely dissolved in both ILs. This can be attributed to their extremely high hydrophobic character. The color of all solutions corresponded to the color of the respective complex, except for the preparation with the IL TEBA FSI. After several months, the color of the solution did not change, which indicates the long-term stability of these complexes in these ionic liquids. The obtained concentrations for $[W(NO)_2(NCCH_3)_4][BF_4]_2$ (**28**) and $[W(NO)_2(NCC(CH_3)_3)_3][BF_4]_2$ (**29**) in all tested ionic liquids are summarized in table 25. The highest concentrations are highlighted in green.

In conclusion, the compounds **28** and **29** are generally soluble in various ionic liquids and reveal a superior solubility compared to all the other used complexes. Especially the ionic liquids HTMA TFSI, MEMP TFSI, MEMPip TFSI and Ach TFSI seem to be very beneficial, in which concentrations of up to 0.25 M are possible. The *tert*-butylnitrile derivative **29** showed a better solubility behavior than **28**. This could also be observed for the other complexes. Furthermore, both complexes could be dissolved quite fast in the ionic liquids.

Table 25 Solubility of $[W(NO)_2(NCR)_{3\text{-}4}][BF_4]_2$ (**28**-**29**) in several ionic liquids. Concentrations are given in [M]. The highest concentrations are highlighted in green.

	Compound	
	28	**29**
	$[W(NO)_2(NCCH_3)_4][BF_4]_2$	$[W(NO)_2(NCC(CH_3)_3)_3][BF_4]_2$
EMIm TFSI	0.13	0.15
BMIm TFSI	0.15	**0.17**
OMIm TFSI	0.15	0.15
EMMIm TFSI	0.15	0.15
BMMIm TFSI	**0.18**	0.17
OMMIm TFSI	0.15	0.16
OTMIm TFSI	0.16	0.17
HTMA TFSI	0.17	**0.20**
DTMA TFSI	0.15	0.18
TEBA FSI	0.10	0.12
ACh TFSI	**0.17**	**0.25**
BMP TFSI	0.15	0.17
MEMP TFSI	0.15	**0.20**
BMPip TFSI	0.13	0.17
MEMPip TFSI	0.16	**0.19**
$P_{6,6,6,14}$ Cl	0.05	0.05
$P_{6,6,6,14}$ TFSI	0.05	0.05

3.2.8 Solubility of the complexes **31**, **32** and **33** in RTILs

The vanadium containing complexes $[V(NCCH_3)_6][BF_4]_2$ (**31**), $[V(NCCH_3)_6][CF_3SO_3]_2$ (**32**) and $[V(NCCH_3)_6][BPh_4]_2$ (**33**) have been synthesized to investigate their solubility in various ionic liquids. The results concerning the solubility and the solubility behavior of the compounds **31**, **32** and **33** are presented in the following.

At the beginning, the alkyl-substituted imidazolium ionic liquids EMIm TFSI, BMIm TFSI and OMIm TFSI were applied. A concentration of 0.01 M and a volume of 0.1 mL were chosen to analyze if the compounds are generally soluble in ionic liquids. By dissolving the complexes **31**-**33** in these three ILs

it was observed that they were thoroughly dissolved in all ILs for a concentration of 0.01 M and a volume of 0.1 mL. Therefore, the volume was increased to 0.5 mL and the solutions were always stirred for at least three hours before the concentration was raised in steps of 0.01 M. **31**-**33** were completely dissolved after about two hours in all ILs for every step of increasing the concentration. In EMIm TFSI concentrations of 0.05 M for **31** and of 0.07 M for **32** were received, whereas a saturated solution was already existent at a concentration of 0.03 M for **33**. **31** and **32** showed an improved solubility in BMIm TFSI and OMIm TFSI, in contrast to **33**, which also exhibited a poor solubility in these ILs. Solubility tests with the higher substituted imidazolium ionic liquids showed a very similar behavior. Whereat concentrations of up to 0.07 M were possible for **31** in EMMIm TFSI, BMMIm TFSI, OMMIm TFSI and OTMIm TFSI, **32** could be dissolved with higher concentrations of 0.10 M in these ILs. Merely **33** showed again a poor solubility in this group of ionic liquids. The highest concentration was 0.04 M in OTMIm TFSI, which is why some other ILs or this group were omitted.

Besides the various alkyl-substituted imidazolium ionic liquids, some alkylammonium, respectively functionalized alkylammonium cations were used in combination with the FSI and TFSI anions in order to investigate the solubility of **31**-**33**. Therefore, HTMA TFSI, DTMA TFSI, TEBA FSI were selected and the ester-functionalized IL, acetylcholine TFSI (ACh TFSI). The starting concentration for these ILs was 0.01 M and the starting volume was 0.1 mL. The compounds were generally soluble in this group of ionic liquids. Although these ILs exhibit a hydrophobic character and most of the examined complexes showed an inferior solubility in HTMA TFSI and DTMA TFSI to the other ILs, **31** and **32** could be thoroughly dissolved with concentrations up to 0.06 M for **31** and 0.09 M for **32** in HTMA TFSI. **33** could only be dissolved up to 0.02 M in HTMA TFSI, which is why it was not tested anymore in DTMA TFSI since the solubility deteriorated a little bit in the most cases by the use of the more hydrophobic IL DTMA TFSI. This was also observed for **31** and **32**. In addition, it took somewhat longer until the complexes dissolved in DTMA TFSI due to its slightly higher hydrophobic character. Nevertheless, concentrations of 0.5 M for **31**, respectively 0.08 M for **32**, were still obtained. TEBA exhibited the same concentration of 0.07 M for **31** and **32**. There were no observations of a color change after the complexes had been dissolved as it appeared for **28** in this IL. The compounds showed a far better solubility in the more polar ionic liquid ACh TFSI. Therefore, the solubility of **33** was investigated for this IL. However, at a concentration of 0.03 M a saturated solution was already existent. In contrast, **31** and **32** actually showed a better solubility. Concentrations of 0.10 M for **31** and even 0.15 M for **32** were obtained. Another beneficial observation was, that **32** was dissolved in under one hour for every step of increasing the concentration in ACh TFSI.

The solubility of the complexes 31-33 was also investigated in some cyclic ammonium ionic liquids such as BMP OTf, BMP TFSI and BMPip TFSI. In addition, these cations were also functionalized with a methoxyethyl group resulting in MEMP TFSI and MEMPip TFSI. In this context, the commercially available ILs $P_{6,6,6,14}$ Cl and $P_{6,6,6,14}$ TFSI were also applied for solubility tests. As for all other solubility tests, the starting concentration for these ILs was also 0.01 M and the starting volume was 0.1 mL. After seeing that the compounds **31**-**33** were generally soluble in these group of ILs as well, the volume was also increased to 0.5 mL. A concentration of 0.07 M was observed for **31** in BMP OTf and **32** was even thoroughly dissolved up to a concentration of 0.15 M. This can probably be attributed to the fact, that

the complex and the IL contain the same anion. Strikingly, all preparations of **32** in the different ionic liquids had a dark green color, just like the complex itself, except for the preparation with BMP OTf. At the beginning the solution also was dark green, but after a few days, the color changed to purple. Independent of further concentration changes, the purple color maintained. Both complexes showed similar concentrations of about 0.07 M in BMP TFSI and BMPip TFSI. Since BMP TFSI is one of the standard ionic liquids for the electrodeposition, the solubility of **33** was investigated. Though it showed again a poor solubility with a concentration of only 0.02 M. The functionalization to MEMP TFSI and MEMPip TFSI caused an improvement of the solubility, especially for **32**. Both complexes were completely dissolved in about 2 h in the ILs for every step of increasing the concentration. **29** again showed the higher possible concentration of 0.12 M for MEMP TFSI and 0.10 M for MEMPip TFSI. As expected, the worst solubility was again received for $P_{6,6,6,14}$ Cl and $P_{6,6,6,14}$ TFSI with the highest concentration of 0.04 M for **31**, respectively 0.03 M for **33**. This can be attributed to their extremely high hydrophobic character. Anyway, **32** could be dissolved up to 0.07 M in $P_{6,6,6,14}$ Cl, although it took almost 10 days until it was thoroughly dissolved. Strikingly, a color change could be observed for this preparation as well. At first it was a clear colorless solution and the dark green complex, but once the complex was fully dissolved, it was a clear light-yellow solution. Just like for the preparation with BMP OTf, a small amount of the solution was withdrawn to crystallize it, but the attempts were not successful. For all other preparations, the color of the solutions corresponded to the color of the respective complex. After several months, the color of the solution did not change, indicating the long-term stability of these complexes in these ionic liquids. The obtained concentrations for $[V(NCCH_3)_6][BF_4]_2$ (**31**), $[V(NCCH_3)_6][CF_3SO_3]_2$ (**32**) and $[V(NCCH_3)_6][BPh_4]_2$ (**33**) in all tested ionic liquids are summarized in table 26. The highest concentrations are highlighted in green.

In conclusion, the compounds **31**, **32** and **33** were generally soluble in various ionic liquids. Some ionic liquids such as MEMP TFSI, ACh TFSI and BMP OTf seem to be very beneficial for these complexes, especially $[V(NCCH_3)_6][CF_3SO_3]_2$ (**32**), in which concentrations of up to 0.15 M were possible. Furthermore, the complexes could be dissolved quite fast in the ionic liquids.

Table 26 Solubility of compounds **31**, **32** and **33** in several ionic liquids. Concentrations are given in [M]. The highest concentrations are highlighted in green.

	Compound		
	31	**32**	**33**
	$[V(NCCH_3)_6][BF_4]_2$	$[V(NCCH_3)_6][CF_3SO_3]_2$	$[V(NCCH_3)_6][BPh_4]_2$
EMIm TFSI	0.05	0.07	0.03
BMIm TFSI	0.07	0.10	0.04
OMIm TFSI	0.06	0.10	0.04
EMMIm TFSI	0.05	0.10	
BMMIm TFSI	0.07	**0.10**	0.03
OMMIm TFSI	0.07	0.10	
OTMIm TFSI	0.07	0.10	0.04
HTMA TFSI	0.06	0.09	0.02
DTMA TFSI	0.05	0.08	
TEBA FSI	0.07	0.07	
ACh TFSI	**0.10**	**0.15**	0.02
BMP OTf	0.07	**0.15**	
BMP TFSI	0.07	0.07	0.02
MEMP TFSI	**0.08**	**0.12**	0.03
BMPip TFSI	0.06	0.07	
MEMPip TFSI	**0.08**	**0.10**	
$P_{6,6,6,14}$ Cl	0.03	0.07	
$P_{6,6,6,14}$ TFSI	0.04	0.05	0.03

3.2.9 Solubility of the complexes **34** and **35** in RTILs

The compounds $[Ti(NCCH_3)_3][BF_4]_3$ (**34**) and $[Nb(NCCH_3)][BF_4]_3$ (**35**) have been synthesized to investigate their solubility in various ionic liquids. Due to the poor yield of both compounds, which could unfortunately not be further improved, it was not possible to conduct thorough solubility tests determining a concentration. However, a small amount of each complex was dissolved in some selected ionic liquids of each group (cf. Figure 19, chapter 3.2) in order to show if the complexes were generally soluble in these ILs. It could be seen that both compounds were either not soluble or exhibited a very poor solubility.

From the first group of ionic liquids BMIm TFSI, BMMIm TFSI and OTMMIm TFSI were chosen, since the previous compounds showed a slightly better solubility in these ILs. However, **34** was soluble in BMIm TFSI and BMMIm TFSI but with a very poor solubility and it took about one week until the small amount of **34** was dissolved. **35** was only slightly soluble in BMIm TFSI and showed a similar behavior as **34**. They were both insoluble in OTMIm TFSI. Both compounds showed a slightly improved solubility for BMP TFSI and MEMP TFSI from the second group of ionic liquids. From the third group HTMA TFSI and ACh TFSI were chosen for solubility tests. Both compounds were only slightly soluble in ACh TFSI but solely **35** could also be dissolved in HTMA TFSI. Both complexes were completely insoluble in $P_{6,6,6,14}$ TFSI from the fourth group of ionic liquids. The received results of the compounds **34** and **35** are summarized in table 27.

Table 27 Solubility of the complexes **34** and **35** in some selected ionic liquids.

Number	Compound	Ionic Liquids			
		BMIm TFSI	**BMMIm TFSI**	**OTMIm TFSI**	**BMP TFSI**
34	$[Ti(NCCH_3)_3][BF_4]_3$	✓	✓	×	✓
		HTMA TFSI	**ACh TFSI**	**MEMP TFSI**	**$P_{6,6,6,14}$ TFSI**
		×	✓	✓	×
		BMIm TFSI	**BMMIm TFSI**	**OTMIm TFSI**	**BMP TFSI**
35	$[Nb(NCCH_3)][BF_4]_3$	✓	×	×	✓
		HTMA TFSI	**ACh TFSI**	**MEMP TFSI**	**$P_{6,6,6,14}$ TFSI**
		✓	✓	✓	×

3.3 Electrochemical Reduction of some Metal Precursors

In order to enable the electrochemical deposition of refractory metals, other precursors than halides have to be used since the deposition of their halides involves some severe detriments, as already mentioned. The approach to overcome these drawbacks was the application of nitrile stabilized metalorganic complexes with weakly coordinating anions. The obtained results concerning the synthesis of such precursors were presented in chapter 3.1. But not only the compounds which are used for the electrodeposition have to be changed, but also the reaction medium. Due to their wide electrochemical window and many other beneficial properties ionic liquids are on principle well suited as medium for the electrodeposition, as it enables the deposition of very ignoble metals from ILs. Thus, the solubility and

the solubility behavior of all synthesized nitrile-stabilized complexes with different weakly coordinating anions were investigated. The received results concerning the solubility were described in chapter 3.2. To date, there is no knowledge about the electrochemical behavior of such compounds in ionic liquids. Therefore, some general electrochemical studies of some selected complexes in various ionic liquids were inquired. The obtained results are presented in the following.

3.3.1 Electrochemical Reduction of **34** and **36**

Due to the fact, that the complex $[Ti(NCCH_3)_3][BF_4]_3$ (**34**) was either only poorly soluble in some ionic liquids or not soluble at all, it was not possible to conduct thorough electrochemical studies. However, the compound $(C_5H_5)_2TiCl_2$ (**36**) was also dissolved in some ionic liquids such as BMMIm TFSI and OTMIm TFSI and some electrochemical studies were undertaken. Figure 20 shows an EQCM study (electrochemical quartz crystal microbalance) to the electrochemical reduction of the compound $(C_5H_5)_2TiCl_2$ in two different ionic liquids, BMMIm TFSI (Figure 20a) and OTMIm TFSI (Figure 20c), as well as the corresponding mass-charge-plot in Figure 20b and Figure 20d. Both systems showed a very similar behavior. In both cases, a first reduction peak C_1 was observed, which was accompanied by an oxidation peak A_1. At the same time, the resonant frequency of the quartz decreased by about 1 kHz, while the damping increased by about 3 kHz. The peaks C_1/A_1 in section a) of Figure 20 are slightly shifted towards more negative values as in section b) of Figure 20, which could be attributed to the applied Pt-quasi-reference electrode. A second reduction peak C_2 was observed at lower potentials, but there was no accompanied oxidation peak. The resonant frequency declined by another 2 kHz, whereas the damping increased by more than 10 kHz. Despite the great change of the damping and the resulting non-applicability of the *Sauerbrey* equation, it was possible to use the mass-charge-plot to estimate which apparent molar mass was associated with the observed reduction reaction. It had to be noticed, that the obtained values must not be overinterpreted. Though, right before the beginning of the reduction peaks C_2 values of 48.0 g/mol für BMMIm TFSI (b), Figure 20) and 41.7 g/mol for OTMIm TFSI (Figure 20d) were found. Because titanium exhibits an oxidation state of +4 in $(C_5H_5)_2TiCl_2$ a value of 12.0 g/mol would be expected for titanium. But it might also be that the peak couple C_1/A_1 could belong to the redox reaction Ti(IV)/Ti(III), in analogy to the known behavior of ferrocene. However, it was not possible to obtain a titanium coating.

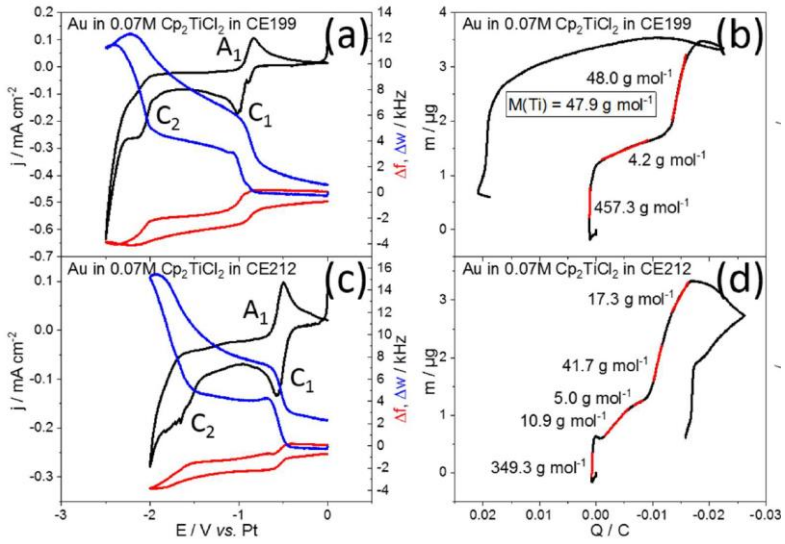

Figure 20 a) EQCM studies on an Au electrode of a solution of 0.07 M **36** in BMMIm TFSI; b) the corresponding mass-charge-plot; c) and d) represent the repetition of the measurement under the same conditions in OTMIm TFSI. The potential scan rate was 2mV/s. For clarification, the designation of the ILs is as follows: BMMIm TFSI: CE199 and OTMIm TFSI: CE212.

3.3.2 Electrochemical Reduction of the Chromium Precursors

A screening of electrolytes to various combinations of the chromium containing complexes with ionic liquids was conducted. Therefor the complexes **8**-**10** of the group $[Cr(NCR)_{3\text{-}4}][BF_4]_2$ were selected, as well as the complexes **12**-**15** of the group $[Cr(NCR)_2][CF_3SO_3]_2$. Especially the different alkyl-substituted imidazolium TFSI ionic liquids were used for this screening. Because some combinations resulted in saturated solutions already at very low concentrations, these complexes were also dissolved in acetonitrile (AN), investigating if there might be a better solubility for the electrochemical studies. Figure 21a shows the EQCM measurement with a saturated solution of $[Cr(NCCH_3)_3][BF_4]_2$ (**8**) in BMP TFSI. There were only small currents concerning the reduction and there was no clear correlation observed in the EQCM data. Every time there was a change in the frequency, the damping changed, but there was no clear evidence of a deposition of chromium. Therefore, the complex was also dissolved in acetonitrile with a concentration of 0.01 M (Figure 21b). The currents were increased by a factor of 20 and a negative shift of the frequency by ca. 2 kHz was detected at the reduction peak below -2.5 V. The damping increased by almost 8 kHz as well, which might be traced back to a change in the viscosity of the electrolyte. Unfortunately, there was no evidence of a Cr deposition as well. In Figure 21c the system of complex **12** dissolved in acetonitrile is seen. The current which belonged to the reduction, was even higher than for the previous system and the reduction peak at -2 V induced a negative change in the frequency of about 7 kHz. At the same time, the damping did not increase by more than 2 kHz. When complex **13** was dissolved in acetonitrile, the currents were very low and there could almost no change be detected in the EQCM signals.

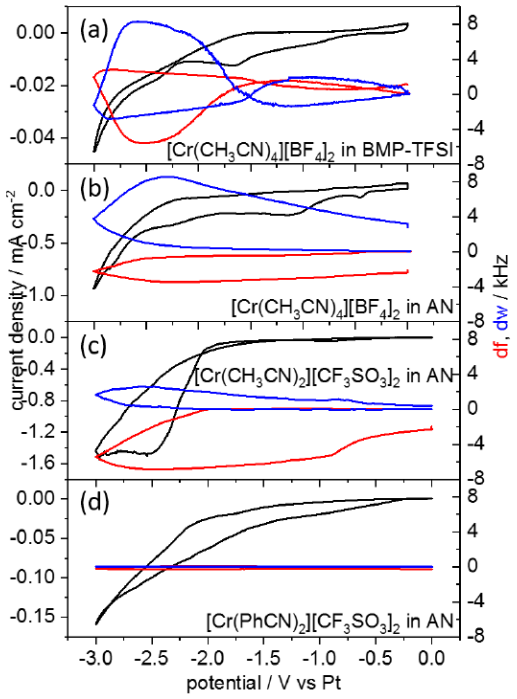

Figure 21 EQCM studies for the electrochemical reduction of the Cr precursors. a) saturated solution of **8** in BMP TFSI; b) solution of **8** in acetonitrile with 0.01 M; c) solution of **12** in acetonitrile with 0.01 M; d) solution of **13** in acetonitrile with 0.01 M. The potential scan rate was 2 mV/s.

The comparison between the CV of the pure IL (purple, Figure 22) with the saturated solution of **8** in BMP TFSI (cf. Figure 21a) showed that the precursors did not take part in the electrochemical processes. As mentioned, higher currents and distinct reduction peaks were observed. In contrast to compound **13**, complex **12** seemed to be a promising precursor. However, so far, a deposition of Cr could not be achieved, and further investigations are necessary.

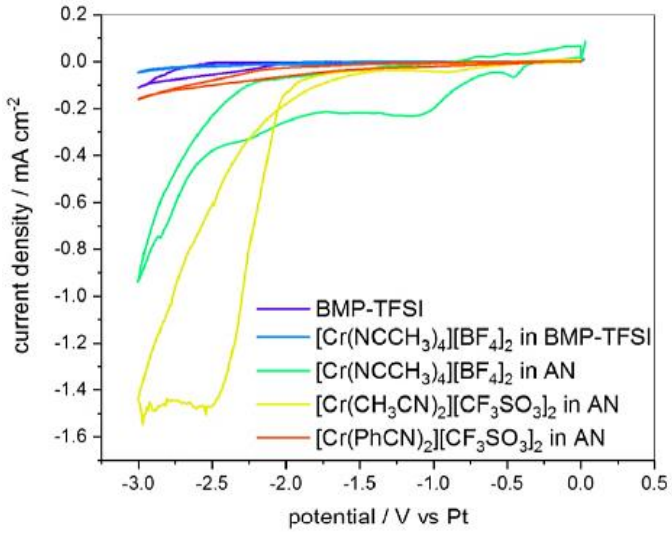

Figure 22 Comparison of the CV measurements of the different Cr precursors. purple: pure IL BMP TFSI; blue: saturated solution of **8** in BMP TFSI; green: 0.01 M solution of **8** in acetonitrile; yellow: 0.01 M solution of **12** in acetonitrile; red: 0.01 M solution of **13** in acetonitrile. The scan rate was 2 mV/s.

The screening of electrolytes was further pursued, and the different chromium complexes were dissolved in the ionic liquids BMIm TFSI and BMMIm TFSI (Figure 23). The ionic liquid BMIm TFSI exhibited a smaller electrochemical window than BMMIm TFSI. The complex **8** was dissolved in various ionic liquids and CV measurements were conducted. For one preparation, CVs were measured at two different temperatures (Figure 24). Though it could be seen that the precursors showed a slightly different electrochemical behavior but unfortunately, within the potential window of the ionic liquids, a deposition of Cr was not detected.

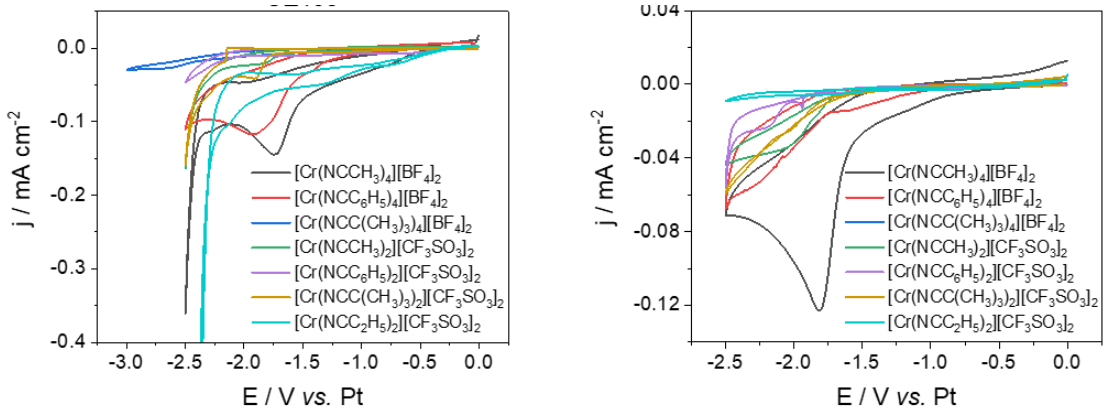

Figure 23 CVs of various chromium precursors in different ILs: left: BMIm TFSI; right: BMMIm TFSI.

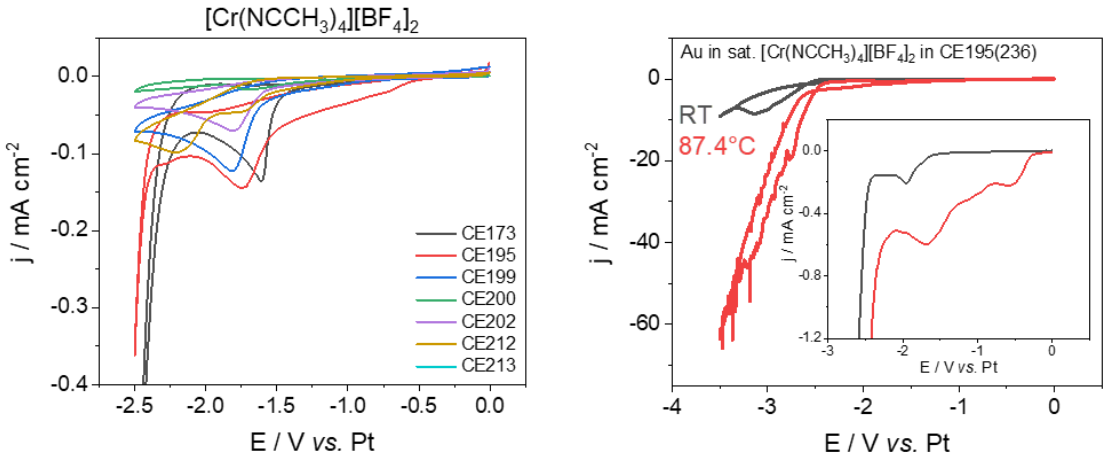

Figure 24 left: CVs of the complex **8** in different ILs: CE173: OMIm TFSI; CE195: BMIm TFSI; CE199: BMMIm TFSI; CE200: EMMIm TFSI; CE202: OMMIm TFSI; CE212: OTMIm TFSI; CE213: BTMIm TFSI. right: influence of the temperature on the CV of the reduction of **8** in BMIm TFSI.

But the complex $[Cr(NCC(CH_3)_3)_4][BF_4]_2$ (**10**) seems to be a promising precursor which was dissolved in BMIm TFSI. The EQCM measurements showed two reduction reactions with very low currents. The resonant frequency did not change for the first reduction peak C_1, while the frequency decreased by

about 3 kHz for the reduction peak C_2. The damping increased significantly. But it had to be noticed, that C_2 is very close to the potential at which the electrolyte might be decomposed. The chromium cation in $[Cr(NCC(CH_3)_3)_4][BF_4]_2$ possesses an oxidation state of +2, whereas an apparent molar mass of 26.0 g/mol results. This value corresponded well with the reduction peak C_2 and a deposition could be observed. However, the appearance of the coating did not seem to be metallic at first sight, but nevertheless, these results were promising for further investigations. The results are summarized in Figure 25.

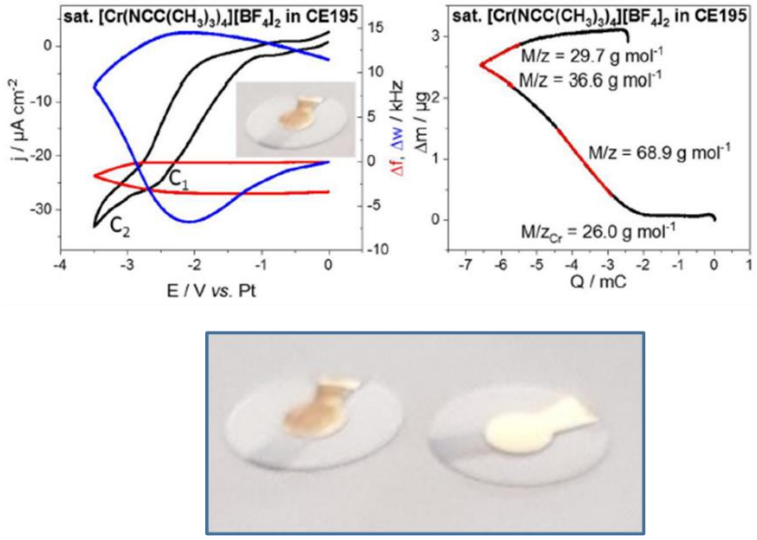

Figure 25 top left: EQCM studies on an Au electrode in a saturated solution of complex **10** in BMIm TFSI; top right: the corresponding mass-charge-plot; bottom: a picture of the deposited layer.

3.3.3 Electrochemical Reduction of the Molybdenum Precursors

A screening of electrolytes to various combinations of the molybdenum containing complexes with ionic liquids was conducted. Therefor the complex **18** of the group $[Mo_2(NCCH_3)_8][BF_4]_4$ was selected, as well as the complex **22** of the group $[Mo_2(NCCH_3)_8][CF_3SO_3]_4$. Especially the different alkyl-substituted imidazolium TFSI ionic liquids were used for this screening. Because the combination of **18** with some ionic liquids resulted in saturated solutions already at very low concentrations, this complex was also dissolved in acetonitrile (AN), investigating if there might be a better solubility for the electrochemical studies. Figure 26a shows an EQCM measurement with a saturated solution of complex **18** in BMP TFSI. The CV exhibits several small reduction peaks, while the resonant frequency in the negative scan nearly did not change (df). If there was a change to observe, then there would be a concurrent change of the damping (dw). Below a potential of -2.75 V the current increased and the damping was increased up to a value of nearly 50 kHz, which resulted in a decrease of the frequency. By dissolving the complex in acetonitrile, greater electrochemical currents were observed (Figure 26b). However, the EQCM measurements did not show any significant changes, which could be attributed to a Mo-deposition.

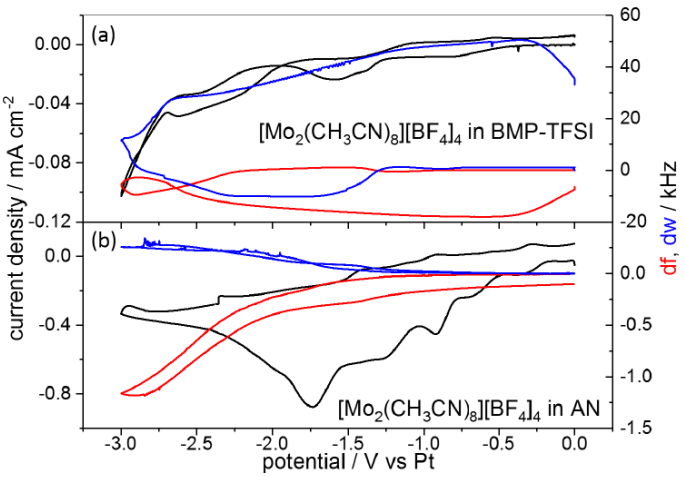

Figure 26 Comparison of an EQCM measurement with an Au electrode in a) a saturated solution of **18** in BMP TFSI and b) a 0.01 M solution of **18** in acetonitrile. The scan rate was 2 mV/s.

The comparison of the CV of complex **18** in BMP TFSI (Figure 26a) with the background CV of the pure ionic liquid BMP TFSI revealed, that the complex nearly did not take part in the electrochemical processes (Figure 27). The CV of pure BMP TFSI (Figure 27, grey) and that with the dissolved complex (Figure 27, red) were nearly identical. The consequence is that this precursor is almost inert in the IL BMP TFSI. The CV of the **18** in acetonitrile is also depicted in Figure 27 (blue) where the greater electrochemical currents can be clearly seen. Unfortunately, for both preparations, a deposition was not detected.

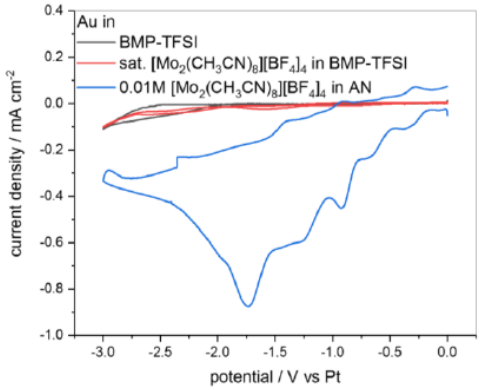

Figure 27 Comparison of the CVs of **18** in BMP TFSI (red); of **18** in acetonitrile (blue); pure BMP TFSI (grey). The scan rate was 2 mV/s.

The electrochemical behavior of $[Mo_2(NCCH_3)_8][CF_3SO_3]_4$ in the ionic liquid BMMIm TFSI was investigated. In Figure 28 the EQCM measurement (a) and the corresponding mass-charge-plot (b) are depicted. A first reduction peak C_1 was observed in the CV, which was neither accompanied by an oxidation peak nor by a change of the EQCM signal. At low potentials of -2.0 V, a second reduction peak C_2 was observed, which was not accompanied by an oxidation peak either, but with a decrease of the frequency by about 40 kHz and an increase of the damping by 60 kHz. Within the complex molybdenum reveals an oxidation state of +2, which corresponds to an apparent molar mass of 48.0 g/mol. The mass-charge-plot (Figure 28b) shows molar masses of 38.7 g/mol in the range of the second reduction peak C_2. Due to the great change of the damping, it might be possible, that this is an evidence of a molybdenum deposition. At first sight, the obtained layer is very thin and unfortunately partly discolored. It is also depicted in Figure 28.

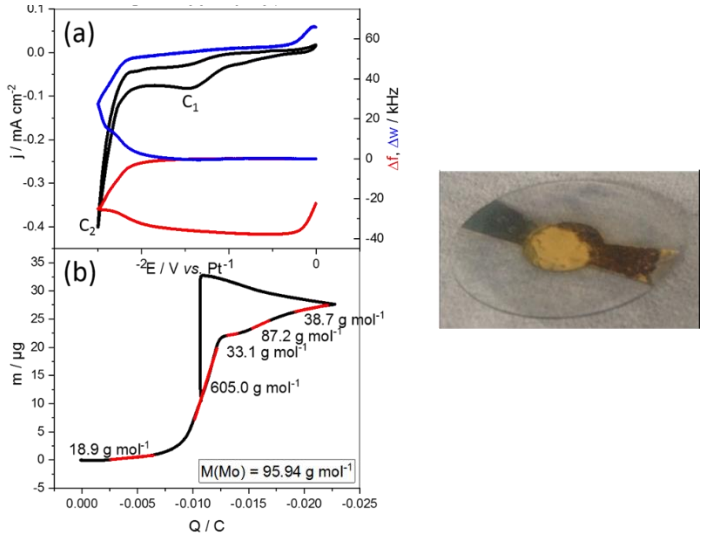

Figure 28 a) EQCM study on an Au electrode in a 0.07 M solution of **22** in BMMIm TFSI; b) the corresponding mass-charge-plot; right: picture of the obtained layer.

3.3.4 Electrochemical Reduction of a Tungsten Precursor

The compound $[W(NO)_2(NCCH_3)_4][BF_4]_2$ (**28**) was dissolved in three ionic liquids and the solutions were investigated by EQCM measurements. The results are depicted in Figure 29. The used ionic liquids were BMMIm TFSI, OMIm TFSI and OTMIm TFSI. Three reduction peaks C_1, C_2 and C_3 were observed for every measurement, but there was no corresponding oxidation reaction. The measured current densities were very low, just as the changes of the resonant frequency. The tungsten ion reveals an oxidation state of +2 in the complex, which is why a slope of 91.7 g/mol would be expected in the mass-charge-plots (Figure 29b,d,f). The obtained results did not correspond with this value at all, and a deposition could not be observed.

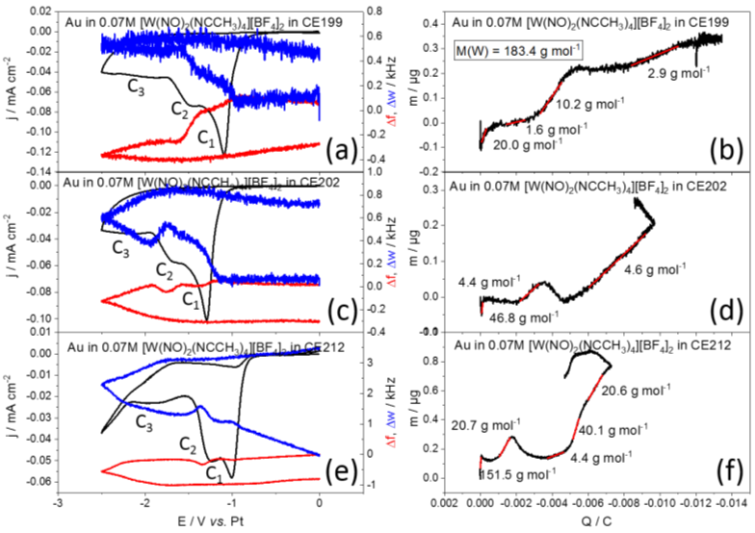

Figure 29 EQCM studies on an Au electrode in a 0.07 M solution of **28** in a) BMMIm TFSI; c) OMMIm TFSI; e) OTMIm TFSI. The corresponding mass-charge-plots: b) BMMIm TFSI; d) OMMIm TFSI; f) OTMIm TFSI.

4. Conclusion and Outlook

The aim of this work was the synthesis of new precursors for the electrodeposition of refractory metals from ionic liquids. Refractory metals are characterized by their many beneficial properties such as their extremely high melting points, which makes them interesting for high-temperature applications. Due to their good biocompatibility this group of metals is suitable for medical implants. Many components are functionalized by coatings with these metals to improve their properties like their corrosion resistance. Currently metallic coatings are realized by electrodeposition from aqueous solutions, but due to the narrow potential window of water this method cannot be used for refractory metals. Hence, the medium was changed to ionic liquids because of their wide electrochemical window and other beneficial properties such as their wider usable temperature range than water and their low vapor pressure. The electrodeposition of some refractory metals could indeed be realized by using ILs, though the obtained metal layers only are of poor quality because of the formation of non-stoichiometric subhalides and other side products which disturb the layers by applying halides as source of refractory metals. Therefore, not only the medium had to be changed but also the precursors which were used for the deposition. The approach was the use of nitrile stabilized metalorganic complexes with weakly coordinating anions with the idea of generating a 'naked' cation to circumvent the mentioned detriments. So, in this work nitrile stabilized metalorganic complexes with titanium, vanadium, niobium, tungsten and especially chromium and molybdenum were synthesized bearing different weakly coordinating anions such as BF_4^-, $CF_3SO_3^-$ or TFSI. Four nitriles with different steric demand were used as ligands, namely acetonitrile, benzonitrile, *tert*-butylnitrile and propionitrile. Furthermore, their solubility was tested in several ionic liquids and some basic electrochemical studies of some selected solutions were conducted. Four different groups of cations were used for the ionic liquids such as alkyl-substituted imidazolium ions, linear and cyclic alkylammonium cations and phosphonium ions. These were combined with anions like Cl^-, $CF_3SO_3^-$, FSI, but mainly TFSI. Some of the cations were also functionalized with more polar ether- or ethoxy-groups. The solubility tests showed that all complexes can be indeed dissolved in all applied ionic liquids and also exhibit a high stability. However, most of the compounds are solely soluble up to a concentration of about 0.07 M in most of the ILs, such as the groups of $[Cr(NCR)_{3\text{-}4}][BF_4]_2$, $[Cr(NCR)_2][CF_3SO_3]_2$ or $[Mo_2(NCCH_3)_8][BF_4]_4$ and $[Mo_2(NCR)_{8\text{-}10}][CF_3SO_3]_4$. But the results also revealed that a slightly better concentration can be obtained if the complex and the IL contain the same anion. Therefore the TFSI anion was incorporated into these complexes, since this anion was the most used for the ionic liquids resulting in $[Cr(\mu\text{-}O_2CCH_3)(NCCH_3)_2][TFSI]$, $[Mo_2(NCCH_3)_8][TFSI]_4$ and $[Mo_2(\mu\text{-}O_2CCH_3)_2(NCC(CH_3)_3)_4][TFSI]_2$. So far, these compounds were only obtained with a significant lower yield compared to the other complexes and that for two of them the exchange of the acetate anions for TFSI was not complete. However, they showed an improved solubility in the tested ILs, especially $[Mo_2(\mu\text{-}O_2CCH_3)_2(NCC(CH_3)_3)_4][TFSI]_2$ is soluble up to concentrations of 0.15 M. In addition, the solubility of $[W(NO)_2(NCR)_4][BF_4]_2$ was also tested in various ILs. It was observed that these complexes reveal the best solubility in most of the ILs compared to the other complexes and concentrations of up to 0.20 M were obtained for some ILs such as ACh TFSI. The complex $[V(NCCH_3)_6][CF_3SO_3]_2$ was also tested in some ionic liquids and showed a better solubility than the corresponding compounds with BF_4^- or BPh_4^- as anions. In general, a slight trend for the different nitrile ligands could be observed, namely

that a better solubility of the complexes can be achieved with the use of *tert*-butylnitrile and benzonitrile than with acetonitrile and propionitrile. Furthermore, higher concentrations are received with the application of ionic liquids with a functionalized substituent such as MEMP TFSI or MEMPip TFSI, and the by far best solubility for most of the compounds was obtained with ACh TFSI. Some basic electrochemical studies were conducted for some chromium and molybdenum complexes. At first a screening of electrolytes for various chromium compounds (**8**-**15**) was conducted, especially in the alkyl-substituted imidazolium ILs. Due to the poor solubility, some complexes were also dissolved in acetonitrile. The EQCM measurements showed only low currents and a Cr deposition could not be observed. However, the complexes **12** and **10** seemed to be promising precursors, because of the higher measured current for **12** and because of a deposition which was possible for **10** from BMIm TFSI. At first sight, the deposit did not exhibit a metallic character and further investigations are necessary. An electrolyte screening was also conducted for the molybdenum complexes **18** and **22** in the alkyl-substituted imidazolium ILs and in acetonitrile. It was recognized for **18** in BMP TFSI that the complex nearly did not take part in the reduction and a deposit could not be detected. Contrary to **18**, the combination of **22** in BMMIm TFSI showed a deposition, which was unfortunately very thin and partly discolored, but this is a promising evidence for further examinations concerning the Mo deposition. For the tungsten complex **28** some EQCM measurements were conducted in three different ionic liquids, BMMIm TFSI, OMIm TFSI and OTMIm TFSI. However, so far it was not possible to obtain a tungsten deposition from this complex despite its superior solubility in various ionic liquids. Interesting points for further investigations concerning this topic would be to test the solubility of the complexes in more ionic liquids in order to further broaden the spectrum in which they can be dissolved. ILs with another heteroatom such as sulfur might be interesting or ILs with dicyanamide as anion, respectively further tests with the FSI anion and the more polar ILs such as ACh TFSI. Since the solubility were all conducted at room temperature, the solubility at higher temperatures might also be worth examining. In the field of the electrochemical studies there are many parameters which have to be taken into consideration and which interact. These are important factors in order to improve the deposition conditions and to realize a homogeneous metal layer. For the synthesis of the nitrile-stabilized complexes the parameters for the TFSI derivatives must be adapted to improve their yield, especially that of complex **16**. Further syntheses of complexes with the TFSI anion might also be interesting as well as the attempt to incorporate another anion such as oxalate, since this should decompose to CO_2 and should therefore be able to escape from the reaction solution as a gas. Moreover, since the compounds with additional acetate or NO molecules as ligands showed a superior solubility in various ionic liquids, it might be interesting to further investigate their influence on the deposition of the metals.

5. Experimental Section

5.1 General Remarks

Unless otherwise stated, all manipulations were performed under dry, oxygen free conditions in an argon atmosphere using standard *Schlenk* and glovebox techniques. The solvents were either dried according to standard purification techniques[98] or obtained from a *M. Braun* Solvent Purification System (SPS-800). Acetic acid and acetic anhydride are refluxed over P_2O_5 for 2 h and afterwards distilled. Prior to use, all solvents as well as all deuterated solvents were degassed using the freeze-pump-thaw method and stored over molecular sieves (3Å, respectively 4Å for diethyl ether). Unless otherwise specified all chemicals were purchased from commercial sources and used without further purification. The following compounds were synthesized according to previously published methods: $Cr_2(OAc)_4$[89] (**7**), $Mo_2(OAc)_4$[92] (**17**), $[Mo_2(\mu\text{-}O_2CCH_3)_2(NCCH_3)_6][BF_4]_2$ (**30**)[94a], $[V(NCCH_3)_6][CF_3SO_3]_2$ (**32**)[99], $[V(NCCH_3)_6][BF_4]_2$ (**31**)[87c], $[V(NCCH_3)_6][BPh_4]_2$ (**33**)[100], $[Ti(NCCH_3)_3][BF_4]_3$ (**34**)[101] and $[Nb(NCCH_3)][BF_4]_3$[87c]. The ionic liquids 1-butyl-1-methylpyrrolidinium triflate (BMP OTf), 1-butyl-1-methylpyrrolidinium bis((trifluoromethyl)sulfonyl)amide (BMP TFSI), Trihexyl(tetradecyl)phosphonium chloride ($P_{6,6,6,14}$ Cl) and Trihexyl(tetradecyl)phosphonium bis((trifluoromethyl)sulfonyl)amide ($P_{6,6,6,14}$ TFSI) were also purchased from commercial sources. All other mentioned ionic liquids were synthesized according to previously published procedures.[97]

NMR spectra were acquired on a *Bruker* Avance Ultrashield 400 MHz or a *Bruker* DPX 400 MHz spectrometer at a temperature of 298 K unless otherwise stated. All ^1H and $^{13}C(^1H)$ chemical shifts δ are reported in parts per million (ppm), with the residual solvent peak serving as internal reference.[102] Abbreviations for NMR multiplicities are: singlet (s), doublet (d), triplet (t), quartet (q) and multiplet (m).

Electrospray ionization mass spectra (ESI-MS) were measured using a *Thermo Scientific LCQ/FLEET* spectrometer.

Elemental analyses were carried out in the microanalytical laboratory of the Catalysis Research Center at the Technical University of Munich. The elements C, H, N and S were determined with a combustion analyzer (EURO EA-CHNS, *HEKAtech*) and are given in mass percentages.

Cyclic voltammograms were recorded using a using a *Ivium Technology* potentiostat employing three-electrode / teflon cell setup in a steel housig in a glovebox with an argon atmosphere. An gold electrode was used as the working electrode and polished before each measurement. Platinum electrodes were used as the counter and reference electrodes. The potential was measured with a scan rate of 2 mV/s. The ionic liquids were used as solvent and electrolyte.

5.2 Synthetic Procedures

5.2.1 Synthesis of $[Cr(NCR)_{3\text{-}4}][BF_4]_2$ (**8**-**11**)

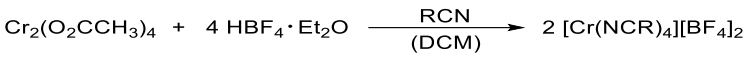

This group of complexes is synthesized according to a literature procedure[87b] with slight modifications. $Cr_2(O_2CCH_3)_4$ (1.00 eq., 3.67 mmol, 1.25 g) is suspended in a mixture of 10 mL of DCM and 5 mL of the respective nitrile at r.t. $HBF_4 \cdot Et_2O$ (5.00 eq., 18.36 mmol, 2.50 mL) is added dropwise to the suspension resulting in an immediate color change from brownish red to turquois. The solution is stirred for 45 min at room temperature to complete the reaction. The solvents are removed under reduced pressure. The remaining oil is washed with diethyl ether (2 x 10 mL) inducing the precipitation of the product. The solid is washed with diethyl ether (3 x 10 mL) and *n*-pentane (3 x 10 mL) and dried *in vacuo*.

5.2.1.1 $[Cr(NCCH_3)_3][BF_4]_2$ (**8**)

The product is obtained as blue powder with a yield of 79 %.

Elemental analysis calculated (%) for $C_6H_9B_2CrF_8N_3$: C, 20.66; H, 2.60; N, 12.05; found: C, 21.71; H, 3.15; N, 9.71.

5.2.1.2 $[Cr(NCC_6H_5)_3][BF_4]_2$ (**9**)

The product is received as two fractions, as a dark blue powder and as blue crystals, with a combined yield of 69 %.

Elemental analysis calculated (%) for $C_{21}H_{15}B_2CrF_8N_3$: C, 47.15; H, 2.83; N, 7.85; found: C, 47.90; H, 3.25; N, 7.43.

5.2.1.3 $[Cr(NCC(CH_3)_3)_4][BF_4]_2$ (**10**)

The product is obtained blue powder with a yield of 85 %.

Elemental analysis calculated (%) for $C_{20}H_{36}B_2CrF_8N_4$: C, 43.04; H, 6.50; N, 10.04; found: C, 42.85; H, 6.31; N, 10.80.

5.2.1.4 $[Cr(NCC_2H_5)_4][BF_4]_2$ (**11**)

The product is received as blue powder with a yield of 73 %.

Elemental analysis calculated (%) for $C_{12}H_{20}B_2CrF_8N_4$: C 32.32; H, 4.52; N, 12.56; found: C, 31.79; H, 4.61; N, 12.01.

5.2.2 Synthesis of $[Cr(NCR)_2][CF_3SO_3]_2$ (**12**-**15**)

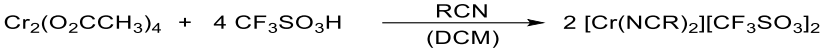

This group of complexes is synthesized according to a literature procedure[103] with slight modifications. To the suspension of $Cr_2(O_2CCH_3)_4$ (1.00 eq., 3.67 mmol, 1.25 g) with 10 mL of dichloromethane and 5 mL of the respective nitrile, trifluoromethanesulfonic acid (5.00 eq., 18.35 mmol, 1.63 mL) is added dropwise at room temperature resulting in an immediate color change from brownish red to blue green. The solution is stirred for 2 h to complete the reaction. The solution is concentrated to 50 % of its original volume inducing the precipitation of the product. 10 mL of diethyl ether are added to complete the precipitation. After filtering off the solvents the remaining solid is washed with diethyl ether (3 x 10 mL) and *n*-pentane (2 x 7 mL) and dried *in vacuo* for about 15 min.

5.2.2.1 $[Cr(NCCH_3)_2][CF_3SO_3]_2$ (**12**)

The product is obtained as green powder with a yield of 65 %.

Elemental analysis calculated (%) for $C_6H_6CrF_6N_2O_6S_2$: C, 16.67; H, 1.40; 6.48; S, 14.83; found: C, 16.82; H, 1.55; N, 5.90; S, 14.50.

5.2.2.2 $[Cr(NCC_6H_5)_2][CF_3SO_3]_2$ (**13**)

The product is received as light green powder with a yield of 66 %.

Elemental analysis calculated (%) for $C_{16}H_{10}CrF_6N_2O_6S_2$: C, 34.54; H, 1.81; N, 5.04; S, 11.52; found: C, 34.27; H, 1.89; N, 5.11; S, 11.39.

5.2.2.3 $[Cr(NCC(CH_3)_3)_2][CF_3SO_3]_2$ (**14**)

The product is obtained as light green powder with a yield of 71 %.

Elemental analysis calculated (%) for $C_{12}H_{18}CrF_6N_2O_6S_2$: C, 27.91; H, 3.51; N, 5.42; S, 12.42; found: C, 27.30; H, 3.47; N, 4.99; S, 11.48.

5.2.2.4 $[Cr(NCC_2H_5)_2][CF_3SO_3]_2$ (**15**)

The product is received as green powder with a yield of 68 %.

Elemental analysis calculated (%) for $C_8H_{10}CrF_6N_2O_6S_2$: C, 20.88; H, 2.19; N, 6.09; S, 13.93; found: C, 20.01; H, 2.14; N, 5.64; S, 14.04.

5.2.3 Synthesis of $[Cr(O_2CCH_3)(NCCH_3)_2][TFSI]$ (**16**)

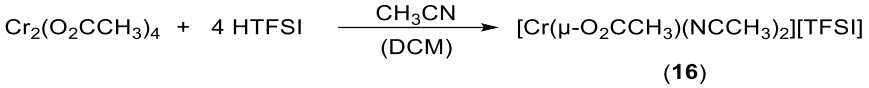

At room temperature dichromium(II) tetraacetate (**7**) (1.00 eq., 0.311 mmol, 106.00 mg) is dissolved in 3 mL of dichloromethane and the acid triflimide (HTFSI) (4.98 eq., 1.55 mmol, 436.80 mg) is dissolved in 3 mL of acetonitrile. The acid solution is added dropwise *via* cannula to the suspension of $Cr_2(O_2CCH_3)_4$ in DCM, resulting in an immediate color change from brownish red to green. The solution is stirred for 2 h to complete the reaction and afterwards it is concentrated to 50 % of its original volume inducing the precipitation of the product. 10 mL of diethyl ether are added to complete the precipitation. After filtering off the solvents the remaining solid is washed with diethyl ether (3 x 5 mL) and *n*-pentane (2 x 3 mL) and dried *in vacuo* for about 15 min. The product is obtained as fine green powder with a yield of 4 %.

^{19}F-NMR (CD_3CN, 298 K, 376 MHz, ppm): δ = -80.12 .

Elemental analysis calculated (%) for $[Cr(\mu\text{-}O_2CCH_3)(NCCH_3)_2][TFSI]$: C, 20.03; H, 1.92; N, 8.88; S, 13.55; found: C, 18.09; H, 1.91; N, 8.23; S, 13.75.

5.2.4 Synthesis of $[Mo_2(NCR)_{8\text{-}10}][BF_4]_4$ (**18**-**21**)

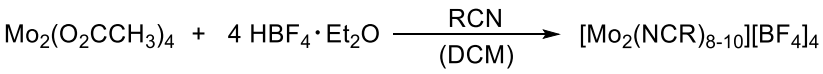

This group of complexes is synthesized according to a literature procedure[93] with slight modifications. At room temperature dimolybdenum(II) tetraacetate (**17**) (1.00 eq., 1.40 mmol, 0.61 g) is dissolved in a solution of 40 mL of dichloromethane and 10 mL of the respective nitrile. $HBF_4 \cdot Et_2O$ (15.75 eq., 22.05 mmol, 3 mL) is added dropwise to the vigorously stirring solution, resulting in an immediate color change from red *via* purple to dark blue within less than 5 min. The reaction mixture is stirred for 30 min at room temperature and then heated to reflux for 3 h. A dark blue solid is formed during the reaction and begins to precipitate by cooling the suspension down to room temperature. To complete the precipitation the suspension is stored in an ice bath for about 2 h and the solvents are filtered off. The remaining solid is washed with diethyl ether (3 x 15 mL) and *n*-pentane (3 x 10 mL) and dried *in vacuo* for about 10 min.

There are slight changes in the procedure for the benzonitrile (**19**) derivative. After cooling down the reaction mixture to room temperature, the solution is concentrated to about 50 % of its original volume. During cooling the reaction mixture in an ice bath, diethyl ether (10 x 15 mL) is added inducing the precipitation of the product. The solution is stored at -32 °C for several days to complete the precipitation. The solvents are filtered off and the product is washed as described above and dried *in vacuo*.

5.2.4.1 $[Mo_2(NCCH_3)_8][BF_4]_4$ (**18**)

The product is obtained as a fine blue powder with a yield of 93 %.

^{1}H-NMR (CD_3CN, 298 K, 400 MHz, ppm): δ = 1.95 (s).

Elemental analysis calculated (%) for $C_{16}H_{24}B_4F_{16}Mo_2N_8$: C, 22.15; H, 2.79; N, 12.92; Mo, 22.12; F, 35.04; found: C, 22.51; H, 3.11; N, 12.92; Mo, 19.60; F, 33.00.

5.2.4.2 $[Mo_2(NCC_6H_5)_8][BF_4]_4$ (**19**)

The product is received as a dark violet solid with a yield of 85 %.

^{1}H-NMR (CD_2Cl_2, 298 K, 400 MHz, ppm): δ = 7.71 (m, 2H), 7.62 (m, 1H), 7.51 (m, 2H).

Elemental analysis calculated (%) for $C_{56}H_{40}B_4F_{16}Mo_2N_8$: C, 49.31; H, 2.96; N, 8.21; found: C, 48.95; H, 2.90; N, 8.00.

5.2.4.3 $[Mo_2(NCC(CH_3)_3)_{10}][BF_4]_4$ (**20**)

The product is received as dark blue powder with a yield of 89 %.

^{1}H-NMR (CD_3CN, 298 K, 400 MHz, ppm): δ = 1.34 (s, $NCC(CH_3)_3$).

Elemental analysis calculated (%) for $C_{50}H_{90}B_4F_{16}Mo_2N_{10}$: C, 43.82; H, 6.62; N, 10.22; found: 43.02; H, 6.00; N, 10.65.

5.2.4.4 $[Mo_2(NCC_2H_5)_{10}][BF_4]_4$ (**21**)

The product is obtained as dark blue powder with a yield of 87 %.

Elemental analysis calculated (%) for $C_{30}H_{50}B_4F_{16}Mo_2N_{10}$: C, 33.06; H, 4.62; N, 12.85; found: C, 32.52; H, 4.13; N, 12.90.

5.2.5 Synthesis of $[Mo_2(NCR)_{8\text{-}10}][CF_3SO_3]_4$ (**22**-**25**)

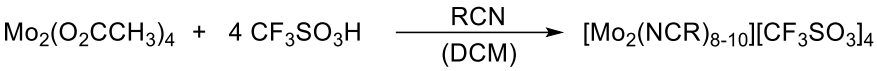

This group of complexes is synthesized according to a literature procedure[93] with slight modifications. At room temperature, $Mo_2(OAc)_4$ (1.00 eq., 1.40 mmol) is dissolved in a solution of 40 mL of dichloromethane and 10 mL of the respective nitrile. Trifluoromethanesulfonic acid is (15.76 eq., 22.07 mmol, 1.96 mL) added dropwise to the vigorously stirring solution, resulting in an immediate color change from red, to purple and to dark blue within less than 5 min. The reaction mixture is stirred for 30 min at room temperature and then heated to reflux for 3 h. A dark blue solid is formed during the reaction and begins to precipitate by cooling to suspension down to room temperature. To complete the precipitation the suspension is stored in an ice bath for about 2 h and the solvents are filtered off. The remaining solid is washed with diethyl ether (3 x 15 mL) and *n*-pentane (3 x 10 mL) and dried *in vacuo* for about 15 min.

5.2.5.1 $[Mo_2(NCCH_3)_7][CF_3SO_3]_4$ (**22**)

The product is obtained as dark blue powder with a yield of 92 %.

^{1}H-NMR (CD_3CN, 298 K, 400 MHz, ppm): δ = 2.53 (s, 21H, $(CH_3CN)_7$).

Elemental analysis calculated (%) for $C_{18}H_{21}F_{12}Mo_2N_7O_{12}S_4$: C, 20.10; H, 1.97; N, 9.12; S, 11.92; found: C, 19,50; H, 2.02; N, 8.37; S, 12.90.

5.2.5.2 $[Mo_2(NCC_6H_5)_7][CF_3SO_3]_4$ (**23**)

The product is received as a fine dark purple powder with a yield of 89 %.

^{1}H-NMR (CD_3CN, 298 K, 400 MHz, ppm): δ = 7.74 – 7.52 (m, 35H, $((C_6H_5)CN)_7$).

Elemental analysis calculated (%) for $C_{53}H_{35}F_{12}Mo_2N_7O_{12}S_4$: C, 42.16; H, 2.34; N, 6.49; S, 8.49; found: C, 41.73; H, 3.05; N, 5.68; S, 6.84.

5.2.5.3 $[Mo_2(NCC(CH_3)_3)_{10}][CF_3SO_3]_4$ (**24**)

The product is received as dark blue solid with a yield of 88 %.

^{1}H-NMR (CD_3CN, 298 K, 400 MHz, ppm): δ = 1.34 (s, 90H, ^{t}BuCN).

Elemental analysis calculated (%) for $C_{54}H_{90}F_{12}Mo_2N_{10}O_{12}S_4$: C, 40.05; H, 5.60; N, 8.65; S, 8.12; found: C, 41.03; H, 5.78; N, 7.96; S, 7.45.

5.2.5.4 $[Mo_2(NCC_2H_5)_8][CF_3SO_3]_4$ (**25**)

The product is obtained as dark blue solid with a yield of 86 %.

Elemental analysis calculated (%) for $C_{28}H_{40}F_{12}Mo_2N_8O_{12}S_4$: C, 27.37; H, 3.28; N, 9.12; S, 10.44; found: C, 26.94; H, 3.35; N, 8.45; S, 8.75.

5.2.6 Synthesis of $[Mo_2(NCCH_3)_8][TFSI]_4$ (**26**)

$$Mo_2(O_2CCH_3)_4 + 4\ HTFSI \xrightarrow[(DCM)]{CH_3CN} [Mo_2(NCCH_3)_8][TFSI]_4$$

At room temperature, dimolybdenum tetraacetate (1.00 eq., 0.58 mmol, 248.82 mg) is dissolved in 10 mL of dichloromethane and trifluoromethanesulfonimide (4.79 eq., 2.80 mmol, 787.22 mg) is dissolved in 8 mL of acetonitrile. The acid solution is added dropwise to the solution of $Mo_2(O_2CCH_3)_4$ in DCM, resulting in an immediate color change from red *via* purple to dark blue. The reaction mixture is stirred for about 30 min at room temperature and afterwards heated to reflux for 1 h to complete the reaction. The dark violet solution is cooled down to room temperature and then cooled in an ice bath to facilitate the precipitation of the product. By concentrating the solution to 50 % of its original volume a dark blue solid begins to precipitate, and the mother liquor is filtered off. The remaining solid is washed with diethyl ether (3 x 10 mL) and *n*-pentane (3 x 10 mL) and dried *in vacuo* for about 30 min. The product is obtained as a fine blue powder with a yield of 57 %.

Dark blue needle shaped single crystals suitable for SC-XRD were grown by slow diffusion of diethyl ether in a solution of the product in acetonitrile.

^{1}H-NMR (CD_3CN, 298 K, 400 MHz, ppm): δ = 2.17 (s, 24H, CH_3CN).

^{13}C-NMR (CD_3CN, 298 K, 101 MHz, ppm): δ = 118.26; 1.28.

^{19}F-NMR (CD_3CN, 298 K, 376 MHz, ppm): δ = -80.13.

Elemental analysis calculated (%) for $[Mo_2(NCCH_3)_{8.5}][TFSI]_4$: C, 18.07; H, 1.55; N, 10.54; S, 15.44; found: C, 18.16; H, 1.56; N, 9.94; S, 16.02.

5.2.7 Synthesis of $[Mo_2(\mu\text{-}O_2CCH_3)_2(NCC(CH_3)_3)_4][TFSI]_2$ (**27**)

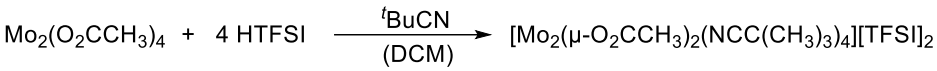

At room temperature, dimolybdenum(II) tetraacetate (1.00 eq., 0.584 mmol, 248.82 mg) is dissolved in 10 mL od DCM and trifluoromethanesulfonimide (4.79 eq., 2.80 mmol, 787.22 mg) is dissolved in 10 mL of *tert*-butylnitrile. The acid solution is added dropwise to the solution of $Mo_2(O_2CCH_3)_4$ in DCM, resulting in an immediate color change from red, to dark red to purple. The reaction mixture is stirred for about 30 min at room temperature and afterwards heated to reflux for 1.5 h. The solution is cooled down to room temperature and concentrated to about 50 % of its original volume. The remaining oil is filtered off from the mother liquor and is washed with diethyl ether (8 x 10 mL) and *n*-pentane (3 x 10 mL) to yield a pink solid, while the mother liquor is also treated with diethyl ether (60 mL) and stored at -32 °C over night to yield the product as fine pink needles. Both fractions are filtered off from the solvents and dried *in vacuo* for about 15 min each. The product is obtained as a fine pink powder and as pink needles with a combined yield of 56%.

^{1}H-NMR (CD_3CN, 298 K, 400 MHz, ppm): δ = 1.34 (s, 36H, ^{t}BuCN); 2.90 (s, 6H, CH_3COO).

^{13}C-NMR (CD_3CN, 298 K, 101 MHz, ppm): δ = 173.12; 125.53; 27.46; 22.73; 13.48.

^{19}F-NMR (CD_3CN, 298 K, 376 MHz, ppm): δ = -80.21.

Elemental analysis calculated (%) for $C_{28}H_{42}F_{12}Mo_2N_6O_{12}S_4$: C, 27.96; H, 3.52; N, 6.99; S, 10.66; found: 28.33; H, 3.41; N, 6.72; S, 10.39.

5.2.8 Synthesis of $[W(NO)_2(NCR)_4][BF_4]_2$ (**28** and **29**)

This group of complexes is synthesized according to a literature procedure[96] with slight modifications. $W(CO)_6$ (1.00 eq., 2.84 mmol, 1.00 g) is dissolved in 20 mL of the respective nitrile at room temperature. $NOBF_4$ (2.00 eq., 5.86 mmol, 0.68 g) is added to the solution resulting in a color change from yellow *via* orange to dark green within few minutes. The reaction mixture is stirred at room temperature overnight. The solution is concentrated to about 50 % of its original volume and cooled in an ice bath to induce the precipitation of the product. 10 mL of diethyl ether are added to complete the precipitation. After filtering off the solvents the remaining solid is washed with diethyl ether (3 x 10 mL) and *n*-pentane (2 x 7 mL) and dried *in vacuo* for about 45 min.

5.2.8.1 $[W(NO)_2(NCCH_3)_4][BF_4]_2$ (**28**)

The product is obtained as dark green solid with a yield of 85 %.

^{1}H-NMR (CD_3NO_2, 298 K, 400 MHz, ppm): δ = 3.04 (s, 6H, CH_3CN), 3.16 (s, 6H, CH_3CN).

^{13}C-NMR (CD_3NO_2, 298 K, 101 MHz, ppm): δ = 135.81; 125.12; 3.38; 2.41.

Elemental analysis calculated (%) for $C_8H_{12}B_2F_8N_6O_2W$: C, 16.52; H, 2.08; N, 14.45; found: C, 16.06; H, 2.38; N, 14.29.

5.2.8.2 $[W(NO)_2(NCC(CH_3)_3)_3][BF_4]_2$ (**29**)

The product is received as light green powder with a yield of 89 %.

^{1}H-NMR (CD_3CN, 298 K, 400 MHz, ppm): δ = 1.54 (s, 9H, $(CH_3)_3CCN$), 1.56 (s, 9H, $(CH_3)_3CCN$).

Elemental analysis calculated (%) for $C_{15}H_{27}B_2F_8N_5O_2W$: C, 27.02; H, 4.08; N, 10.50; found: C, 28.95; H, 4.68; N, 10.29.

6. Supplementary Data

6.1 Single crystal X-ray Structure Determination

6.1.1 General Data

X-ray crystallographic data were collected on a single crystal X-ray diffractometer with the following setup: *Bruker* APEX II, κ-CCD, with a CCD detector, a FR591 rotating anode and a MONTEL mirror optic using the APEX2 software package.[20]

All measurements used MoK_α radiation (λ = 0.71073 Å). The measurements were performed on single crystals coated with perfluorinated ether. The crystal was fixed on top of a glass fiber or kapton micro sampler and frozen under a stream of cold nitrogen. A matrix scan was used to determine the initial lattice parameters. Reflections were corrected for Lorentz and polarization effects, scan speed and background using SAINT.[21] Absorption corrections, including odd and even ordered spherical harmonics were performed using SADABS.[21] Space group assignments were based upon systematic absences, E statistics and successful refinement of the structures. Structures were solved by direct methods (SHELXS) or charge flipping (SHELXT) with the aid of successive difference Fourier maps and were refined against all data using SHELXL-2014 in conjunction with SHELXLE.[22] Hydrogen atoms were calculated in ideal positions as follows: Methyl hydrogen atoms were refined as part of rigid rotating groups, with a C-H distance of 0.98 Å and $U_{iso(H)} = 1.5 \cdot U_{eq(C)}$. Other H atoms were placed in calculated positions and refined using a riding model, with methylene and aromatic C-H distances of 0.99 Å and 0.95 Å, respectively, other C-H distances of 1.00 Å and $U_{iso(H)} = 1.2 \cdot U_{eq(C)}$. Non-hydrogen atoms were refined with anisotropic displacement parameters. Full matrix least-squares refinements were carried out by minimizing $\Sigma w(F_o^2 F_c^2)^2$ with SHELXL weighting scheme.[22b] Neutral atom scattering factors for all atoms and anomalous dispersion corrections for the non-hydrogen atoms were taken from *International Tables for Crystallography*.[23] Images of the crystal structures were generated with Mercury.[24]

6.1.2 Detailed crystallographic Data

	Compound (**26**)	Compound (**27**)
Chemical formula	$C_{24}H_{24}F_{24}Mo_2N_{12}O_{16}S_8$	$C_{28}H_{42}F_{12}Mo_2N_6O_{12}S_4$
Formula weight [g mol^{-1}]	1640.89	1202.79
Temperature [K]	100(2)	100(2)
Wavelength [Å]	0.71073	0.71073
Crystal size [mm^3]	0.326 x 0.601 x 0.701	0.115 x 0.123 x 0.197
Crystal habit	clear colorless block	clear pink plate
Crystal system	tetragonal	triclinic
Space group	P -4 21 c	P -1
a [Å]	13.0869(4)	10.7587(18)
b [Å]	13.0869(4)	10.8540(18)
c [Å]	17.9800(7)	20.924(3)
α [°]	90	82.097(5)
β [°]	90	88.166(5)
γ [°]	90	82.065(5)
Volume [Å^3]	3079.4(2)	2396.8(7)
Z	2	2
Density calculated [g cm^{-3}]	1.858	1.667
μ [mm^{-1}]	0.820	0.801
F(000)	1704	1208
Θ range for data collection [°]	2.20 to 27.50	2.55 to 26.37
Index ranges (h, k, l)	-15 ≤ h ≤ 17 -16 ≤ k ≤ 9 -23 ≤ l ≤ 23	-13 ≤ h ≤ 13 -13 ≤ k ≤ 13 -26 ≤ l ≤ 26
Reflections collected	13170	104812
Independent reflections	3499 [R(int) = 0.0199]	9810 [R(int) = 0.0267]
Coverage of independent reflections [%]	99.7	99.9
Max. and min. transmission	0.7760 and 0.5970	0.9140 and 0.8580
Data / restraints / parameters	3499 / 258 / 287	9810 / 0 / 591
Goodness-of-fit on F^2	1.082	1.068
Δ/σ_{max}	0.011	0.003
Final R indices (I>2σ(I))	3342 data R_1 = 0.0491; wR_2 = 0.1385	9205 data R_1 = 0.0491; wR_2 = 0.1385
Final R indices (all data)	R_1 = 0.0513, wR_2 = 0.1414	R_1 = 0.0212; wR_2 = 0.0479
Largest difference peak and hole [eÅ^{-3}]	1.411 and -0.728	0.373 d -0.724

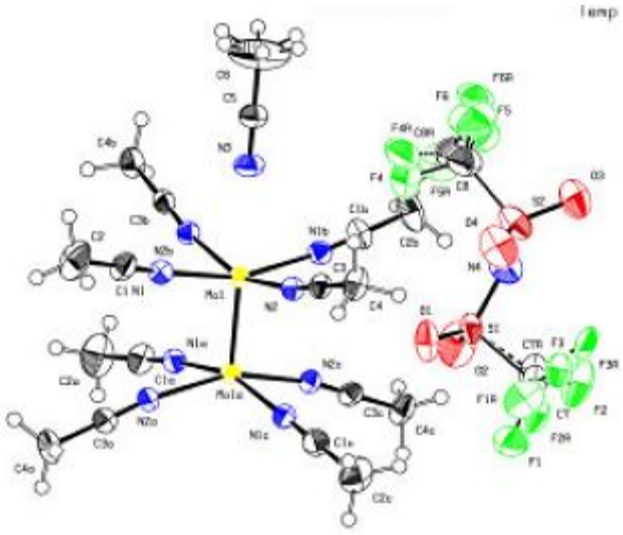

Figure 30 ORTEP style representation of the $[Mo_2(NCCH_3)_8]^{4+}$ core of the complex **26** with ellipsoids shown at a 50 % probability level. Hydrogen atoms are omitted for clarity. One TFSI anion is also shown. An additional acetonitrile molecule can be seen above the cation which is located between two cations and is 'shared'. Color scheme: yellow, molybdenum; blue, nitrogen.

6.2. ^{1}H- and ^{13}C-NMR spectroscopy Data

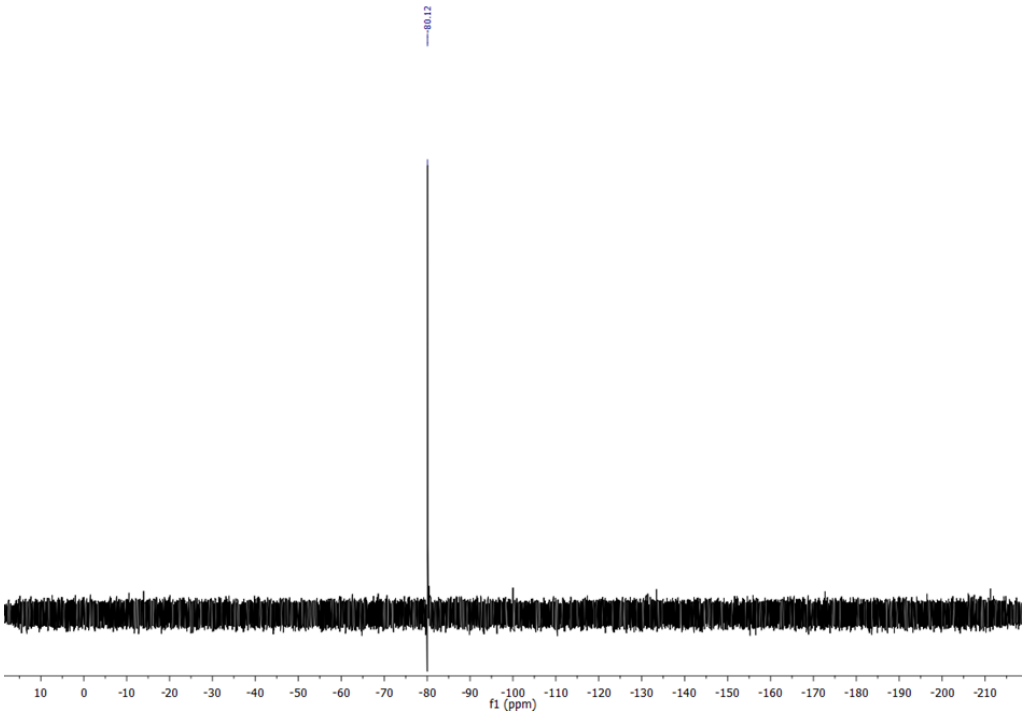

Figure 31 ^{19}F-NMR of complex **16** in CD_3CN at 298 K.

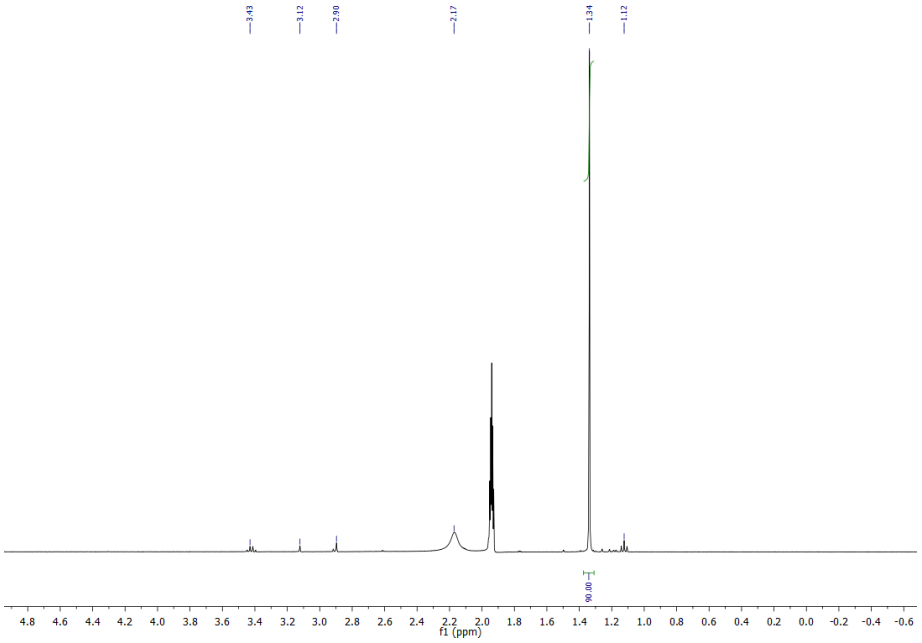

Figure 32 ^{1}H NMR of complex **20** in CD_3CN at 298 K. Small impurities of diethyl ether and water were still present.

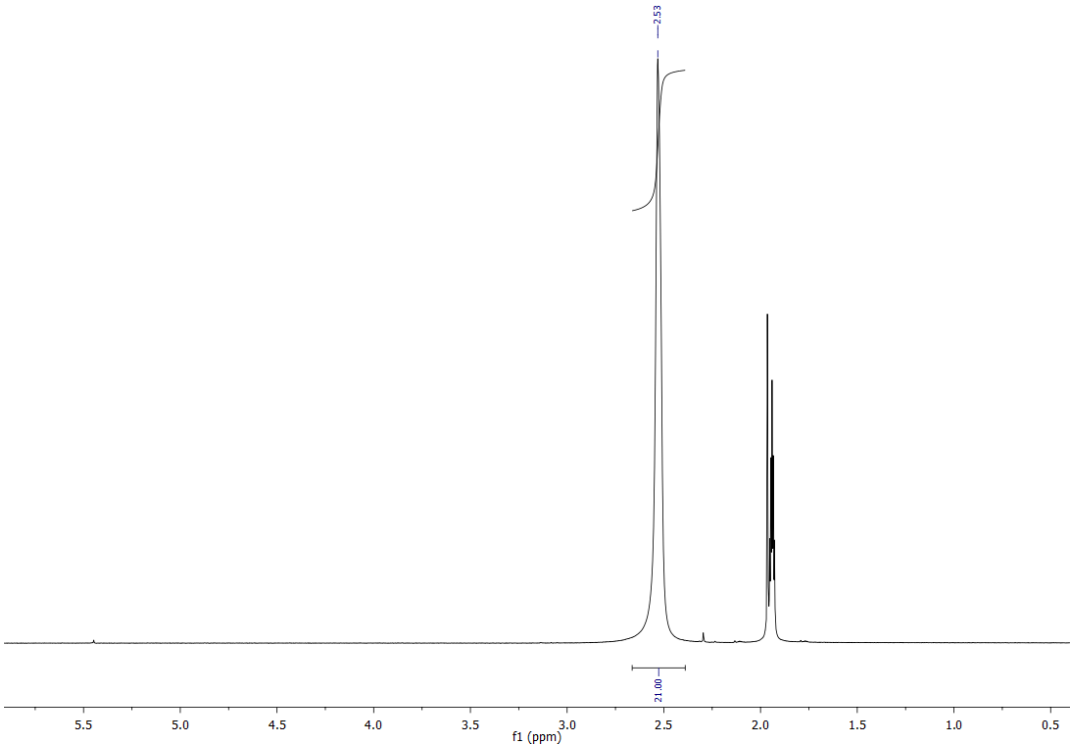

Figure 33 ^{1}H NMR of complex **22** in CD_3CN at 298 K.

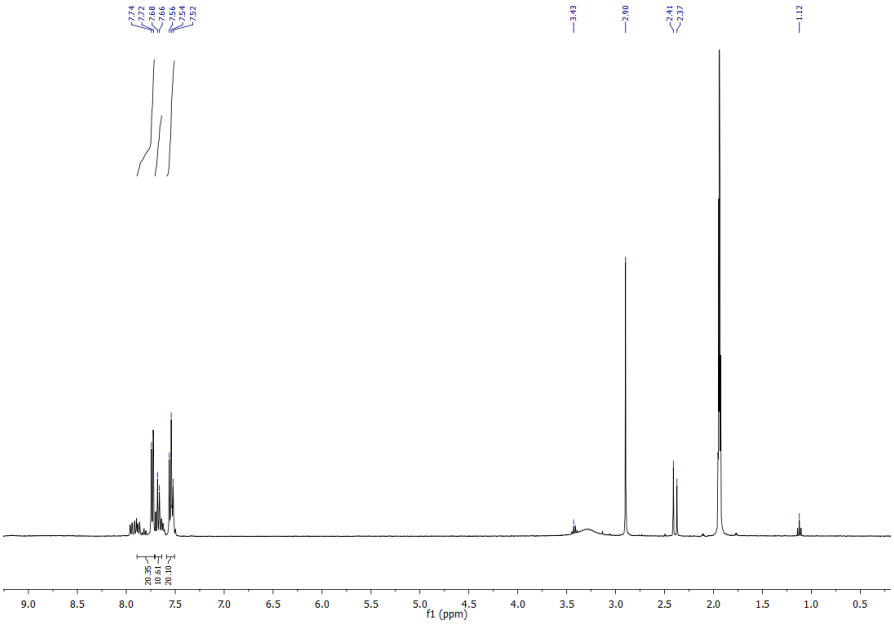

Figure 34 ^{1}H NMR of complex **23** in CD_3CN at 298 K. Impurities of diethyl ether were still present and at 2.37 ppm as well at 2.41 ppm which could not be assigned.

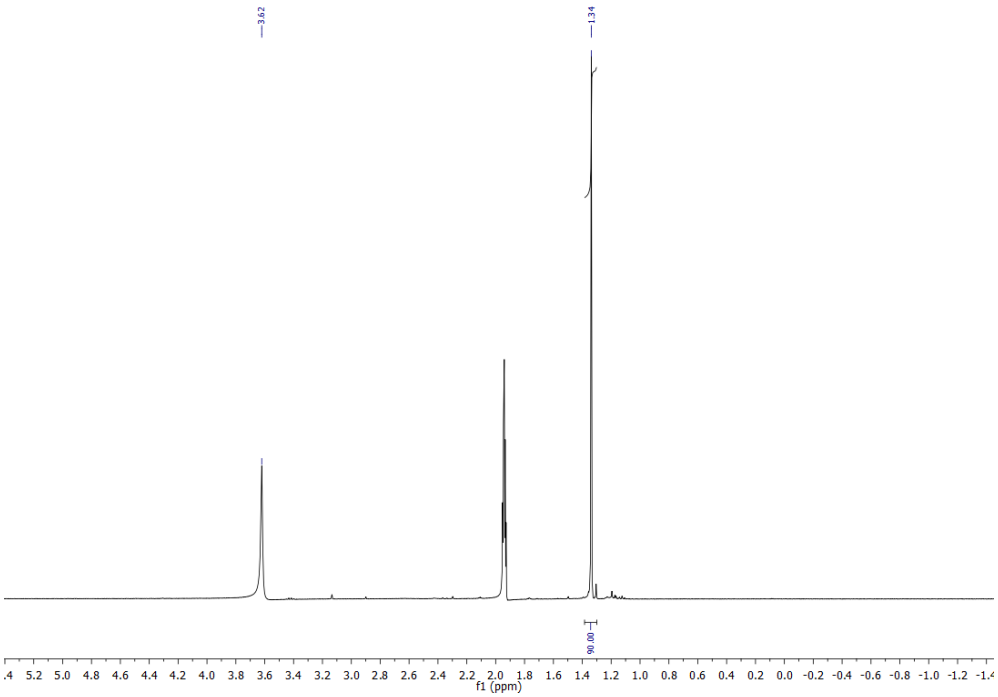

Figure 35 ^{1}H NMR of complex **24** in CD_3CN at 298 K. An impurity at 3.62 ppm was still present and could not be assigned.

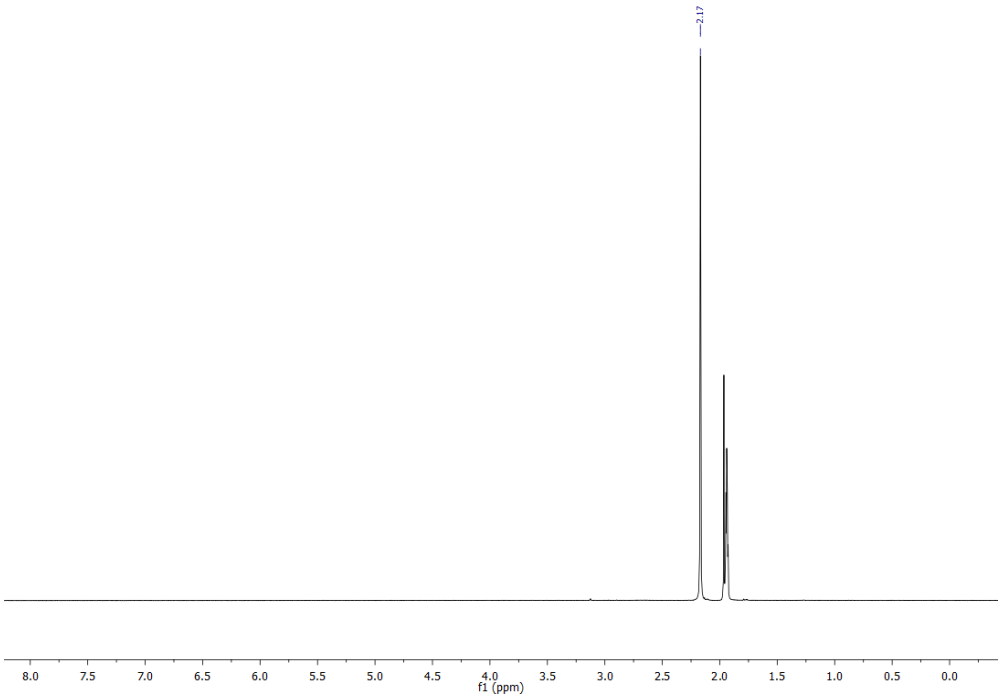

Figure 36 ^{1}H NMR of complex **26** in CD_3CN at 298 K.

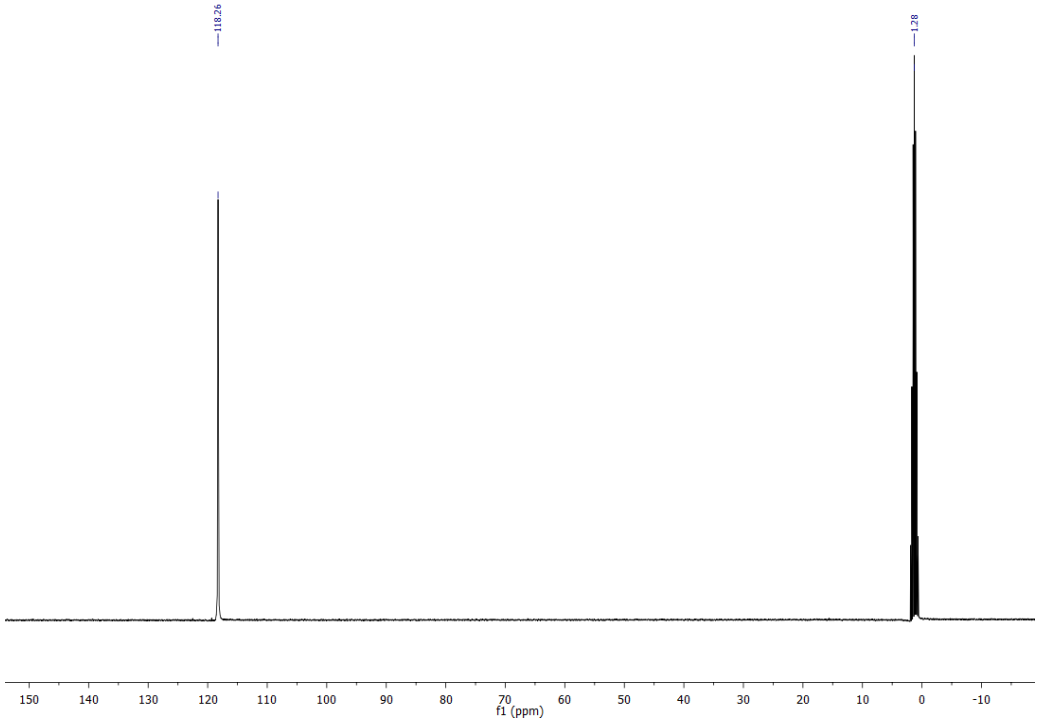

Figure 37 $^{13}C(^{1}H)$ NMR of complex **26** in CD_3CN at 298 K.

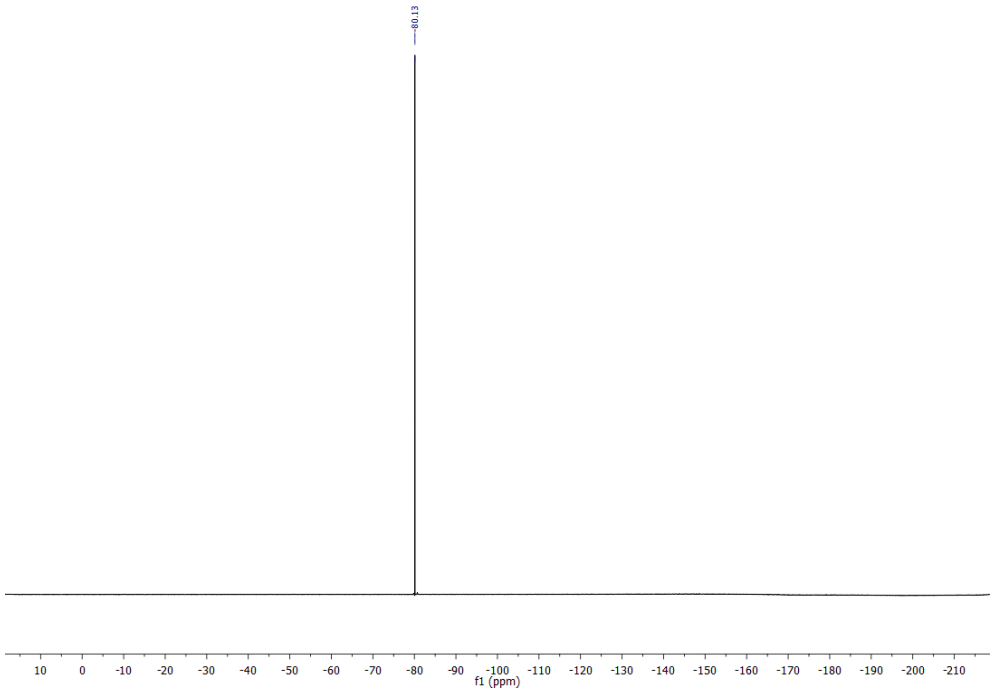

Figure 38 ^{19}F NMR of complex **26** in CD_3CN at 298 K.

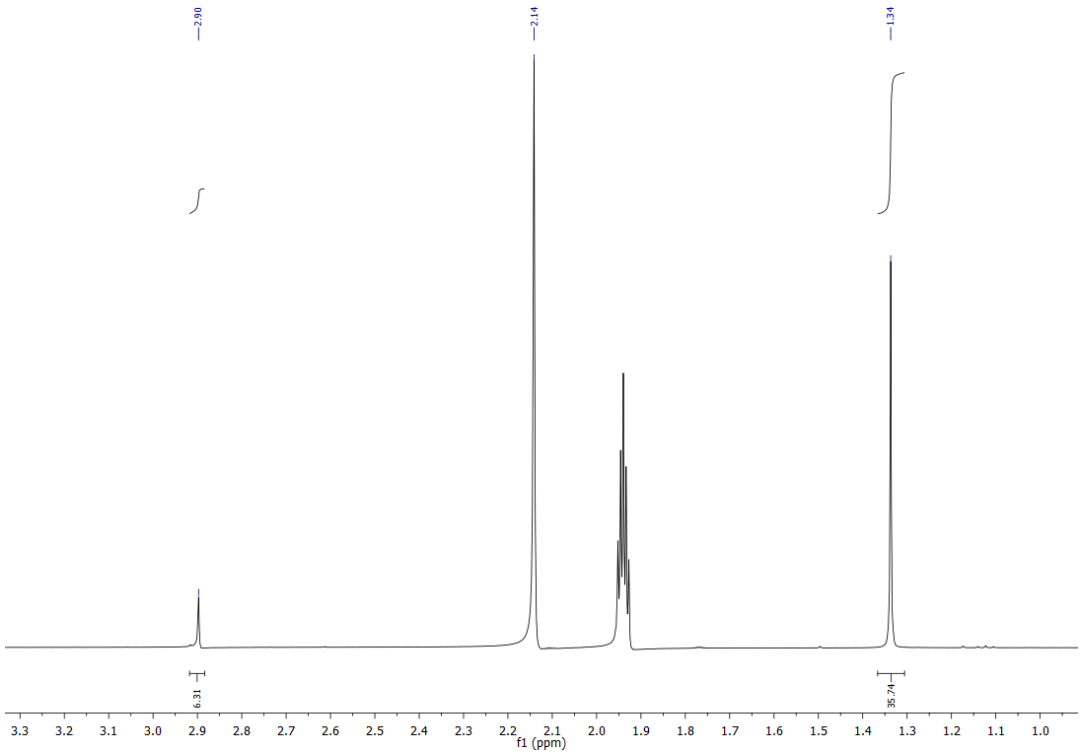

Figure 39 ^{1}H NMR of complex **27** in CD_3CN at 298 K. There is an impurity of water at 2.14 ppm since there was not used dried CD_3CN.

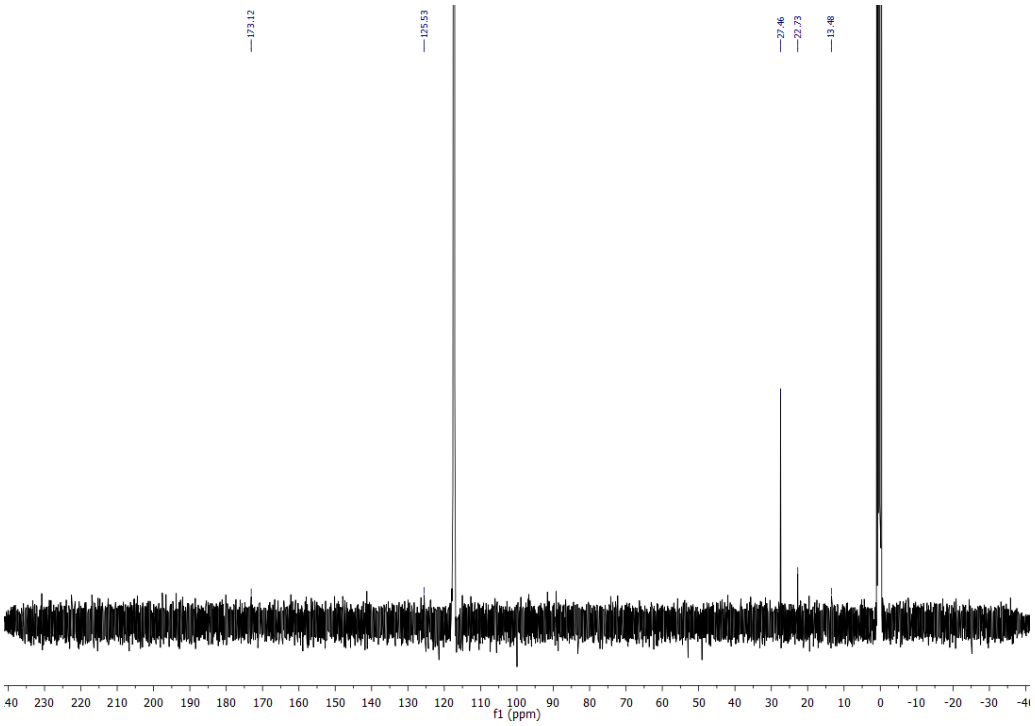

Figure 40 $^{13}C(^{1}H)$ NMR of complex **27** in CD_3CN at 298 K.

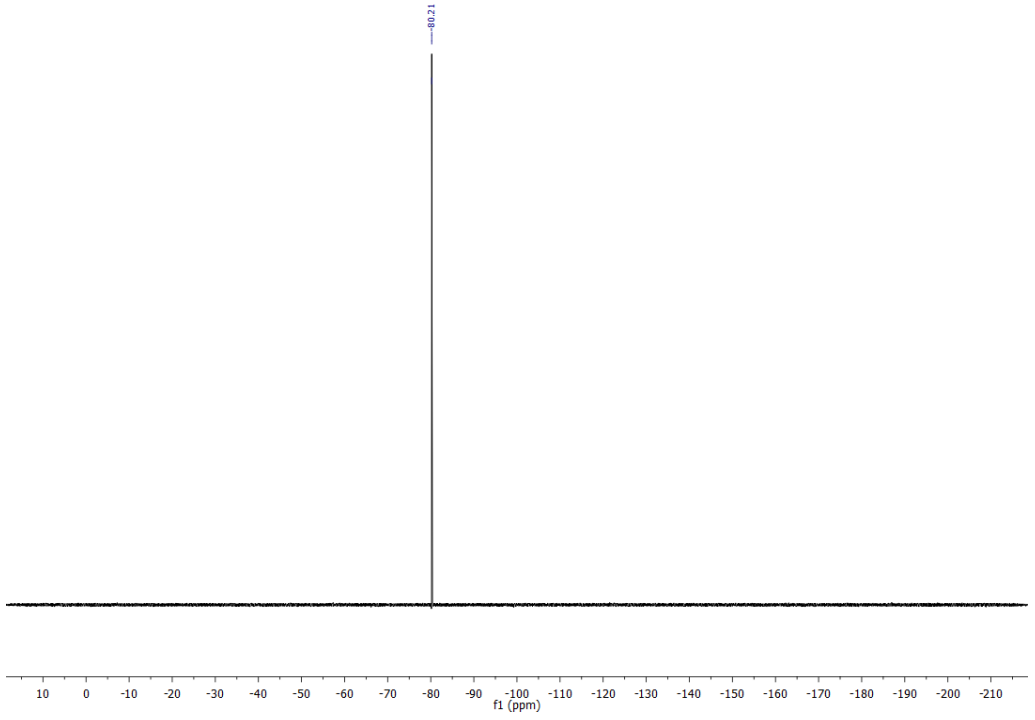

Figure 41 ^{19}F NMR of complex **27** in CD_3CN at 298 K.

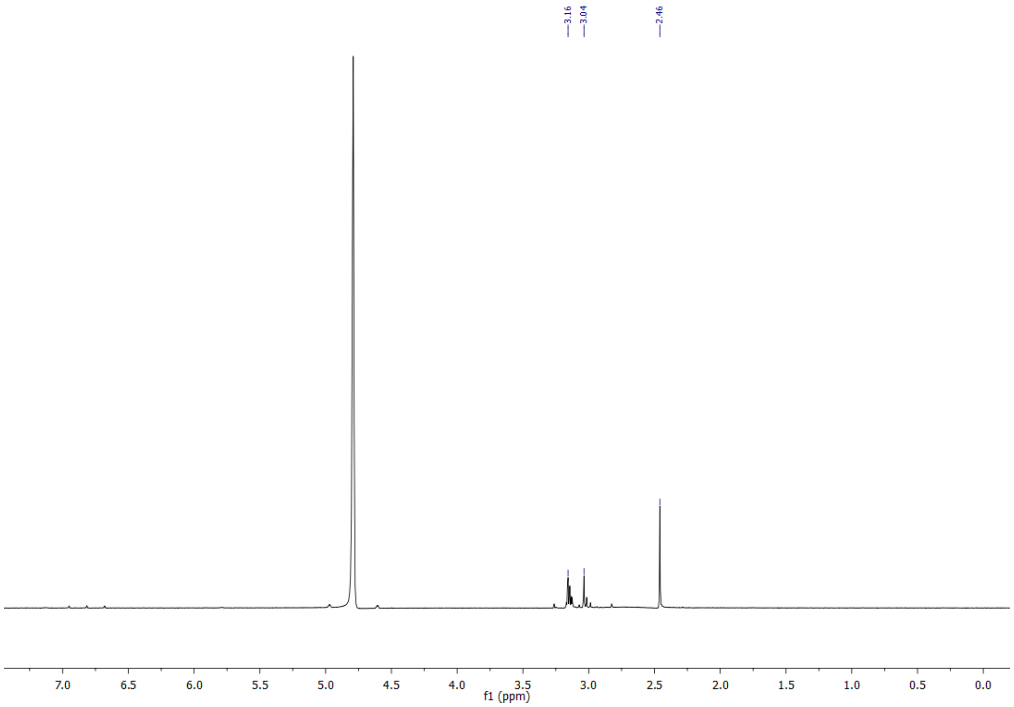

Figure 42 ^{1}H NMR of complex **28** in CD_3NO_2 at 298 K.

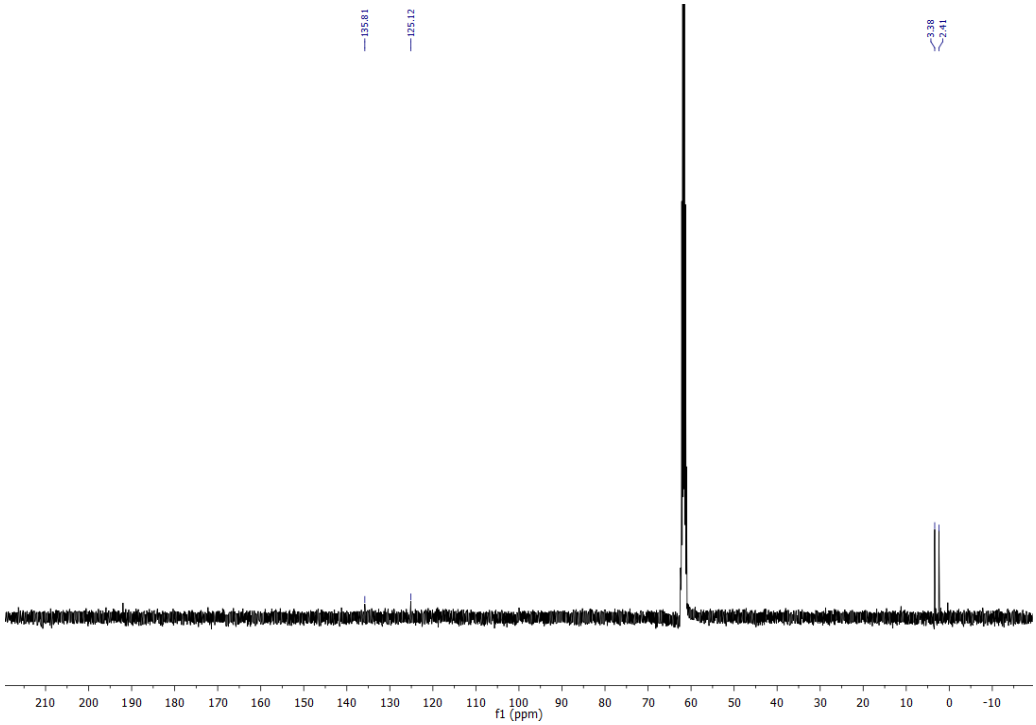

Figure 43 $^{13}C(^{1}H)$ NMR of complex **28** in CD_3NO_2 at 298 K.

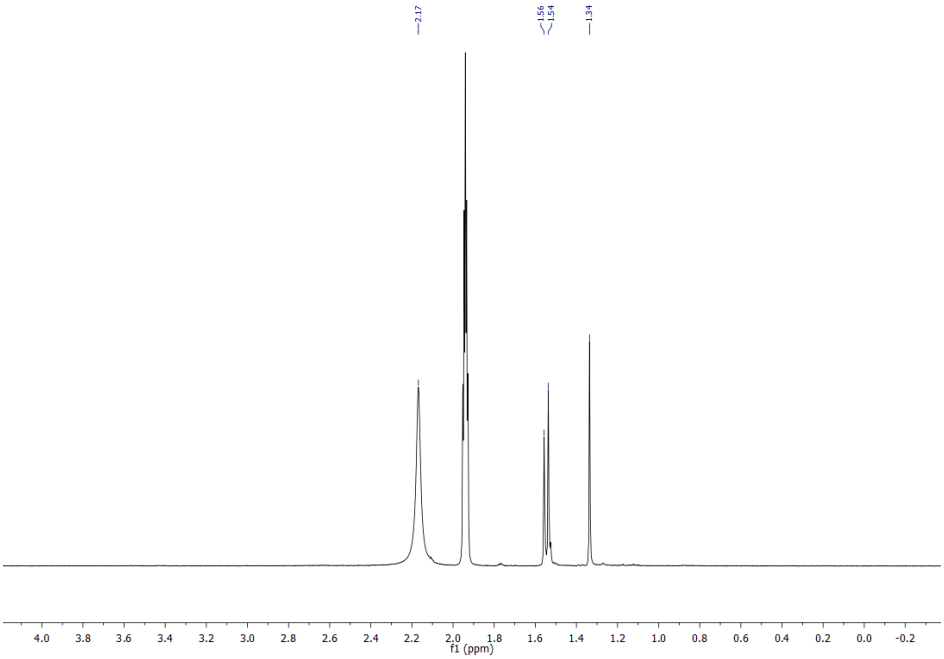

Figure 44 ^{1}H NMR of complex **29** in CD_3CN at 298 K. Free acetonitrile as well as free *tert*-butylnitrile ligands were also detected due to constant ligand exchange in solution.

III. References

[1] C. M. Egger, C. H. G. Jakob, F. Kaiser, O. Rindle, P. J. Altmann, R. M. Reich, F. E. Kühn, *Eur. J. Inorg. Chem.* **2019**, *2019*, 5059-5065.

[2] a) Y. Matsumura, H. Maeda, *Cancer Res.* **1986**, *46*, 6387-6392; b) H. Maeda, J. Wu, T. Sawa, Y. Matsumura, K. Hori, *J. Controlled Release* **2000**, *65*, 271-284; c) D. Wang, S. J. Lippard, *Nat. Rev. Drug Discovery* **2005**, *4*, 307; d) T. C. Johnstone, K. Suntharalingam, S. J. Lippard, *Chem. Rev.* **2016**, *116*, 3436-3486.

[3] D. A. McMorran, P. J. Steel, *Angew. Chem. Int. Ed.* **1998**, *37*, 3295-3297.

[4] F. Kaiser, A. Schmidt, W. Heydenreuter, P. J. Altmann, A. Casini, S. A. Sieber, F. E. Kühn, *Eur. J. Inorg. Chem.* **2016**, *2016*, 5189-5196.

[5] B. Therrien, G. Süss-Fink, P. Govindaswamy, A. K. Renfrew, P. J. Dyson, *Angew. Chem. Int. Ed.* **2008**, *47*, 3773-3776.

[6] A. Schmidt, A. Casini, F. E. Kühn, *Coord. Chem. Rev.* **2014**, *275*, 19-36.

[7] a) B. J. Holliday, C. A. Mirkin, *Angew. Chem. Int. Ed.* **2001**, *40*, 2022-2043; b) J. K. Klosterman, Y. Yamauchi, M. Fujita, *Chem. Soc. Rev.* **2009**, *38*, 1714-1725; c) A. M. Johnson, O. Moshe, A. S. Gamboa, B. W. Langloss, J. F. K. Limtiaco, C. K. Larive, R. J. Hooley, *Inorg. Chem.* **2011**, *50*, 9430-9442; d) Z. Li, N. Kishi, K. Hasegawa, M. Akita, M. Yoshizawa, *Chem. Commun.* **2011**, *47*, 8605-8607; e) J. E. M. Lewis, A. B. S. Elliott, C. J. McAdam, K. C. Gordon, J. D. Crowley, *Chem. Sci.* **2014**, *5*, 1833-1843.

[8] Z. Li, N. Kishi, K. Yoza, M. Akita, M. Yoshizawa, *Chem. Eur. J.* **2012**, *18*, 8358-8365.

[9] Y.-B. Xie, J.-R. Li, C. Zhang, X.-H. Bu, *Cryst. Growth Des.* **2005**, *5*, 1743-1749.

[10] a) Z. Chen, Y. Zhou, L. Weng, D. Zhao, *Cryst. Growth Des.* **2008**, *8*, 4045-4053; b) Y. Qi, F. Luo, Y. Che, J. Zheng, *Cryst. Growth Des.* **2008**, *8*, 606-611; c) H.-D. Guo, X.-M. Guo, S. R. Batten, J.-F. Song, S.-Y. Song, S. Dang, G.-L. Zheng, J.-K. Tang, H.-J. Zhang, *Cryst. Growth Des.* **2009**, *9*, 1394-1401; d) L.-L. Wen, Z.-D. Lu, X.-M. Ren, C.-Y. Duan, Q.-J. Meng, S. Gao, *Cryst. Growth Des.* **2009**, *9*, 227-238.

[11] a) S. Wang, S. Xiong, Z. Wang, J. Du, *Chem. Eur. J.* **2011**, *17*, 8630-8642; b) X. Zhang, L. Hou, B. Liu, L. Cui, Y.-Y. Wang, B. Wu, *Cryst. Growth Des* **2013**, *13*, 3177-3187; c) S. Bommakanti, U. Venkataramudu, S. K. Das, *Cryst. Growth Des.* **2019**, *19*, 1155-1166.

[12] a) K. A. Hofmann, F. Küspert, *Z. Anorg. Allg. Chem.* **1897**, *15*, 204-207; b) J. H. Rayner, H. M. Powell, *J. Chem. Soc.* **1952**, 319-328.

[13] S. R. Batten, N. R. Champness, X.-M. Chen, J. Garcia-Martinez, S. Kitagawa, L. Öhrström, M. O'Keeffe, M. P. Suh, J. Reedijk, *CrystEngComm* **2012**, *14*, 3001-3004.

[14] T. R. Cook, Y.-R. Zheng, P. J. Stang, *Chem. Rev.* **2013**, *113*, 734-777.

[15] a) O. M. Yaghi, G. Li, H. Li, *Nature* **1995**, *378*, 703-706; b) D. J. Tranchemontagne, J. R. Hunt, O. M. Yaghi, *Tetrahedron* **2008**, *64*, 8553-8557.

[16] H. Li, M. Eddaoudi, M. O'Keeffe, O. M. Yaghi, *Nature* **1999**, *402*, 276-279.

[17] a) A. Schmidt, M. Hollering, M. Drees, A. Casini, F. E. Kühn, *Dalton Trans.* **2016**, *45*, 8556-8565; b) A. Schmidt, V. Molano, M. Hollering, A. Pöthig, A. Casini, F. E. Kühn, *Chem. Eur. J.* **2016**, *22*, 2253-2256.

[18] J. Han, A. F. B. Räder, F. Reichart, B. Aikman, M. N. Wenzel, B. Woods, M. Weinmüller, B. S. Ludwig, S. Stürup, G. M. M. Groothuis, H. P. Permentier, R. Bischoff, H. Kessler, P. Horvatovich, A. Casini, *Bioconjugate Chem.* **2018**, *29*, 3856-3865.

[19] O. M. Yaghi, M. O'Keeffe, N. W. Ockwig, H. K. Chae, M. Eddaoudi, J. Kim, *Nature* **2003**, *423*, 705-714.

[20] *APEX suite of crystallographic software, APEX 2, version 2008.4,* APEX 2, Version 2017-9.0 and APEX 3, Version 2015-5.2, Bruker AXS Inc., Madison, Wisconsin, USA, **2014/2015**.

[21] SAINT, Versions 8.34A and 8.37A and SADABS, Versions 2014/5 and 2016/2, Bruker AXS Inc., Madison, Wisconsin, USA, **2014/2016**.

[22] a) C. B. Hübschle, G. M. Sheldrick, B. Dittrich, *J. Appl. Crystallogr.* **2011**, *44*, 1281-1284; b) G. Sheldrick, *Acta Crystallogr., Sect. C* **2015**, *71*, 3-8; c) G. Sheldrick, *Acta Crystallogr., Sect. A* **2015**, *71*, 3-8.
[23] *International Tables for Crystallography;* A. J. Wilson, Ed.; Kluwer Academic Publishers: dordrecht, The Netherlands, **1992**; Vol. C, *Tables 6.1.1.4 (pp 500-502), 4.2.6.8 (pp 219-222), and 4.2.4.2 (pp 193-199).*
[24] C. F. Macrae, I. J. Bruno, J. A. Chisholm, P. R. Edgington, P. McCabe, E. Pidcock, L. Rodriguez-Monge, R. Taylor, J. van de Streek, P. A. Wood, *J. Appl. Crystallogr.* **2008**, *41*, 466-470.
[25] A. S. f. Metals, *ASM metals reference book*, ASM Internat., Materials Park, OH, **1993**.
[26] a) T. E. Tietz, J. W. Wilson, *Behavior and Properties of Refractory Metals*, Stanford University Press, **1965**; b) J. R. Davis, *Alloying: Understanding the Basics*, ASM International, **2001**.
[27] C. L. Briant, *Mater. Res. Soc. Symp. Proc.* **1994**, *322*, 305.
[28] a) I. Mukhopadhyay, C. L. Aravinda, D. Borissov, W. Freyland, *Electrochim. Acta* **2005**, *50*, 1275-1281; b) H. Matsuno, A. Yokoyama, F. Watari, M. Uo, T. Kawasaki, *Biomaterials* **2001**, *22*, 1253-1262; c) F. Endres, MacFarlane D. R., A. P. Abbott (Eds.) *Electrodeposition from Ionic Liquids*, Wiley-VCH, **2008**; d) E. Boland, R. Lanam, A. Shchetkovskiy, A. Smirnov, *Proc. - Electrochem. Soc.* **2002**, *2002-19*, 797-802; e) V. A. Borisenko, *Powder Metall. Met. Ceram.* **1963**, *1*, 182-186; f) F. Habashi, *Miner. Process. Extr. Metall. Rev.* **2001**, *22*, 25-53; g) A. Weronski, *Thermal Fatigue of Metals*, Taylor & Francis, **1991**; h) A. Ravi Shankar, U. Kamachi Mudali, *Surf. Coat. Technol.* **2013**, *235*, 155-164.
[29] a) D. Inman, S. H. White, *J. Appl. Electrochem.* **1978**, *8*, 375-390; b) R. E. Smallwood, A. S. f. Testing, Materials, A. C. B.-o. Reactive, R. Metals, Alloys, *Refractory Metals and Their Industrial Applications: A Symposium*, ASTM, **1984**; c) D. S. Lee, *Mater. Manuf. Processes* **1990**, *5*, 121-123; d) Q. Wu, G. Pulletikurthi, T. Carstens, F. Endres, *J. Electrochem. Soc.* **2018**, *165*, D223-D230; e) S. Romankov, Y. C. Park, I. V. Shchetinin, *Surf. Coat. Technol.* **2019**, *357*, 473-482.
[30] Q. Zhang, Q. Wang, S. Zhang, X. Lu, X. Zhang, *ChemPhysChem* **2016**, *17*, 335-351.
[31] a) M. Schlesinger, M. Paunovic, *Modern electroplating*, Wiley, Hoboken, N.J., **2010**; b) *Electrochemical Aspects of ionic liquids* John Wiley & Sons, Inc., **2011**; c) A. P. Abbott, K. J. McKenzie, *Phys. Chem. Chem. Phys.* **2006**, *8*, 4265-4279.
[32] H. Ohno, *Electrochemical aspects of ionic liquids*, Wiley, Hoboken, N.J., **2011**.
[33] a) F. Endres, M. Bukowski, R. Hempelmann, H. Natter, *Angew. Chem. Int. Ed.* **2003**, *42*, 3428-3430; b) K. Izutsu, *Electrochemistry in nonaqueous solutions*, Wiley-VCH, Weinheim [u.a.], **2009**; c) D. J. Fray, G. Z. Chen, *Mater. Sci. Technol.* **2004**, *20*, 295-300.
[34] P. Walden, *Bull. Acad. Imp. Sci. St.-Petersbourg* **1914**, 405-422.
[35] a) H. L. Chum, V. R. Koch, L. L. Miller, R. A. Osteryoung, *J. Am. Chem. Soc.* **1975**, *97*, 3264-3265; b) R. J. Gale, B. Gilbert, R. A. Osteryoung, *Inorg. Chem.* **1978**, *17*, 2728-2729; c) J. Robinson, R. A. Osteryoung, *J. Am. Chem. Soc.* **1979**, *101*, 323-327.
[36] a) J. S. Wilkes, J. A. Levisky, R. A. Wilson, C. L. Hussey, *Inorg. Chem.* **1982**, *21*, 1263-1264; b) T. M. Laher, C. L. Hussey, *Inorg. Chem.* **1983**, *22*, 3247-3251; c) T. B. Scheffler, C. L. Hussey, K. R. Seddon, C. M. Kear, P. D. Armitage, *Inorg. Chem.* **1983**, *22*, 2099-2100; d) T. B. Scheffler, C. L. Hussey, *Inorg. Chem.* **1984**, *23*, 1926-1932.
[37] J. S. Wilkes, M. J. Zaworotko, *J. Chem. Soc. Chem. Commun.* **1992**, 965-967.
[38] F. Endres, S. Z. E. Abedin, N. Borissenko, *Z. Phys. Chem.* **2006**, *220*, 1377.
[39] F. Endres, *Chem. Ing. Tech.* **2011**, *83*, 1485-1492.
[40] a) F. Endres, *ChemPhysChem* **2002**, *3*, 144-154; b) W. Simka, D. Puszczyk, G. Nawrat, *Electrochim. Acta* **2009**, *54*, 5307-5319.
[41] P. Wasserscheid, *Ionic liquids in synthesis*, Wiley-VCH, Weinheim, **2004**.
[42] A. Ispas, A. Bund, *Interface magazine* **2014**, *23*, 47-51.
[43] C. A. Berger, M. Arkhipova, A. Farkas, G. Maas, T. Jacob, *Phys. Chem. Chem. Phys.* **2016**, *18*, 4961-4965.
[44] N. V. Plechkova, K. R. Seddon (Eds.), *Ionic Liquids Uncoiled*, WILEY-VCH, **2012** pp. 1-27.
[45] P. Wasserscheid, W. Keim, *Angew. Chem. Int. Ed.* **2000**, *39*, 3772-3789.
[46] G. M. Haarberg, W. Rolland, Å. Sterten, J. Thonstad, *J. Appl. Electrochem.* **1993**, *23*, 217-224.
[47] A. P. Abbott, A. Bettley, D. J. Schiffrin, *J. Electroanal. Chem.* **1993**, *347*, 153-164.

[48] X.-Y. Zhang, Y.-X. Hua, C.-Y. Xu, Q.-B. Zhang, X.-B. Cong, N. Xu, *Electrochim. Acta* **2011**, *56*, 8530-8533.
[49] a) Y. Katayama, K. Ogawa, T. Miura, *Electrochemistry* **2005**, *73*, 576-578; b) Y. Andriyko, U. Fastner, H. Kronberger, G. E. Nauer, *Z. Naturforsch. A* **2007**, *62*, 529; c) Y. Andriyko, G. E. Nauer, *Electrochim. Acta* **2007**, *53*, 957-962.
[50] F. Endres, S. Zein El Abedin, A. Y. Saad, E. M. Moustafa, N. Borissenko, W. E. Price, G. G. Wallace, D. R. MacFarlane, P. J. Newman, A. Bund, *Phys. Chem. Chem. Phys.* **2008**, *10*, 2189-2199.
[51] J. Ding, J. Wu, D. MacFarlane, W. E. Price, G. Wallace, *Electrochem. Commun.* **2008**, *10*, 217-221.
[52] J. Ding, J. Wu, D. R. MacFarlane, W. E. Price, G. Wallace, *Phys. Chem. Chem. Phys.* **2008**, *10*, 5863-5869.
[53] Y. Andriyko, A. Andriiko, O. B. Babushkina, G. E. Nauer, *Electrochim. Acta* **2010**, *55*, 1081-1089.
[54] a) H. Chandler (Ed.), *Metallurgy for the Non-Metallurgist*, ASM International, **1998**; b) J. Verhoeven, Materials Park, Ohio, *ASM Int.* **2007**; c) G. F. Hardy, J. K. Hulm, *Phys. Rev.* **1953**, *89*, 884-884; d) W. Markiewicz, E. Mains, R. Vankeuren, R. Wilcox, C. Rosner, H. Inoue, C. Hayashi, K. Tachikawa, *IEEE Trans. Magn.* **1977**, *13*, 35-37.
[55] T. Tsuda, Hussey C.L., *J. Min. Metall., Sect. B* **2003**, *39*, 3-22.
[56] G. W. Mellors, S. Senderoff, *J. Electrochem. Soc.* **1965**, *112*, 266-271.
[57] V. Van, A. Silný, J. Híveš, V. Daněk, *Electrochem. Commun.* **1999**, *1*, 295-300.
[58] B. Gillesberg, J. H. V. Barner, N. J. Bjerrum, F. Lantelme, *J. Appl. Electrochem.* **1999**, *29*, 939-949.
[59] S. Krischok, A. Ispas, A. Zuhlsdorff, A. Ulbrich, A. Bund, F. Endres, *ECS Trans.* **2013**, *50*, 229-237.
[60] P. Giridhar, S. Zein El Abedin, A. Bund, A. Ispas, F. Endres, *Electrochim. Acta* **2014**, *129*, 312-317.
[61] M. Mascia, A. Vacca, L. Mais, S. Palmas, E. Musu, F. Delogu, *Thin Solid Films* **2014**, *571*, 325-331.
[62] A. Vacca, M. Mascia, L. Mais, S. Rizzardini, F. Delogu, S. Palmas, *Electrocatalysis* **2014**, *5*, 16-22.
[63] O. B. Babushkina, E. O. Lomako, W. Freyland, *Electrochim. Acta* **2012**, *62*, 234-241.
[64] a) M. Mehmood, N. Kawaguchi, H. Maekawa, Y. Sato, T. Yamamura, M. Kawai, K. Kikuchi, Mater. Trans. **2003**, *44*, 259-267; b) N. Borisenko, A. Ispas, E. Zschippang, Q. Liu, S. Zein El Abedin, A. Bund, F. Endres, *Electrochim. Acta* **2009**, *54*, 1519-1528.
[65] a) S. Senderoff, G. W. Mellors, *Science* **1966**, *153*, 1475; b) G. M. Haarberg, J. Thonstad, *J. Appl. Electrochem.* **1989**, *19*, 789-801.
[66] a) S. Zein El Abedin, H. K. Farag, E. M. Moustafa, U. Welz-Biermann, F. Endres, *Phys. Chem. Chem. Phys.* **2005**, *7*, 2333-2339; b) S. Zein El Abedin, U. Welz-Biermann, F. Endres, *Electrochem. Commun.* **2005**, *7*, 941-946; c) Z. E. S. Abedin, *Trans. IMF* **2008**, *86*, 220-226.
[67] a) A. Ispas, B. Adolphi, A. Bund, F. Endres, *Phys. Chem. Chem. Phys.* **2010**, *12*, 1793-1803; b) A. Ispas, A. Bund, *Trans. IMF* **2012**, *90*, 298-304; c) S. Krischok, A. Ispas, A. Zühlsdorff, A. Ulbrich, A. Bund, F. Endres, *ECS Trans.* **2013**, *50*, 229-237; d) T. Carstens, A. Ispas, N. Borisenko, R. Atkin, A. Bund, F. Endres, *Electrochim. Acta* **2016**, *197*, 374-387.
[68] S. Martens, A. Ispas, L. Asen, L. Seidl, U. Stimming, O. Schneider, A. Bund, *ECS Trans.* **2016**, *75*, 287-295.
[69] a) E. Hayes, *Ind. Eng. Chem.* **1961**, *53*, 105-107; b) A. P. Abbott, G. Capper, D. L. Davies, R. K. Rasheed, *Chem. Eur. J.* **2004**, *10*, 3769-3774; c) S. Eugénio, C. M. Rangel, R. Vilar, S. Quaresma, *Electrochim. Acta* **2011**, *56*, 10347-10352.
[70] Z. Zeng, Y. Chen, D. Wang, J. Zhang, *Electrochem. Solid-State Lett.* **2007**, *10*, D85-D87.
[71] A. P. Abbott, G. Capper, D. L. Davies, R. K. Rasheed, J. Archer, C. John, *Trans. IMF* **2004**, *82*, 14-17.
[72] E. S. C. Ferreira, C. M. Pereira, A. F. Silva, *J. Electroanal. Chem.* **2013**, *707*, 52-58.

[73] a) S. Eugénio, C. M. Rangel, R. Vilar, A. M. Botelho do Rego, *Thin Solid Films* **2011**, *519*, 1845-1850; b) S. Survilienė, S. Eugénio, R. Vilar, *J. Appl. Electrochem.* **2011**, *41*, 107-114.

[74] a) X. He, B. Hou, C. Li, Q. Zhu, Y. Jiang, L. Wu, *Electrochim. Acta* **2014**, *130*, 245-252; b) X. He, C. Li, Q. Zhu, B. Hou, Y. Jiang, L. Wu, *RSC Adv.* **2014**, *4*, 64174-64182; c) X. He, Q. Zhu, B. Hou, Y. Cai, C. Li, L. Fu, L. Wu, *J. Nanosci. Nanotechnol.* **2015**, *15*, 9431-9437; d) X. He, Q. Zhu, B. Hou, C. Li, Y. Jiang, C. Zhang, L. Wu, *Surf. Coat. Technol.* **2015**, *262*, 148-153; e) L. Sun, J. F. Brennecke, *Ind. Eng. Chem. Res.* **2015**, *54*, 4879-4890; f) H. Khani, J. F. Brennecke, *Electrochem. Commun.* **2019**, *107*, 106537; g) E. B. Molodkina, M. R. Ehrenburg, P. Broekmann, A. V. Rudnev, *J. Electroanal. Chem.* **2020**, *860*, 113892.

[75] a) D. R. Ervin, D. L. Bourell, C. Persad, L. Rabenberg, *Mater. Sci. Eng., Sect. A* **1988**, *102*, 25-30; b) J. R. Davis, A. S. M. I. H. Committee, *ASM Specialty Handbook: Heat-Resistant Materials*, ASM International, **1997**; c) N. A. Yefimov, S. Naboychenko, O. D. Neikov, I. B. Mourachova, V. G. Gopienko, I. V. Frishberg, D. V. Lotsko, *Handbook of Non-Ferrous Metal Powders: Technologies and Applications*, Elsevier Science, **2009**.

[76] a) N. W. Hovey, A. Krohn, G. M. Hanneken, *J. Electrochem. Soc.* **1963**, *110*, 362; b) E. Gómez, E. Pellicer, E. Vallés, *J. Electroanal. Chem.* **2001**, *517*, 109-116; c) E. Gómez, E. Pellicer, E. Vallés, *J. Appl. Electrochem.* **2003**, *33*, 245-252.

[77] H. Nakajima, T. Nohira, R. Hagiwara, *Electrochim. Acta* **2006**, *51*, 3776-3780.

[78] a) B. Gao, T. Nohira, R. Hagiwara, *ECS Trans.* **2007**, *3*, 323-331; b) T. Nohira, K. Kitagawa, R. Hagiwara, K. Nitta, M. Majima, S. Inazawa, *Electrochemistry* **2009**, *77*, 687-689.

[79] a) T. Tsuda, S. Arimoto, S. Kuwabata, C. L. Hussey, *J. Electrochem. Soc.* **2008**, *155*, D256-D262; b) M. H. Allahyarzadeh, B. Roozbehani, A. Ashrafi, S. R. Shadizadeh, *Surf. Coat. Technol.* **2011**, *206*, 137-142; c) M. H. Allahyarzadeh, B. Roozbehani, A. Ashrafi, S. R. Shadizadeh, A. Seddighian, E. Kheradmand, *J. Electrochem. Soc.* **2012**, *159*, D473-D478.

[80] X.-T. Hu, J.-G. Qian, Y. Yin, X. Li, T.-J. Li, J. Li, *Rare Met.* **2018**.

[81] a) E. Lassner, W. D. Schubert, *Tungsten: Properties, Chemistry, Technology of the Elements, Alloys, and Chemical Compounds*, Springer US, **1999**; b) T. Nohira, K. Kitagawa, R. Hagiwara, K. Nitta, M. Majima, S. Inazawa, *Trans. Mater. Res. Soc. Jpn.* **2010**, *35*, 35-37; c) T. Tsuda, Y. Ikeda, T. Arimura, A. Imanishi, S. Kuwabata, C. L. Hussey, G. R. Stafford, *ECS Trans.* **2012**, *50*, 239-250.

[82] S. Senderoff, G. W. Mellors, *J. Electrochem. Soc.* **1967**, *114*, 586.

[83] a) A. Katagiri, *J. Electrochem. Soc.* **1991**, *138*, 767; b) M. Masuda, H. Takenishi, A. Katagiri, *J. Electrochem. Soc.* **2001**, *148*, C59; c) Y. Liu, Y. Zhang, Q. Liu, X. Li, F. Jiang, *Int. J. Refract. Met. Hard Mater.* **2012**, *35*, 241-245.

[84] a) K. B. Kushkhov, M. N. Adamokova, *Russ. J. Electrochem.* **2007**, *43*, 997-1006; b) K. Nitta, M. Majima, S. Inazawa, T. Nohira, R. Hagiwara, *Electrochemistry* **2009**, *77*, 621-623; c) F. Jiang, Y. Zhang, N. Sun, J. Leng, *Appl. Surf. Sci.* **2015**, *327*, 432-436.

[85] a) T. Tsuda, Y. Ikeda, T. Arimura, M. Hirogaki, A. Imanishi, S. Kuwabata, G. R. Stafford, C. L. Hussey, *J. Electrochem. Soc.* **2014**, *161*, D405-D412; b) T. Tsuda, Y. Ikeda, S. Kuwabata, G. R. Stafford, C. L. Hussey, *ECS Trans.* **2014**, *64*, 563-574.

[86] a) W. Henke, *Justus Liebigs Ann. Chem.* **1858**, *106*, 280-287; b) B. J. Hathaway, A. E. Underhill, *J. Chem. Soc.* **1960**, 3705-3711; c) B. J. Hathaway, D. G. Holah, J. D. Postlethwaite, *J. Chem. Soc.* **1961**, 3215-3218; d) B. J. Hathaway, D. G. Holah, A. E. Underhill, *J. Chem. Soc.* **1962**, 2444-2448; e) D. W. Meek, R. S. Drago, T. S. Piper, *Inorg. Chem.* **1962**, *1*, 285-289.

[87] a) F. A. Cotton, J. L. Eglin, K. J. Wiesinger, *Inorg. Chim. Acta* **1992**, *195*, 11-23; b) R. T. Henriques, E. Herdtweck, F. E. Kühn, A. D. Lopes, J. Mink, C. C. Romão, *J. Chem. Soc., Dalton Trans.* **1998**, 1293-1298; c) D. Coucouvanius (Ed.), *Inorganic Syntheses,* John Wiley & Sons Inc., New York, *Vol. 33*, **2002**, pp. 75-121; d) S. F. Rach, F. E. Kühn, *Chem. Rev.* **2009**, *109*, 2061-2080.

[88] a) S. N. Bernstein, K. R. Dunbar, *Angew. Chem. Int. Ed.* **1992**, *31*, 1360-1362; b) J. C. Bryan, F. A. Cotton, L. M. Daniels, S. C. Haefner, A. P. Sattelberger, *Inorg. Chem.* **1995**, *34*, 1875-1883; c) M. E. Prater, L. E. Pence, R. Clérac, G. M. Finniss, C. Campana, P. Auban-Senzier, D. Jérome, E. Canadell, K. R. Dunbar, *J. Am. Chem. Soc.* **1999**, *121*, 8005-8016.

[89] O. Levy, B. Bogoslavsky, A. Bino, *Inorg. Chim. Acta* **2012**, *391*, 179-181.

[90] a) D. L. Reger, A. E. Pascui, P. J. Pellechia, A. Ozarowski, *Inorg. Chem.* **2013**, *52*, 12741-12748; b) A. J. Pell, G. Pintacuda, C. P. Grey, *Prog. Nucl. Magn. Reson. Spectrosc.* **2019**, *111*, 1-271.
[91] a) I. Nicotera, C. Oliviero, W. A. Henderson, G. B. Appetecchi, S. Passerini, *J. Phys. Chem., Sect. B* **2005**, *109*, 22814-22819; b) I. Favier, E. Duñach, *Tetrahedron Lett.* **2004**, *45*, 3393-3395; c) I. Favier, E. Duñach, *Tetrahedron Lett.* **2003**, *44*, 2031-2032; d) J. M. Griffin, A. C. Forse, H. Wang, N. M. Trease, P.-L. Taberna, P. Simon, C. P. Grey, *Faraday Discuss.* **2014**, *176*, 49-68.
[92] J. C. Menezes, C. C. Romão, *Polyhedron* **1990**, *9*, 1237-1239.
[93] F. E. Kühn, J. R. Ismeier, D. Schön, W.-M. Xue, G. Zhang, O. Nuyken, *Macromol. Rapid Commun.* **1999**, *20*, 555-559.
[94] a) F. A. Cotton, A. H. Reid, W. Schwotzer, *Inorg. Chem.* **1985**, *24*, 3965-3968; b) F. A. Cotton, K. J. Wiesinger, *Inorg. Chem.* **1991**, *30*, 871-873.
[95] F. A. Cotton, F. E. Kühn, *Inorg. Chim. Acta* **1996**, *252*, 257-264.
[96] H. D. Kaesz (Ed.), *Inorganic Syntheses*, **1989** Vol. 26, 128-134.
[97] a) J. Sun, D. R. MacFarlane, M. Forsyth, *Ionics* **1997**, *3*, 356-362; b) L. Cammarata, S. G. Kazarian, P. A. Salter, T. Welton, *Phys. Chem. Chem. Phys.* **2001**, *3*, 5192-5200; c) O. O. Okoturo, T. J. VanderNoot, *J. Electroanal. Chem.* **2004**, *568*, 167-181; d) Z.-B. Zhou, H. Matsumoto, K. Tatsumi, *Chem. Eur. J.* **2006**, *12*, 2196-2212; e) N. Sasaya, M. Matsumiya, K. Tsunashima, *Polyhedron* **2015**, *85*, 888-893; f) A. R. Neale, P. Li, J. Jacquemin, P. Goodrich, S. C. Ball, R. G. Compton, C. Hardacre, *Phys. Chem. Chem. Phys.* **2016**, *18*, 11251-11262.
[98] W. L. F. Armarego (Ed.), *Purification of Laboratory Chemicals, 8th Edition*, Butterworth-Heinemann, **2017**, 95-634.
[99] D. E. Freedman, D. M. Jenkins, J. R. Long, *Chem. Commun.* **2009**, 4829-4831.
[100] S. J. Anderson, F. J. Wells, G. Willkinson, B. Hussain, M. B. Hursthouse, *Polyhedron* **1988**, *7*, 2615-2626.
[101] J. J. Habeeb, F. F. Said, D. G. Tuck, *J. Chem. Soc., Dalton Trans.* **1981**, 118-120.
[102] a) G. R. Fulmer, A. J. M. Miller, N. H. Sherden, H. E. Gottlieb, A. Nudelman, B. M. Stoltz, J. E. Bercaw, K. I. Goldberg, *Organometallics* **2010**, *29*, 2176-2179; b) N. R. Babij, E. O. McCusker, G. T. Whiteker, B. Canturk, N. Choy, L. C. Creemer, C. V. D. Amicis, N. M. Hewlett, P. L. Johnson, J. A. Knobelsdorf, F. Li, B. A. Lorsbach, B. M. Nugent, S. J. Ryan, M. R. Smith, Q. Yang, *Org. Process Res. Dev.* **2016**, *20*, 661-667.
[103] J. Oldengott, C.-G. Frhr. v. Richthofen, S. Walleck, A. Stammler, H. Bögge, T. Glaser, *Eur. J. of Inorg. Chem.* **2018**, *2018*, 4987-4996.

IV. Appendix

1. Publication in Scientific Journals

Parts of this dissertation have been published.

Full Paper

Reactivity Studies of a Dipyridine Ethinyl Ligand with Zinc(II)

C. M. Egger, C. H.G. Jakob, F. Kaiser, O. Rindle, P. J. Altmann, R. M. Reich, F. E. Kühn;

Eur. J. Inorg. Chem., **2019**, Vol. 2019, Iss. 48, p. 5059-5065.

2. Active Participation in a Scientific Conference

Poster Presentation

Synthesis and characterization of metalorganic complexes for the electrochemical deposition of refractory metals out of ionic liquids

C. M. Egger, R. M. Reich, O. Schneider, F. E. Kühn

258th ACS Fall National Meeting, 25.-29.08.2019, San Diego, CA, USA.

3. Talks

[7] Synthese neuer Präkursoren zur Refraktärmetallabscheidung aus ionischen Flüssigkeiten

C. M. Egger, F. E. Kühn

7th project meeting of GALACTIF, 28.-29.05.2019, TU München, Garching.

[6] Synthese neuer Präkursoren zur Refraktärmetallabscheidung aus ionischen Flüssigkeiten

C. M. Egger, F. E. Kühn

6th project meeting of GALACTIF, 08.-09.01.2019, Fraunhofer-IST, Braunschweig.

[5] Synthese neuer Präkursoren zur Refraktärmetallabscheidung aus ionischen Flüssigkeiten

C. M. Egger, F. E. Kühn

5th project meeting of GALACTIF, 24.-25.07.2018, TU Clausthal, Clausthal-Zellerfeld.

[4] Synthese neuer Präkursoren zur Refraktärmetallabscheidung aus ionischen Flüssigkeiten

C. M. Egger, F. E. Kühn

4th project meeting of GALACTIF, 22.-23.02.2018, TU Ilmenau, Ilmenau.

[3] Synthese neuer Präkursoren zur Refraktärmetallabscheidung aus ionischen Flüssigkeiten

C. M. Egger, F. E. Kühn

3rd project meeting of GALACTIF, 10.10.2017, TU Chemnitz, Chemnitz.

[2] Synthese neuer Präkursoren zur Refraktärmetallabscheidung aus ionischen Flüssigkeiten

C. M. Egger, F. E. Kühn

2nd project meeting of GALACTIF, 22.02.2017, FEM, Schwäbisch-Gmünd.

[1] Synthese neuer Präkursoren zur Refraktärmetallabscheidung aus ionischen Flüssigkeiten

C. M. Egger, F. E. Kühn

1st project meeting of GALACTIF, 24.08.2016, TU München, Garching.

4. Reprint Permission

JOHN WILEY AND SONS LICENSE
TERMS AND CONDITIONS

Jul 06, 2020

This Agreement between Christiane Egger ("You") and John Wiley and Sons ("John Wiley and Sons") consists of your license details and the terms and conditions provided by John Wiley and Sons and Copyright Clearance Center.

License Number	4863121321873
License date	Jul 06, 2020
Licensed Content Publisher	John Wiley and Sons
Licensed Content Publication	European Journal of Inorganic Chemistry
Licensed Content Title	Reactivity Studies of a Dipyridine Ethinyl Ligand with Zinc(II)
Licensed Content Author	Christiane M. Egger, Christian H. G. Jakob, Felix Kaiser, et al
Licensed Content Date	Dec 17, 2019
Licensed Content Volume	2019
Licensed Content Issue	48
Licensed Content Pages	7
Type of use	Dissertation/Thesis
Requestor type	Author of this Wiley article
Format	Print and electronic
Portion	Full article
Will you be translating?	No
Title	Time and Temperature dependent Reactivity Studies of a Dipyridine Ethinyl Ligand with Zinc(II) and Synthesis and Characterization of new Precursors for the Deposition of Refractory Metals from Ionic Liquids
Institution name	Technical University of Munich, Department of Chemistry, Professorship of Molecular Catalysis
Expected presentation date	Sep 2020
Requestor Location	Christiane Egger Lichtenbergstrasse 4 Garching bei München, 85747 Germany Attn: Professorship for Molecular Catalysis
Publisher Tax ID	EU826007151
Total	0.00 EUR

Terms and Conditions

TERMS AND CONDITIONS

This copyrighted material is owned by or exclusively licensed to John Wiley & Sons, Inc. or one of its group companies (each a"Wiley Company") or handled on behalf of a society with which a Wiley Company has exclusive publishing rights in relation to a particular work (collectively "WILEY"). By clicking "accept" in connection with completing this licensing transaction, you agree that the following terms and conditions apply to this transaction (along with the billing and payment terms and conditions established by the Copyright Clearance Center Inc., ("CCC's Billing and Payment terms and conditions"), at the time that you opened your RightsLink account (these are available at any time at http://myaccount.copyright.com).

Terms and Conditions

- The materials you have requested permission to reproduce or reuse (the "Wiley Materials") are protected by copyright.
- You are hereby granted a personal, non-exclusive, non-sub licensable (on a stand-alone basis), non-transferable, worldwide, limited license to reproduce the Wiley Materials for the purpose specified in the licensing process. This license, **and any CONTENT (PDF or image file) purchased as part of your order**, is for a one-time use only and limited to any maximum distribution number specified in the license. The first instance of republication or reuse granted by this license must be completed within two years of the date of the grant of this license (although copies prepared before the end date may be distributed thereafter). The Wiley Materials shall not be used in any other manner or for any other purpose, beyond what is granted in the license. Permission is granted subject to an appropriate acknowledgement given to the author, title of the material/book/journal and the publisher. You shall also duplicate the copyright notice that appears in the Wiley publication in your use of the Wiley Material. Permission is also granted on the understanding that nowhere in the text is a previously published source acknowledged for all or part of this Wiley Material. Any third party content is expressly excluded from this permission.
- With respect to the Wiley Materials, all rights are reserved. Except as expressly granted by the terms of the license, no part of the Wiley Materials may be copied, modified, adapted (except for minor reformatting required by the new Publication), translated, reproduced, transferred or distributed, in any form or by any means, and no derivative works may be made based on the Wiley Materials without the prior

permission of the respective copyright owner.**For STM Signatory Publishers clearing permission under the terms of the STM Permissions Guidelines only, the terms of the license are extended to include subsequent editions and for editions in other languages, provided such editions are for the work as a whole in situ and does not involve the separate exploitation of the permitted figures or extracts,** You may not alter, remove or suppress in any manner any copyright, trademark or other notices displayed by the Wiley Materials. You may not license, rent, sell, loan, lease, pledge, offer as security, transfer or assign the Wiley Materials on a stand-alone basis, or any of the rights granted to you hereunder to any other person.

- The Wiley Materials and all of the intellectual property rights therein shall at all times remain the exclusive property of John Wiley & Sons Inc, the Wiley Companies, or their respective licensors, and your interest therein is only that of having possession of and the right to reproduce the Wiley Materials pursuant to Section 2 herein during the continuance of this Agreement. You agree that you own no right, title or interest in or to the Wiley Materials or any of the intellectual property rights therein. You shall have no rights hereunder other than the license as provided for above in Section 2. No right, license or interest to any trademark, trade name, service mark or other branding ("Marks") of WILEY or its licensors is granted hereunder, and you agree that you shall not assert any such right, license or interest with respect thereto
- NEITHER WILEY NOR ITS LICENSORS MAKES ANY WARRANTY OR REPRESENTATION OF ANY KIND TO YOU OR ANY THIRD PARTY, EXPRESS, IMPLIED OR STATUTORY, WITH RESPECT TO THE MATERIALS OR THE ACCURACY OF ANY INFORMATION CONTAINED IN THE MATERIALS, INCLUDING, WITHOUT LIMITATION, ANY IMPLIED WARRANTY OF MERCHANTABILITY, ACCURACY, SATISFACTORY QUALITY, FITNESS FOR A PARTICULAR PURPOSE, USABILITY, INTEGRATION OR NON-INFRINGEMENT AND ALL SUCH WARRANTIES ARE HEREBY EXCLUDED BY WILEY AND ITS LICENSORS AND WAIVED BY YOU.
- WILEY shall have the right to terminate this Agreement immediately upon breach of this Agreement by you.
- You shall indemnify, defend and hold harmless WILEY, its Licensors and their respective directors, officers, agents and employees, from and against any actual or threatened claims, demands, causes of action or proceedings arising from any breach of this Agreement by you.
- IN NO EVENT SHALL WILEY OR ITS LICENSORS BE LIABLE TO YOU OR ANY OTHER PARTY OR ANY OTHER PERSON OR ENTITY FOR ANY SPECIAL, CONSEQUENTIAL, INCIDENTAL, INDIRECT, EXEMPLARY OR PUNITIVE DAMAGES, HOWEVER CAUSED, ARISING OUT OF OR IN CONNECTION WITH THE DOWNLOADING, PROVISIONING, VIEWING OR USE OF THE MATERIALS REGARDLESS OF THE FORM OF ACTION, WHETHER FOR BREACH OF CONTRACT, BREACH OF WARRANTY, TORT, NEGLIGENCE, INFRINGEMENT OR OTHERWISE (INCLUDING, WITHOUT LIMITATION, DAMAGES BASED ON LOSS OF PROFITS, DATA, FILES, USE, BUSINESS OPPORTUNITY OR CLAIMS OF THIRD PARTIES), AND WHETHER OR NOT THE PARTY HAS BEEN ADVISED OF THE POSSIBILITY OF SUCH DAMAGES. THIS LIMITATION SHALL APPLY NOTWITHSTANDING ANY FAILURE OF ESSENTIAL PURPOSE OF ANY LIMITED REMEDY PROVIDED HEREIN.

- Should any provision of this Agreement be held by a court of competent jurisdiction to be illegal, invalid, or unenforceable, that provision shall be deemed amended to achieve as nearly as possible the same economic effect as the original provision, and the legality, validity and enforceability of the remaining provisions of this Agreement shall not be affected or impaired thereby.
- The failure of either party to enforce any term or condition of this Agreement shall not constitute a waiver of either party's right to enforce each and every term and condition of this Agreement. No breach under this agreement shall be deemed waived or excused by either party unless such waiver or consent is in writing signed by the party granting such waiver or consent. The waiver by or consent of a party to a breach of any provision of this Agreement shall not operate or be construed as a waiver of or consent to any other or subsequent breach by such other party.
- This Agreement may not be assigned (including by operation of law or otherwise) by you without WILEY's prior written consent.
- Any fee required for this permission shall be non-refundable after thirty (30) days from receipt by the CCC.
- These terms and conditions together with CCC's Billing and Payment terms and conditions (which are incorporated herein) form the entire agreement between you and WILEY concerning this licensing transaction and (in the absence of fraud) supersedes all prior agreements and representations of the parties, oral or written. This Agreement may not be amended except in writing signed by both parties. This Agreement shall be binding upon and inure to the benefit of the parties' successors, legal representatives, and authorized assigns.
- In the event of any conflict between your obligations established by these terms and conditions and those established by CCC's Billing and Payment terms and conditions, these terms and conditions shall prevail.
- WILEY expressly reserves all rights not specifically granted in the combination of (i) the license details provided by you and accepted in the course of this licensing transaction, (ii) these terms and conditions and (iii) CCC's Billing and Payment terms and conditions.
- This Agreement will be void if the Type of Use, Format, Circulation, or Requestor Type was misrepresented during the licensing process.
- This Agreement shall be governed by and construed in accordance with the laws of the State of New York, USA, without regards to such state's conflict of law rules. Any legal action, suit or proceeding arising out of or relating to these Terms and Conditions or the breach thereof shall be instituted in a court of competent jurisdiction in New York County in the State of New York in the United States of America and each party hereby consents and submits to the personal jurisdiction of such court, waives any objection to venue in such court and consents to service of process by registered or certified mail, return receipt requested, at the last known address of such party.

WILEY OPEN ACCESS TERMS AND CONDITIONS

Wiley Publishes Open Access Articles in fully Open Access Journals and in Subscription journals offering Online Open. Although most of the fully Open Access journals publish open access articles under the terms of the Creative Commons Attribution (CC BY) License only, the subscription journals and a few of the Open Access Journals offer a choice of Creative Commons Licenses. The license type is clearly identified on the article.

The Creative Commons Attribution License

The Creative Commons Attribution License (CC-BY) allows users to copy, distribute and transmit an article, adapt the article and make commercial use of the article. The CC-BY license permits commercial and non-

Creative Commons Attribution Non-Commercial License

The Creative Commons Attribution Non-Commercial (CC-BY-NC)License permits use, distribution and reproduction in any medium, provided the original work is properly cited and is not used for commercial purposes.(see below)

Creative Commons Attribution-Non-Commercial-NoDerivs License

The Creative Commons Attribution Non-Commercial-NoDerivs License (CC-BY-NC-ND) permits use, distribution and reproduction in any medium, provided the original work is properly cited, is not used for commercial purposes and no modifications or adaptations are made. (see below)

Use by commercial "for-profit" organizations

Use of Wiley Open Access articles for commercial, promotional, or marketing purposes requires further explicit permission from Wiley and will be subject to a fee.

Further details can be found on Wiley Online Library http://olabout.wiley.com/WileyCDA/Section/id-410895.html

Other Terms and Conditions:

v1.10 Last updated September 2015

Questions? customercare@copyright.com or +1-855-239-3415 (toll free in the US) or +1-978-646-2777.